Evaluation of Deficit Irrigation Strategies and Management Zones Delineation for Corn Production in Alabama

by

Guilherme Trimer Morata

A thesis submitted to the Graduate Faculty of
Auburn University
in partial fulfillment of the
requirements for the Degree of
or Master of Science

Auburn, Alabama
August 8, 2020

Keywords: Variable Rate Irrigation, Irrigation Scheduling, Irrigation Management Zones, Irrigated Corn, DSSAT

Approved by

Brenda V. Ortiz, Chair, Professor, Department of Crop, Soil and Environmental Sciences
Di Tian, Assistant Professor, Department of Crop, Soil and Environmental Sciences
Frances O'Donnell, Assistant Professor, Department of Civil Engineering
Stephanie Rogers, Assistant Professor, Department of Geosciences
William Batchelor, Professor, Department of Biosystems Engineering

ABSTRACT

The adoption of center pivot irrigation in Alabama has increased in recent years. The reason is that farmers are achieving high crop yield by avoiding crop water stress. Although, irrigation adoption has increased, Alabama farmers still require more training to increase knowledge on irrigation timing and rate in order to increase irrigation water use efficiency. Technologies such as variable rate irrigation (VRI) and soil sensors to monitor soil water status are available to help farmer to increase their irrigation water use efficiency. Variable Rate Irrigation allows farmers to change irrigation rate as the pivot traverse the field, therefore, meeting crop water needs in relation to soil conditions of field terrain changes. Irrigation management zones (MZ) are required to create an irrigation prescription map that allows the VRI system to modify that irrigation rates according to the field and crop variability. Soil properties and topography are the most common data analyzed to delineate irrigation MZ because these properties affect soil water content on crop fields.

The objectives of this study were to: (i) identify which terrain attribute, or combination of terrain attributes and soil properties better explain the variability in soil water content in a crop field, and then, can be used for irrigation management zone delineation; (ii) use a crop growth simulation modeling software CERES-Maize model (DSSAT v.4.7.5) to identify deficit irrigation strategies to initiate irrigation; and (iii) to identify irrigation amount that maximize net returns and irrigation efficiency.

For the first study of this thesis (Chapter II), the experiment was conducted in Tanner and Town Creek, Alabama in 2018 and 2019. Both fields were irrigated by a center pivot irrigation system that covered 24 and 120 hectares in Tanner and Town Creek, respectively. Tanner field

was planted with corn in 2018 and cotton in 2019, and Town Creek was planted with corn on both years. Spatial and temporal changes in soil water content were assessed by soil water tension sensors installed at 15, 30 and 60 cm soil depth. The daily average soil tension values were converted in volumetric water content using soil water retention curves generated through these studies. Topographic wetness index (TWI), topographic position index (TPI), elevation, and slope were considered as terrain attributes for this analysis. Apparent soil electrical conductivity (Soil EC_a) collected at Tanner field and clay, silt and sand content from the Town Creek field were included in the analyses as part of the characterization of soil properties. Principal component analysis (PCA) was used to reduce the dimensionality of the volumetric water content data set and to test the hypothesis of spatial and temporal differences in soil water content. A second step involved a Spearman correlation analysis between the scores of the principal components retained in the PCA and terrain attributes and soil properties to identify parameter with significant correlation with changes in soil water content. The results of PCA indicated that three principal components were sufficient to retain more than 95% of the variance of the entire volumetric water content data set. The principal component one (PC1) was found related to soil water content spatial variability and PC2 and PC3 with temporal variability on both fields and years. At Tanner field, the PC1 explained the most of soil water content variance for the three soil layers analyzed and was high correlated only with TPI for both years. In 2018, PC2 was correlated with elevation, slope and TWI. In 2019, PC3 showed only correlation with slope and soil EC_a . At the Town Creek field, PC1 was significantly correlated with slope, TWI, and sand content in 2018 and TPI in 2019. PC2 was significantly correlated with TWI, clay, and silt content in 2018 and elevation in 2019. PC3 only showed significant collection with clay and silty content in 2019. For both fields, both topographic indices were significant explaining the

variability in soil water content and therefore could be considered for irrigation management zones delineation.

The crop growth simulation modeling study, chapter III on this thesis, was conducted in Decatur silty clay loam soil type at Town Creek, Alabama on an irrigated corn field. The CERES-Maize model, part of the Decision Support System for Agrotechnology Transfer (DSSAT) software application program, was calibrated and validated using data collected in 2019 and 2018, respectively. Plant biomass, leaf area index, volumetric water content, phenology dates, crop yield, and yield components were used to calibrate the model. Deficit irrigation scenarios assumed for this study were considered to trigger irrigation at 20, 30, 40, 50, 60, 70, 80, and 90% of soil water depletion. This analysis was conducted using the seasonal analysis tool in DSSAT. Daily weather data used in the seasonal analyses corresponded to the period 1984 to 2019. Three different fixed irrigation rates of 12.7, 19, 25.4 mm and full rate were evaluated to refill the soil back to field capacity and the criteria for selecting the most efficient treatment was based on maximization of the net returns. The results of the calibrated model showed prediction of crop yield with RMSE = 69 kg ha^{-1} (0.5%) and RMSE = 450 kg ha^{-1} (3.5%) for the validation data set. The deficit irrigation strategy that maximized net returns resulted on triggering irrigation at 70% of soil water depletion with an average crop yield of 11,175.5 kg ha^{-1}. Yield started to decrease when irrigation was triggered at 80% and 90% of soil water depletion. The irrigation strategies that maximized net results considered applying irrigation at the rate of 25.4 mm every time the soil reached 70% of soil water depletion. These results will require field testing to prove the results from the crop growth modeling and the results will guide Alabama farmers to manage better irrigation decisions related to irrigation timing and rate to help them increase water use efficiency, achieve higher yield and improve the profitability.

Acknowledgments

I would like to thank my advisor, Dr. Brenda V. Ortiz, for all the opportunities provided, the encouragement and friendship during my entire masters at Auburn. I would like to also thank all of my committee members: Dr. Di Tian, Dr. William Batchelor, Dr. Frances O'Donnell and Dr. Stephanie Rogers for all the support.

I would like to thank my family so much for encouraging me to come to the United States and for all the support that they provided me during my period far from them. I am so grateful for the best family that I could have asked for. My dad Julio, my mom Regina, my sister Juliana and my brother Murilo.

I am so thankful for my friends that were always by my side helping me with everything that was needed (Hemendra Kumar, Luca Bondesan, Bruno Lena, Luan Pereira, Mailson, Tayler Schillerberg, Kyle Stewart, Taylor Putman and Mary Herron) and my friends from Brazil that always kept me motivated to move forward (Octavio Schichi, Murillo Oliveira, Fabio Alvares, Rafael Contiero, Amaro Neto and Davi Rinaldo)

I would like to thank Emily Yates and Vinci so much for all of the encouragement, motivation, love, friendship and the help provided throughout my two and a half years at Auburn. I am extremely happy to have you both in my life.

Table of Contents

List of Tables

List of Figures

I. LITERATURE REVIEW

1. Irrigation Scenario

Irrigation adoption has been increasing in the United States every year. In the last fifteen years, the total irrigated land in the country increased by almost 5% (NASS, 2017). The states with larger irrigated land are Nebraska, California, Arkansas, Texas and Idaho. These states represent 50% of the total irrigated land in the United States. Meanwhile, the southeast represents only 10% of the total irrigated land in the country. Mississippi, Florida and Georgia are the largest irrigated areas in the southeast. The Alabama State has around 58,000 hectares irrigated, which is 5% of the total agricultural land in the state. However, the irrigation adoption in Alabama increased by 25% between 2012 and 2017 (NASS, 2017). The main reasons that farmers are increasing irrigation are due to high yield achievement and to avoid water stress. Moreover, the changes in climate directly influence the rainfall distribution during the growing season and irrigation is required in the periods without rainfall to minimize yield losses by crop water stress. In addition, the climate change in the southeast has demonstrated higher temperatures, heavy rainfall and decreases in water availability for human health and agriculture (Carter et al., 2018). The main water sources for irrigation are drilled wells, surface water and ponds. The drilled wells use groundwater from the aquifers. The main problem for this source is related to water depletion in the aquifer related to the increase in irrigation land. Surface water includes lakes, creeks and rivers and this is the most common water source used by farmers. However, the main concern is water availability during the growing season. Typically, low water levels in rivers or creeks do not allow farmers to pump water and it can reflect in yield losses according to the crop growth stage (Chen et al., 2016). Lastly, the pond water source has been a good option for water conservation and a good strategy to have water available for irrigation when there is no water available in the creeks. This strategy allows farmers to store water in

periods of drought and during the winter by collecting water from rainfall and runoff and to have it available during the crop growing season. The Agricultural Water Enhancement Program provides training and support for farmers to implement and build ponds.

In terms of irrigation types, the most common irrigation systems are center pivots, drip irrigation and surface irrigation. The difference between these three methods is related to price, efficiency and maintenance of the system. The adoption of center pivot, drip irrigation and surface irrigation is 85%, 10% and 5% respectively in Alabama (NASS, 2013). In terms of efficiency, the highest efficiency is found in drip irrigation as 85-95%, followed by center pivots systems as 80-90% and surface irrigation as 45-80% (Irmak et al., 2011). Even though irrigation is still increasing in the United States, the main barriers to irrigation adoption in the United States are related to financial issues. Improvements in irrigation will not reduce costs enough to cover the installation costs and uncertainty about the future availability of water (NASS, 2013).

2. Approaches to Increase Irrigation Water Use Efficiency

Irrigation plays an important role in increasing yield especially in dry years when lack of precipitation during periods of high crop water demand is limited. Although irrigation can minimize the risks of yield losses due to water stress issues such as over-irrigation could also have negative impacts to crops and the environment. The issues with over-irrigation could be linked to the crop type, soil type, crop stage, irrigation system used and its maintenance. The main impacts of over-irrigation are related to nitrogen leaching, runoff, favorable environment for crop diseases, low soil aeration, decrease in soil temperature, crop yield impact, and consequently net returns (Irmak and Rathje, 2008). As farmers can over-irrigate a field, under-irrigation is also common. Under-irrigation is related to application small irrigation amounts that are not enough to provide the appropriate plant available water for crop to growth and

development. Farmers can under- or over- irrigate fields frequently when there is a lack of knowledge regarding soil water holding capacities, daily crop water use, and soil water depletion status that potentially could cause crop stress. Irrigation water use efficiency is characterized as the relationship between crop yield and total amount applied of water applied by irrigation. Meanwhile, crop water use efficiency is used to describe the irrigation effectiveness in terms of crop yield (Irmak et al., 2011). Increasing water use efficiency could be possible through the use of several management practices such as the use of cover crops and conservation tillage (Hatfield et al., 2001), and better irrigation management practices (Perry et al., 2012). Typically, agricultural fields in any part of the world have their own field variability related to different soil types, topography, fertility, organic matter and soil compaction. In order for farmers to increase water use efficiency, it is necessary to apply the right irrigation rate at the right place, and right time meeting then field and crop growth variability (Reyes et al., 2019). Technologies such as soil water monitoring to decide irrigation timing and irrigation scheduling methods as well as variable rate irrigation systems are available for farmers to support irrigation decisions and therefore, increase water use efficiency.

3. Irrigation Scheduling

Irrigation scheduling is a science-based tool that determines irrigation application timing and amount (Liang et al., 2016). Irrigating at the right time and right rate to meet crop water needs provides economic and agronomic benefits. The main benefits of irrigation scheduling are related to minimization of crop water stress, maximization of yield, reduction of energy costs and labor, minimization of fertilizer costs due leaching or runoff, minimization of waterlogging problems (Evans and Sadler, 2008) and increase in profitability (Perry et al., 2012; Broner, 2005). The key factors to irrigation scheduling are linked to tracking soil moisture content in the

root zone, the amount of water lost by plants evapotranspiration (ET) during each crop growth stage, water lost by soil evaporation and soil water holding capacity.

There are several methods to schedule irrigation and each method uses different criteria to trigger irrigation. Based on the 2012 Census of Agriculture the most commons method used for farmers to schedule irrigation are crop condition, feel of soil, personal calendar schedule, soil moisture device, evapotranspiration method, commercial or governmental scheduling or when neighbors begin to irrigate.

3.1 Crop condition

The most common method of irrigation scheduling used by farmers in the United States and southeast is to evaluate crop conditions. This method works by farmers watching the crop during the growing season and as soon as the plants show signs of water stress, (wilted leaves) farmers begin to irrigate. This method is easy to use by farmers because it associates their knowledge of the crops and in the field to determine irrigation timing. The main problem with this method is the low accuracy. Plants can show signs of wilting caused by a number of factors, not only water stress. On the other hand, it is not easy to determine irrigation when the field shows high spatial variability that could lead to different levels and frequency of crop water stress.

3.2 Feeling the soil

The second most adopted irrigation scheduling method is feeling the soil by hand. This method consists of farmers grabbing soil samples in the field to check the soil moisture by feeling the soil by hand. Farmers believe it is an easy method, is simple and can be improved with experience. The disadvantages are the low accuracy, the field work to take samples and time consumed when a field exhibits high soil within-field variability.

3.3 Soil Moisture Sensor

Technologies similar to soil moisture sensors have the advantage of having a high accuracy of measuring soil water status, instantaneous readings and, if telematics are available, remote access to data. However, the use of this technology has not been fully adopted by farmers due the sensors price, difficult to interpret the data and lack of knowledge. Different soil moisture sensor devices are currently available in the market. The differences between them are related to how the sensors operate, how they are installed, the unit of measurement and prices. One typical sensor utilized for irrigation scheduling is the soil water tension or soil matric potential sensor. This sensor works as an electrical resistance sensor (Irmak et al., 2016). A current is applied to the sensor to obtain a resistance value. As the soil water content increases, the electrical resistance decreases. The electrical resistance is then converted into tension values using a non-linear equation developed by Shock et al. 1998. The tension value is going to be used to determine how much water is in the soil at the moment of the reading and how much is available for the plants if other soil properties are known. The tension values increase as the soil water content decreases (Irmak and Haman, 2001; Vellidis et al., 2008). Soil water tension sensors can be installed at different soil depths, and then, monitoring soil water changes over the crop root zone during the growing season. In addition, sensors can be connected into a network system to be able to have remote access to the data every hour or daily. Data from soil sensors is important to determine when to start irrigation and the appropriate rate, and then to prevent any crop water stress.

Monitoring soil water content with soil sensors allows farmers to increase water use efficiency due to the high accuracy of the measurement. Irmak et al., 2012 using soil water

tension sensors and 100 kPa as an irrigation threshold in silt loams soils for corn, increased irrigation water use efficiency, which considers the ratio of crop yield by irrigation amount applied, by 34% on average compared to farmer's management irrigation. Steele et al., 1994 found that using a threshold as 50 kPa in a sandy loam also for corn soil decreased in 40% the total amount of water applied in comparison to water balance method. The thresholds for irrigation using soil water tension vary from soil to soil, crop to crop and also vary by growth stages on the same crop. Fisher et al., 2009 concluded that using soil water tension provided good guidance for irrigation timing and yield for cotton.

There are other types of sensors available in the market to measure volumetric water content. It can be electromagnetic sensors, capacitance probes or neutron probes. Those sensors are, in general, more expensive than soil water tension sensors. However, those sensors have a longer life span in comparison to soil water tension sensors.

3.4 Evapotranspiration

Evapotranspiration (ET) is defined as a combination of water lost by evaporation from the soil surface and plant transpiration (Allen et al., 1998). The evaporation is related to the water loss in the soil surface to the atmosphere. This process depends on the amount of radiation that the soil receives. As the crop starts to grow and increase the biomass, the soil starts to be covered by the crop canopy and the evaporation decreases. At the same time, the transpiration increases. The transpiration is the process where the plant loses water to the atmosphere by the stomata. Most of the water uptake by the plant is lost through transpiration. Weather conditions, crop characteristics and management conditions directly influence evapotranspiration. The ET estimation for agricultural crops is a hard process. Some known methods for the determination of ET are lysimeters (Lena, 2013) and eddy covariance systems, but these are complex and

expensive. The easiest method used to estimate ET for a crop is using a reference crop evapotranspiration (ET_o) and a crop coefficient (Djaman et al., 2018). The ET_o is calculated from a hypothetical grass reference crop and weather parameters (Allen et al., 1998). The most accurate equation to estimate ET_o is the Penman-Monteith equation. Radiation, air temperature, air humidity and wind speed are the variables required for ET_o estimation. The ET_o needs to be multiplied by a crop coefficient (Kc) to determine the evapotranspiration for the desired crop at a specific growth stage. The Kc value is different for each crop and changes during the crop growing season. The Kc values increase from the beginning of the growing season, reaches the maximum value at mid-season and decreases at the late-season stage where maturity or senescence happens (Allen et al., 1998). The Kc is calculate by the ratio of the evapotranspiration of the crop to a reference crop.

The ability of the use of evapotranspiration as irrigation scheduling depends on several factors. Weather data is one of the most important factors and a weather station needs to be as close as possible to a crop field where the irrigation is desired. The crop coefficient also changes from different regions and possibly also between need crop varieties and old varieties. These differences can affect the irrigation prescription. Djaman et al., 2018 compared the Kc values using FAO and a local value and they found different irrigation amounts required using these two different values. Fisher et al., 2009 using ET method for irrigation scheduling achieved higher cotton yield in conventional and minimum tillage systems. Vellidis et al., 2016 compared ET irrigation scheduling using a smartphone application against the traditional checkbook (Section 3.5) method for cotton and the ET method performed better than the checkbook method for over two years. The use of the smartphone ET-Based irrigation scheduling method resulted in a yield increase and decrease in total water amount applied over the growing season.

3.5 Checkbook

The checkbook is a method that is based on soil moisture balance. This method works as a checking account (Melvin and Yonts, 2009). Irrigation and rainfall are the deposits and evapotranspiration (crop water use) and percolation are the withdrawals (Perry et al., 2012). The methods required information related to soil type, crop and rooting depth, growth stage, soil water holding capacity, minimum allowable balance and estimation of soil water content during the growing season. The soil storage will be a key information for this method to determine the amount of water required to replenish the soil profile. This method is easy to use, does not require fieldwork, and is used to forecast irrigation (Broner, 2005). The calculation of the soil water balance can be done on a daily basis by adding any irrigation or precipitation and subtracting the crop water use for the day. Based on the calculation, it is possible to know how depleted your soil is and if irrigation is required. The main concern of the checkbook method is that it does not work properly when significant within-field variability which results in over-irrigation (Vellidis et al., 2016).

4. Crop growth modeling to assess deficit irrigation strategies

Since the 1970s, the use of crop growth simulation models in agriculture has been a powerful strategy to yield prediction under different management and environmental scenarios. Crop growth models are able to simulate and evaluate for example the effects on crop growth and yield under climate change, increases in CO_2 concentration and temperature as well as different management practices such as fertilization, seed rates, tillage systems, and different irrigation strategies. Considering different management scenarios, some of the objectives of crop

growth simulation modeling are to reduce risks, increase crop yield and profitability by choosing the most assertive management for the current environment condition (Yadav et al., 2012). Different crop models are available for the evaluation of water management and irrigation strategies. The most commons models are the Environmental Policy Integrated Climate (EPIC), Decision Support System for Agro-Technology Transfer (DSSAT), CROPWAT, USDA-ARS Root Zone Water Quality Model (RZWQM). Ko et al. (2009) evaluated the EPIC model to determine crop yield, water use efficiency and to simulate the variability in crop yields under different irrigation management for corn and cotton. They concluded that EPIC model is useful as a tool for irrigation decision support for crops in South Texas and to achieve the maximum crop yield it was required 700 mm of water input and 650 mm of ETc. Ma et al., (2003) evaluated RZWQM model to simulate yield response and growth for corn in northeastern Colorado under different levels of irrigation. They concluded that the model can be used as a tool to simulate different irrigation scenarios to optimize water management. Saseendran et al., 2015 evaluated different deficit irrigation strategies for corn in Colorado and concluded that initiating irrigation at 80% of soil water depletion resulted was the best strategy to increase net returns.

Decision of irrigation timing or soil water depletion thresholds to initiate irrigation and amounts could be supported by the use of crop growth simulation models. Most times farmers are looking for decisions that balance agronomy and profitability. The best irrigation threshold usually does not represent the most profitable scenario due to the costs of irrigation and crop prices. Kisekka et al. (2015) investigated the optimum plant available water threshold to initiate irrigation that maximizes net returns using CERES-Maize (DSSAT). Their results showed that 50% of soil water depletion was the best plant available water depletion threshold that maximized net returns considering corn price and costs to run the irrigation system. Crop growth

simulation models are a powerful tool in studying irrigation water management under multiple biotic and abiotic conditions. Several studies have shown one strategy does not fill all; therefore , it is necessary to be careful in implementing the same strategy for different fields and/or regions because differences in variety, hybrids, soil type, climate, size of the field and irrigation system capacity influence the decision of when to initiate irrigation.

5. Management Zone Delineation

The differences in crop yield in agricultural fields are driven by a combination of several factors such as soil type and fertility, topography and soil compaction (Fridgen et al., 2004). These factors can change drastically even within the same field and independently of field size (Koestel et al., 2013). Farmers recognize the impact of the field variability in the potential crop yield and they are seeking new management practices to implement in order to increase their profitability (Pinter et al., 2018). Areas in the field that have homogenous characteristics (terrain attributes, soil properties, fertility and yield) should be grouped as the same site-specific zone. The site-specific zones are called management zones (MZ) (Fraisse et al., 2001). The objectives of delineating MZs are to increase crop productivity, reduce environmental issues and increase nutrient and water use efficiency (Lowrance et al., 2016). The selection of the variables that will be used for zone delineation is an important step, but this selection should consider the problem being addressed (e.g., nutrient, water, pesticide).

Each MZ should receive different irrigation rates to increase water use efficiency, decrease under or over-irrigation and increase nutrients efficiency. Soil properties are one of the most important factors affecting plant available water and, therefore, key factors for irrigation management and zone delineation. Each soil type has its own properties and these properties are important for irrigation management decisions. The soil texture is determined by the content of

soil particles of different sizes and it varies from sandy soils (large particle sizes) to clay soils (small particle sizes). Based on the United States Department of Agriculture (Soil Survey Staff, 2014), there are a total of 12 soil texture classification (sand, loamy sand, sandy loam, sandy clay loam, sandy clay, loam, silt loam, clay loam, silty clay loam, silt, silty clay, clay). Two key factors influencing irrigation water management are linked to soil texture, soil water holding capacity and water infiltration rate through the soil profile. Sandy soils are characterized by having low soil water holding capacity and rapid water movement through the soil profile. Meanwhile, clay soils have high soil water holding capacity and much lower infiltration rate than sandy soils. These differences in soil properties are important when characterizing field variability and delineating irrigation management zones.

A good field measurement to describe the variability related to soil properties is the soil electrical conductivity (EC_a) (Yan et al., 2007). The soil EC_a has been identified as a surrogate data for soil salinity, clay content, cation exchange capacity (Sudduth et al.,2001), soil water holding capacity and plant available water (McNeill, 1992). There are two commercial sensor types to measure soil EC_a, the contact sensors and non-contact sensors. The contact sensor, or electrode-based, is produced by Veris Technologies in Salina, Kansas which have two available sensors Veris 3100 and 2000XA. These type of sensors vary from four to six disks in the equipment that penetrates the soil and act as electrodes. One pair of disk induces a current in the soil and the other one or two pairs measures the change in voltage that is used to calculate a value for apparent soil resistivity and converted to EC_a (Sudduth et al., 2013). The Veris 3100 has six disks and measures soil EC_a from 0-30 cm (shallow) and 0-90 cm (deep), and the 2000XA measures at 30 cm with four disks. The second type of sensor (non-contact) uses an electromagnetic induction (EMI) that does not require contact between equipment and soil. The

sensor that is most used for agricultural measurements is the EM38 which is produced by Geonics Limited of Mississauga, Ontario – Canada. The EM38 represents the total EC_a in 1.5 m depth. This type of sensor has two coils, one is the transmitter coil and the other is the receiver coil. The transmitter sends an electric current in the soil that induces a response that is measured by the receiver. The strength of the induced magnetic is converted to the apparent electrical conductivity of the soil (Stanley et al., 2014).

Soil EC_a is a measurement that is relatively easy to obtain and is highly correlated to crop yield. The correlation with yield is mainly explained by the differences in soil water holding capacity which is the major factor that affects crop yield (Grisso et al., 2009). This measurement is useful not only for MZ delineation for variable rate irrigation, but also for variable rate fertilization and seeding (Wang et al., 2003; Jeschke et al., 2012; Anderson-Cook et al., 2002).

Topography attributes have also been used for irrigation MZ delineation due to the correlation with crop yield, soil water movement and availability (Fraisse et al., 2000; Maestrini and Basso, 2018; Kravchenko and Bullock, 2000). Changes in field terrain can be measured using several methods such us farm vehicle's equipment real-time kinematic global positions systems (RTK GPS), GPS mounted on drones collecting field images, or Light Detection and Ranging (LIDAR) digital elevation models. The most common and easy way to collect terrain elevation data is through the use of any farm equipment with a RTK GPS. The terrain elevation data can be processed to obtain other terrain attributes like slope, curvature, wetness index and drainage lines that are useful to characterize water movement and accumulation (Miller et al., 2014). Several studies have investigated the relationship between terrain elevation and yield. Typically, in dry years, locations with higher slopes usually have less available water and lower yield in comparison to areas with low slopes (Kaspar et al., 2004). Kravchenko and Bullock,

2000 found that topographic attributes such as elevation, slope, curvature and flow accumulation explained about 20% of yield variability and combining this parameter with soil properties explained 40% of grain yield variability. Kaspar et al., 2003 found that a multiple linear regression using elevation, slope and curvature explained 78% of the corn yield spatial variability over 4 years and they concluded that terrain attributes were a good tool for management zone delineation. Da Silva and Alexandre (2005) found that the wetness index had the highest correlation with yield and concluded that this index could be used for management zone delineation. The same results found by Miller et al., (2014) concluded that topographic position index could be a source for management zone delineation.

Remote sensing imagery has increasingly been used for the management zone delineation of agricultural fields (Varvel et al., 1999). This increase has been related to a low cost to obtain and process the data (Schepers et al., 2004). The remote sensing imagery can provide information about crop stress through the reflectance properties of the leaves, vegetation indices, crop canopies and spectral reflectance properties of soils (Pinter et al., 2018). This type of information is relevant to characterize the field variability with a different perspective and is useful to delineate management zones, not only for irrigation, but also for fertilization and seeding rates.

6. Variable Rate Irrigation (VRI)

Variable rate irrigation is a technology developed to increase irrigation efficiency. This technology gives farmers the ability to apply different irrigation rates across a single field, therefore addressing the spatial and temporal variability of the soil and terrain that influence soil moisture and yield (Sui and Yan, 2017). Variable rate systems are most commonly used in center pivot irrigation systems.

Although VRI technology has been available for decades, farmers have not widely adopted it. The reasons for the low adoption could be related to inexpensive water cost, difficulty prescribing different rates for different parts of the field, lack of water regulation (Cook, 2015), and high costs to implement the technology (Evans et al., 2013). However, in recent years the pressure of population increase and the decrease of groundwater levels has increased the environmental pressure for adopting the best irrigation management practices that can reduce water use and increase irrigation water use efficiency (Khan et al., 2006).

For variable rate irrigation to address the spatial and temporal variability of crop water needs, it is necessary to first to identify and quantify the sources of the within-field soil's plant available water variability because those will constitute the basis of irrigation prescription maps. These prescription maps could be represented by zones with different crop water needs.

Delineation of field management zones that describe features influencing spatio-temporal variability of plant available water and crop growth is key to VRI implementation and impact. The VRI systems will be able to apply different irrigation rates while meeting crop water needs and replenishing soil water storage over each management zone. Speed control and zone control are currently the two variable rate control methods used on VRI systems (LaRue & Evans, 2012). The variable rate speed control method modifies the travel speed of the center pivot irrigation system to change the irrigation rate over an area. The higher the speed, the lower the irrigation rate and vice-versa. The speed control system is less expensive and easier to implement. However, this system can only vary the application in the travel direction of the pivot. The variable rate zone control method is able to control individual sprinklers or groups of sprinklers. This method allows the pivot to control the time each sprinkler will be on and off to achieve the irrigation rate prescribed. This method is more flexible and efficient in applying

water to non-uniform shape areas of the field resulted from variable soil properties, terrain changes, and growth (Yang et al., 2016). Although this method provides more advantages compared to the speed control, this method is more expensive due the cost of valves, nozzles and software to run the system (Cook, 2015).

Variable rate irrigation has several environmental, economic and agronomic benefits. One of the most important benefits of VRI systems is the potential to reduce or increase the amount of water applied during the growing season over specific parts of a field and therefore, increasing water use efficiency. Sadler et al., (2005) reduced 8 to 21% water using VRI over three seasons of corn. A similar result was found by Irmak et al., (2012) that estimated a 33% of water savings over two seasons of corn. Decreasing the amount of water applied in the crop season can lead to energy savings and reduction in labor costs (Perry et al., 2012). In addition, the potential of water savings can be higher if the non-cropped area is located inside of the field (Sadler et al., 2005) or overlapping between two center pivots. As far as agronomic benefits, VRI can potentially favor yield gains, reduce the risk of nutrient leaching and runoff issues. All the agronomic benefits will have a direct impact on profitability due to the high nutrient use efficiency, potentially higher yields and lower cost of energy to run the irrigation system.

RESEARCH OBJECTIVES

The thesis was focused on irrigation. Two fields located in Tanner and Town Creek, Alabama were used for the two chapters of this thesis. This thesis covered only portion of the work realized in both fields. In both locations, the use of variable rate irrigation (VRI) technology was used to compare with farmers uniform irrigation practice. Part of this project was related to train farmers and crop consultants the steps necessary to implement the variable rate irrigation system and irrigation scheduling tools. Because of this reason, farmers focus groups were created for

each field. Two group of neighbor farmers were invited to participate of the trainings and discussion about results and to listen from farmers their experiences. Meetings were realized before and during the growing season during 2018 and 2019 to demonstrate to farmers the benefits of using VRI and soil sensors.

In order to implement variable rate irrigation, irrigation management zones (MZ) were delineated. The delineation considered several sources of data such as crop yield data from previous years, soil properties, topographic indices and features, apparent soil electrical conductivity and satellites images. Based on the MZ, soil sensors were installed in the field to monitor soil water tension. A total of 31 sensors were installed in Town Creek and 21 in Tanner in both years. The field was divided in strips trials that covered the different irrigation management zones. The soil sensors monitored the changes in soil water content for both treatments (farmer and VRI). The irrigation scheduling was done through the calculations using the data recorded from the soil sensors.

During the two years of this project, it was clear that farmers required more training related to irrigation time and rate. The project also demonstrated to the farmers that based on the field variability, it was necessary to change irrigation rates throughout the field to meet the variability, crop water needs and soil water holding capacity. By changing the rates, water could be saved, decrease the runoff problems, nutrients leaching and increase the profitability. In Town Creek field, the farmer had 7 hectares of non-crop areas in the middle of the field. The VRI system was able to turn off the water in these locations and in 2019, a total of 6 million liters of water were saved just by turning off the nozzles where irrigation was not needed.

Farmers were able to understand and check daily the sensor information, to detect issues and to realize how they could improve irrigation based on the knowledge acquired during the two years working with the Precision Ag. Team from Auburn University.

Therefore the objectives of this study were:

1. Identify a terrain attribute or a combination of terrain attributes and soil properties that explains the variability in soil water content to delineate irrigation management zones
2. Calibrate and validate a crop growth model for the North Alabama conditions
3. Identify the best deficit irrigation strategy to initiate irrigation and the best irrigation rate

II. EVALUATION OF TERRAIN ATTRIBUTES AND SOIL PROPERTIES TO CHARACTERIZE SOIL WATER CONTENT VARIABILITY FOR IRRIGATION MANAGEMENT ZONES DELINEATION

Abstract

Differences in soil characteristics and topography is the most common factor that affect soil water availability for crops. The use of variable rate irrigation (VRI) allows farmers to apply different irrigation rates, to meet soil and crop needs and to improve the impact of the terrain attributes in soil water content and crop yield. The implementation of VRI systems required to identify and quantify the within field variability in terms of soil, topography and crop yield. Management zones need to be delineated to potentially receive different irrigation rates during the growing season to meet the field variability. The objective of this study was to identify which terrain attribute, or combination of terrain attributes and soil properties that better explains the variability in soil water content in a crop field and therefore, can be used for irrigation management zone delineation. The study was conducted in two fields located in Town Creek and Tanner, Alabama in 2018 and 2019. Both fields were irrigated by a center a pivot irrigation system that covered 120 and 24 hectares respectively. Soil water content changes were assessed by installing soil water tension sensors at 15, 30 and 60 cm soil depths at different location across the field. The soil sensors recorded the tension data every hour since the V4 growth stage until physiological maturity and tension values were converted to volumetric water content. Topographic wetness index (TWI), topographic position index (TPI), elevation and slope were calculated as terrain attributes. Apparent soil electrical conductivity was collected in Tanner and clay, silt and sand in Town Creek to characterize the soil properties. Principal component analysis was used to identify patterns and to reduce the dimensionality of the volumetric water content data set. A correlation analysis between scores of the principal components retained in the analysis with terrain attributes and soil properties were used to identify which parameter had significant correlation. The results showed that for both fields and years, three principal

components were able to explain more than 95% of the variance of the original data set. The PC1 demonstrated spatial variability and explained well all the variances of soil water content for all depths for both fields. At Tanner field, PC1 was significant correlated with TPI for both years and in Town Creek, with TWI, slope and sand content in 2018 and TPI in 2019. The PC2 and PC3 had effect of temporal variability in both location and years. The PC2 was significant correlated with Elevation, TWI and slope at Tanner in 2018 and TWI, clay and silt in 2018 and only elevation in 2019 at Town Creek field. The results showed that for different locations, the terrain attribute that explained the variability in soil water content was different. Although for both fields TWI and TPI were significant with the first principal component, which explained most of the variance in soil water content. These two indices could be used for farmers and crop consultants to delineate irrigation management zones to use for variable rate irrigation, to increase water use efficiency and maximize net returns.

INTRODUCTION

Irrigation adoption in the USA is continuously increasing. In the past 15 years, an increase of 5% in the total irrigated land has been reported (NASS, 2017). While the southeast USA only represents 10% of the USA total irrigated land, irrigation land in states like Alabama increased by 25% from 2012 to 2017 and currently has 57,465 hectares irrigated that represents 5% to the total farmland (NASS, 2017). Irrigation expansion in the USA has continued in part because irrigation help farmers achieving higher crop yields by avoiding crop water stress. Although irrigation is being considered by farmers as a risk management tool, the water used for irrigation corresponds to approximately 70% of the available freshwater (Liakos et al., 2018). This demand for water along with the population growth, climate change, and the lack of good water management practices by farmers, suggest the need for adoption of practices that increase irrigation water use efficiency (WUE) (FAO, 2018).

Irrigation strategies such as irrigation scheduling and variable rate irrigation (VRI) are available now and allow farmers to increase WUE. The VRI technology has the ability to apply different irrigation rates over the landscape allowing farmers to address the spatial and temporal variability on crop fields which affects soil moisture and crop yield (Sui and Yan, 2017). This technology has been available for many years but the adoption is still low due to the inexpensive water costs, lack of water regulation and complexity for farmers to operate. The main goal of VRI is to increase WUE through the application of the right water rate at the right place, reduce energy cost through the increased efficiency of water application then, maximizing crop yield and profitability. Perceiving the full benefits of the VRI approach, addressing the spatio-temporal charges of crops water needs through site-specific irrigation, require first the identification and quantification of the spatial variability of crop fields and estimation of how those features

influence crop water availability. Areas within the field that have homogenous landscape and soil properties should be grouped as a single area or management zone (MZ). The goal of the MZ delineation is to have areas that differ between each other in terms of field variability but homogenous within the same MZ. The number of management zones changes from year to year due the weather differences and crop planted (Fraisse et al., 2000). The MZ delineation has been the first step toward optimization of input application which could increase crop yield, reduce environmental issues and increase nutrient, pesticide, fungicide, and water use efficiency (Fridgen et al., 2004; Lowrance et al., 2016; Ortiz et al., 2011).

There are many approaches to delineate management zones. These approaches vary in terms of the type of information relevant to describe within-field variability and which of them are needed to consider. Usually, what many researchers use as data for zone delineation correspond to soil properties, crop yield, or topography (Fraisse et al., 2000; Li et al., 2008; Reyes et al., 2019). As far as irrigation water management and VRI, the within-field variability in crop growth, soil and topography are strongly related to irrigation needs (Haghverdi et al., 2015; Maestrini and Basso, 2018; Yari et al., 2017), therefore these layers of data are key to irrigation zones delineation because indicate areas that could receive different rates of water.

As far as soil properties, soil texture, soil structure, soil infiltration and soil depth affect soil water holding capacity and the availability for plants. There are many methods available to characterize soil variability but three basic approaches have been widely used (Fraisse et al., 2000). The first is the use of the soil surveys (SSURGO) generated by the National Cooperative Soil Survey (NCSS), which is a free source available but its spatial resolution is low for precision agriculture applications. The second method is the collection of georeferenced soil samples for soil analysis and generation of a surface map from the interpolation of data. The

downside of this method is the high number of data points needed to produce an accurate map, which then could increase labor costs and time. The third method of characterization of soil variability using apparent soil electrical conductivity (EC_a) mapping. This measurement provides information of soil salinity, clay content, cation exchange capacity (Ortiz et al., 2011), soil water holding capacity and plant available water (Ortiz et al., 2011) . The EC_a data has shown a good relationship with crop yield and therefore, it is useful for MZ delineation (Reyes et al., 2019; Schepers et al., 2004; Kitchen et al., 2003). Chiericati et al., 2007 also suggested that the use of EC and multispectral radiometer with eight narrowband wavelengths (460-810mm) data could be an efficient and cost-effective approach for irrigation MZ delineation.

Besides the soil properties, the topography is one of the most important factors used to characterize soil water content variability and plant available water (Robert et al., 1996). The topography is the main responsible factor that affects water availability for plants due to the horizontal and vertical movement. Terrain attributes have been widely used for MZ delineation (Fridgen et al., 2004). Different topographic indices can be generated to characterize soil water content variability on a crop field. The most common topographic indices used to describe field variability are elevation, slope, curvature, topographic position index, and topographic wetness index (Huang et al., 2008; Maestrini and Basso, 2018; Moore et al., 1993). Digital elevation models can be processed from different sources such as elevation data collected by farmers grain combines equipped with Real-Time Kinematic (RTK) GPS systems, existing soil maps (Reyes et al., 2019), or high-resolution LiDAR data (James et al., 2006). Terrain attributes affect directly crop yield through their effect of soil development, soil erosion, soil deposition, and soil water movement and accumulation (Kaspar et al., 2003). Areas in the field located in lower slopes often receive water from higher positions and it can result in higher yield in dry years (Maestrini

and Basso, 2018). Elevation was found to have the most influence on soil water content and crop yield in Illinois and Indiana (Kravchenko and Bullock, 2000). Kaspar et al. (2003) concluded that elevation, slope, profile curvature, and plan curvature combined along with crop yield data helped to identify spatial yield patterns and this data was useful for management zones delineation. Miller et al. (2014) concluded that topographic wetness index (TWI) and soil EC_a might be used to explain crop yield variability and could be considered for MZ delineation. Jiang and Thelen (2004) found that slope showed a high correlation with crop yield and soil moisture.

The success of a VRI practice will depend on how accurate the MZ-based irrigation prescription map represents the within-field variability of soil plant water available. Several layers of soil properties and topographic indices could be considered for MZ delineation; however, statistical analyses should be used to identify the most important or a combination of layers that best describe the field variability. Fraisse et al., (2000) used principal component analysis to identify the most important variables that described the field variability. Fridgen et al., (2004) and Yari et al., (2017) delineated management zones using the fuzzy c-means unsupervised clustering procedure. Kravchenko and Bullock, (2000) used Pearson correlation to determine the correlation between corn and soybean yield with topography and soil properties for management zones delineation.

The objectives of this study were (1) to apply principal component analysis to reduce the dimensionality of the volumetric water content data set and (2) correlate the scores of the principal components with terrain attributes to identify which terrain attribute or attributes that best explain volumetric water content variability that could be potentially used in irrigation management zones delineation at two fields in Alabama.

MATERIAL AND METHODS

Site Description

The study was conducted at two farms located in Town Creek (34º 43’ 6.67” N, 87º 23’ 13.52” W, 181 m above sea level) and Tanner (34º 41’ 30.6” N, 87º 0’ 54.63” W, 203 m above sea level), Alabama during 2018 and 2019 crop growing season.

The predominant soil type at the Tanner field was a Decatur silty clay loam with 2 to 10 percent slope, and the elevation changes that ranged from 180 to 191 meters. The field was 44 hectares in size with 24 hectares irrigated by a Valley© center pivot (Valmont Irrigation, Valley, Nebraska) irrigation system of 284 meters length. The historic average precipitation during the corn growing season, April to August, at this location is 485 mm. During the season in 2018 and 2019, the total precipitation was above the historic average with a total of 650 mm and 600 mm, respectively. However, the precipitation was below the historic average in July (-26 mm) and August (-15 mm) of 2018 and May (-15 mm) and June (- 40 mm) of 2019 (Figure 1.1).

For the Town Creek field, the predominant soil type is a Decatur silty clay loam however, soil texture across the field varies from silty clay loam to clay with 2 to 10 percent slope variation, and elevation ranges from 169 to 180 meters. The field was 190 hectares in size with 125 irrigated hectares under a Reinke© center pivot irrigation system of 623 meters length. The historic average precipitation during the growing season, April to August, for this location is 520 mm. For 2018 and 2019, the total precipitation was above the historic average with a total of 640 mm and 590 mm, respectively. Even though growing season precipitation was above historic values, in 2018 the precipitation was below the historic average for the months of July (-72 mm)

and in 2019, May (-28 mm), Jun (-17 mm) and August (-40 mm) precipitation was below average (Figure 1.2).

In 2018, both fields were cultivated with corn planted at 0.76 m spacing between rows and population around 84,000 plants per hectare under the center pivot irrigation system. In 2019, the Town Creek field was cultivated with corn again and the Tanner field was planted with cotton at 0.96 m row spacing and plant population of 111,000 plants per hectare. These two study fields represent two different irrigation farming scenarios in north Alabama, either large cropped field or small rolling terrain fields.

Monitoring the volumetric water content

The soil water content, in both sites, was monitored using a wireless soil sensor probes that measure soil matric potential (Watermark®). Each soil sensor probe is composed of three Watermark® sensors arranged vertically to measure soil matric potential at 15, 30 and 60 cm soil depths and a thermocouple at 30 cm. The soil probes were connected to a circuit board and a radio transmitter that was sending the data to a laptop computer installed outside of the field. The laptop was connected into an online server that allowed fully remote access to the soil tension data. The sensors were recording soil matric potential very hour starting 30 days after planting and until the crop physiological maturity.

This type of soil matric potential sensor measures the electrical resistance by two electrodes installed inside of the sensor. The resistance value is then converted into tension values expressed in Kilopascal (kPa) using the equation developed by Shock et al. (1998):

$$\Psi(\Omega) = -\frac{(4.093 + (3.213 * k\Omega))}{1 - (0.009733 * k\Omega) - (0.01205 * T_s)} \quad (1)$$

where

$\Psi(\Omega)$ is the soil matric potential in kPa; $k(\Omega)$ is the resistance value; T_s is soil temperature in ºC.

The soil water tension indicates the strength that the plants need to exert to extract water from the soil (Irmak et al. 2014). The higher the tension value is, the lower is the volumetric water content and vice-versa.

Soil water tension was converted into volumetric water content through the use of five soil water retention curves (SWRC). Those curves were generated from soil samples collected at each field from locations near to each soil sensor location used for this analysis. Undisturbed soil samples at 15, 30 and 60 cm were collected and analyzed for determination of soil water characteristic curve using the Hyprop® 2 sensor (METER Group- Pullman, WA). The permanent wilting point was determined using disturbed soil samples in the WP4 sensor (METER Group- Pullman, WA). The parameters from each SWRC were determined and the Van Genuchten equation (2) was used to convert soil matric potential into volumetric water content.

$$\theta(\psi) = \theta_r + \frac{\theta_s + \theta_r}{[1 + (\alpha|\psi|)^n]^m} \quad (2)$$

where

$\theta(\psi)$ is the soil volumetric water content (cm^3/cm^3); θ_r is residual water content (cm^3/cm^3); θ_s is saturated water content (cm^3/cm^3); α is related to the inverse of the air entry suction (cm^{-1}); $|\Psi|$ is suction pressure (cm of water); *m* and *n* is the empirical shape-defining parameters (dimensionless).

The soil sensors were installed between plants, and at different locations (Figures 1.3 and 1.4) within the center pivot area that covered most of the field variability in terms of soil, crop yield and topography. The fields were delineated in different irrigation management zones using different sources of information such as historic crop yield maps, elevation, and soil properties.

Both fields had three different irrigation management zones (MZ) (Figure 1.5). The management zone, one for both fields, was considered the highest yield zone, zone two the intermedium and zone three the lowest yield zone. At the Tanner field, MZ 1, 2, and 3 had 14, 5.5, and 4.5 hectares, respectively. At the Town Creek field, MZ 1, 2, and 3 had 35, 50, and 35 hectares.

Volumetric soil water content collected at both study fields comprised the core of the data used in this study. In 2018, volumetric water content data collected at 17 different days from 16 probes installed at the Town Creek field and 24 different days recorded from 12 probes installed at Tanner field were selected for these analyses. In 2019, data collected at 23 different days from nine probes in the Town Creek field and 29 days from 11 probes installed at the Tanner field were selected. The measurement dates were selected based on three days after precipitation events during the growing season, where the entire field received a uniform amount of water. This criteria for data selection might ensure that the differences on soil water content were driven mainly by water movement, lateral and horizontal, influenced by terrain attributes. The data selected corresponds mainly to dates during the growth periods that correspond to high water use. Terrain attributes explaining variability in volumetric water content during those periods will be more useful for irrigation zone delineation. In 2018, dates in the months of June and July from both fields were analyzed due to the frequent and precipitation period that occurred during the growing season and because of that period corresponded to high water demand for the corn crop. In 2019, date from the same months, June and July, were selected for Town Creek corn planted field and July and August dates for Tanner cotton planted field.

Assessment of Field Terrain Attributes

Two topographic features and two topographic indices were analyzed to determine which terrain attribute or a combination of attributes could explain the volumetric water content variability in both fields. The topographic data analyzed were elevation, slope, topographic position index (TPI) and topographic wetness index (TWI).

The elevation is one of the most commonly used attributes for interpretation of yield, water movement, and surface runoff (Kitchen et al., 2003; Kaspar et al., 2003; Jiang & Thelen, 2004). The elevation data for this study was obtained for both sites from the StarFire™ 6000 GPS system installed on each John Deere© grain combine. This system works as real time kinematic (RTK) GPS and provides a high horizontal and vertical accuracy of 5 and 2.5 centimeters respectively. Moreover, farmers use the same GPS unit during precision planting, fertilization, chemical application, and harvest. The elevation data was recorded when the farmer's combine was harvesting the field. The data was downloaded and processed using a QGIS Geographic Information System (version 3.8.1).

A digital elevation model (DEM) with 6.5 meters resolution was generated from the elevation data through the kriging interpolation method using ArcMAP™ software (version 10.3.1) by ESRI®. The slope of the terrain, TPI and TWI were processed from the DEM and generated using the System for Automated Geoscientific Analyses (SAGA) version 2.3.2.

The topographic wetness index (TWI) has been related to soil moisture and sediment transport processes (Moore et al., 1993; Radula et al., 2018). The TWI describes areas that potentially have higher or lower water accumulation based on the landscape position (Da Silva and Alexandre, 2005; Qin et al., 2011). High values of TWI indicate high water accumulation, high water content and lower slope. In contrast, low TWI values indicate low water

accumulation, low water content and higher slope. It is known that there is a high correlation between crop yield, topography and plant available water during the growing season. Da Silva and Alexandre (2005) found that TWI showed a high correlation with yield when compared to other topographic indices. Same results found by Maestrini and Basso (2018) proved that areas on the field allowing right water accumulation, neither runoff nor waterlogging, exhibiting high TWI values, resulted in high crop yield. Topographic wetness index (TWI) was calculated as defined by Moore et al. (1993):

$$TWI = \ln\left(\frac{A_s}{tan\beta}\right) \quad (3)$$

where

A_s is the specific catchment area (m^2m^{-1}) and β is the slope angle (degrees).

Topographic position index (TPI) measures the difference in elevation of a central point (z) and the average elevation ($\bar{z}$) of neighboring points around it separated by specific radius (R) (Mieza et al., 2016). This index is calculated as:

$$TPI = z_0 - \bar{z} \quad (4)$$

$$\bar{z} = \frac{1}{n_r} \sum i \in R^{z_i} \quad (5)$$

where z_0 is the central point and $\bar{z}$ is the average elevation around the central point.

TPI values can be positive or negative. Positive values mean that the central point or selected point is at a higher elevation than the average of the neighborhood cells, while negative

values are locations with elevation lower than the surrounding cells. According to Ali et al. (2013), TPI can be used to identify is a point is on a hilltop, a valley bottom, an exposed ridge, or another topographic feature over an area. TPI also can have values close to zero, which represent flat areas or areas with constant slopes within the radius used for the TPI estimation. This index has been used for studies related to geomorphology, geology, hydrology, agricultural science, risk management and climatology (De Reu et al., 2012). Among agriculture and water movement studies using TPI, Mieza et al. (2016) concluded that TPI performed better to characterize field variability than topographic maps for management zones delineation applied to operational applications in agriculture.

The other topographic data included in this study was the slope of the terrain, which refers to the angle of inclination in comparison to the horizontal. The slope is also related to water movement and has a high impact on crop yield (Kravchenko and Bullock, 2000). The slope in this study was considered in percentage, which is calculated based on the changes in elevation in meters considering a horizontal distance of 100 meters.

Assessment of Soil Properties

The soil information was assessed for both fields in 2018. At the Tanner field, the apparent soil electrical conductivity (EC_a) was collected to assess the soil variability. The EC_a has been identified as a surrogate data for soil salinity, clay content, cation exchange capacity (Sudduth et al.,2001), soil water holding capacity and plant available water (McNeill, 1992). The EC_a data was collected using the Veris 3100 equipment produced by Veris Technologies in Salina, Kansas. The equipment has six number of disks in the equipment that penetrates the soil and act as electrodes. One pair of disk induce a current in the soil and the other two pairs measure the change in voltage that is used to calculate a value for apparent soil resistivity and

converted to EC_a (Sudduth et al., 2013). The EC_a was assessed at shallow layers and deep layers. The shallow layer corresponds to 0-30 cm and the deep layers from 0-90 cm.

At Town Creek field, only soil texture was collected and analyzed for soil properties. A sample at 15, 30, and 60 cm were collected at each soil sensor location. The samples were sent to a commercial laboratory to quantify the total percentage of clay, silt, and sand.

Statistical analysis

The principal component analysis (PCA) is a multivariate statistical technique that facilitates the analysis of multiple variables at the same time. It transforms a data set of correlated variables into a small linearly independent variables, principal components (PCA) (Martini et al., 2017). The objectives of this method are dimension reduction and interpretation. The linear transformation reduces the original dimensions of the data set that contains all the variability into a few newly generated variables called principal components (PC). These principal components are orthogonal and uncorrelated and they represent most of the information using reduced dimensions of the data rather than the original data set. The assumptions for the PCA are there are a correlation between the variables, large data set and suitable for data reduction.

The principal component analysis was used to reduce the dimensionality of the data and to interpret the variance of spatial and temporal patterns of volumetric water content. In 2018, volumetric water content comprised data collected from 16 sensors on 17 different measurement dates at the Town Creek field and 12 sensors on 24 measurement dates at the Tanner field. In 2019, volumetric water content data from nine sensors on 23 measurement dates at the Town Creek field and 11 sensors on 29 measurement dates at the Tanner field were selected for

analysis. Based on this, the matrix *m* x *n* was constructed for PCA, where *n* was the volumetric water content at three different depths and dates (dates x three depths), and *m* was the number of sensors included in the analysis. In 2018, the matrix was 12x72 for the Tanner field and 16x51 in Town Creek. In 2019, the matrices were 11x87 and 9x69 for Tanner and Town Creek, respectively. The PCA was conducted using R software package (R Core Team, 2019). Loadings, scores, and variances of each PC were analyzed and interpreted. The loadings determine the importance and contribution of each variable of the data set in the principal component being analyzed. The scores are considered the transformed variable values in the new coordinate system. The variance explained by each PC is the fraction of the variance explained by the PC over the total variance. The first principal component carries the highest variance, the second PC the second highest and so on.

The next step in the analyses was to evaluate the spatial terrain attributes and soil characteristics and their relationship with volumetric water content variability within each field. Topographic features and indices (TPI, TWI, elevation and slope), EC_a (Tanner), and percentage of clay, silt and sand (Town Creek) were correlated with the scores of the principal components that explained most of the variance in the original data set. The Spearman's rank correlation method was used for the correlation analysis (Spearman, 1904).

RESULTS AND DISCUSSION

Volumetric Water Content Variability

In 2018 and 2019, the number of soil sensors installed in the Tanner field was 12 and 11 and in the Town Creek field 16 and 13, respectively. The sensors were installed on locations that will cover most of the soil and terrain field variability. Both study fields exhibit changes in field terrain that might influence soil water movement and therefore volumetric water content. Figure

1.3 and Figure 1.4 shows the topographic features, topographic indices, and soil sensor locations for Tanner and Town Creek fields, respectively.

In the Tanner field, the TPI values ranged from -2.17 to 1.92. The negative values for TPI are related to areas in the field that are in low elevation positions when compared to the neighboring cells. The low elevation positions correspond to the areas where water will move into and potentially water accumulation occurs. In contrast, the TWI values ranged from 0.29 to 8.10. High TWI values correspond to the wettest areas in the field. The low values for TWI also show the areas where water infiltration will be low and consequently potentially dry when compared to high TWI values (Qin et al., 2011). The average values for the topographic features, topographic indices, and apparent soil electrical conductivity for each soil sensor location are shown in Table 1.1. Two examples of how these topographic characteristics will influence soil water content and movement are as follow. Soil sensor five and sensor nine were installed in two contrasting locations of the field. The soil sensor location five was installed in a location with a high slope value (4.21%) and TPI (1.19) and the lowest TWI (2.58). In contrast, soil sensor location nine was installed in a location with a low slope value (3.87%), low TPI (-0.90) and high TWI (3.42). These two contrasting locations showed that sensor five was located at a dry area in the field and the soil sensor nine was located in a wet area. The differences in soil water tension between both soil sensor locations are shown in the Figure 1.6. The higher the tension value is, lower is the volumetric water content and vice-versa. The soil sensor five showed higher tension values throughout the growing season when compared to sensor nine. Sensor nine did not achieve tension values higher than 100 kPa, meanwhile sensor five achieved values of 200 kPa. Those differences in soil water tension and the different characteristics of these

locations with respect to TWI, TPI, and slope values suggest that geographic data could be a good tool to determine areas in the field with different irrigation requirements.

The slope of the field ranged from 0.5% to 7.0% and elevation from 180 m to 191 m. The elevation data has been used for many researchers to characterize the differences in topography (Kaspar et al., 2003) and used to delineate irrigation management zones. The problem using only elevation as topography source is that elevation alone is not able to capture the detail of the field variability. In the field, the same elevation can represent two different contrasting areas. For example, soil sensor three and six (Figure 1.3 – C) shows almost the same elevation but the slope is almost the double (Table 1.1). Therefore, the volumetric water content in these two different locations was different during the growing season.

At the Town Creek field, the TPI ranged from -1.93 to 2.06, TWI from 4.84 to 17.88, elevation from 168 m to 180.45 m and slope from 0.5% to 8.8% (Figure 1.4). There were sensors installed in contrasting locations in respect of different TPI, TWI, elevation and slope as described as in Tanner Field. The values for the topographic features, indices, and soil texture for each soil sensor location for both years are shown in Table 1.2. For example, the differences in soil water tension between soil sensor six and soil sensor 19 are shown in Figure 1.7. The soil sensor six had low TPI (-0.16) and slope (1.74%), and high TWI (11.43) when compared to location 19 that had the greatest TPI (2.98) and slope (4.79%) and lowest TWI (6.85). The differences in soil water tension show that sensor location 19 achieved higher tension values during the growing season, which means less water content and dry conditions compared to location five. The sensor five did not reach values higher than 70 kPa for all soil depths during the entire growing season. However, location 19 had values of 200 kPa for 15 cm and high values for 30 and 60 cm. The topographic features and topographic indices could be also a guide

to understand the soil water content at deep layers. High slopes increase the chances of water moving in a lateral orientation and decrease the soil water infiltration (Huat et al., 2006). Sensors located in high values of slopes (sensor 19) showed high soil water tension values in deep layers which means that water was not infiltrating to these layers due to the lateral movement. This information is important to characterize the field variability, especially for irrigation management zones delineation.

Principal Component Analysis

The results of the principal component analysis for each location and year are presented in Table 1.3 and 1.4. There is not a fixed rule to determine the number of PCs that have to be retained. However, many researchers consider the PCs to be retained that demonstrate eigenvalue higher than one, as proposed by Kaiser (1960). Another method used is to consider the principal components that explain most of the variance. In this research, the first three principal components (PCs) for both locations and years were selected for further analysis based on the high variance explained by them. At the Tanner field, PC1 was able to explain alone 96% and 93% of the total variance of soil moisture data in 2018 and 2019, respectively. At the Town Creek field, the first PC explained 76% and 77% of the variance in 2018 and 2019, respectively. The cumulative variance explained by the first three PCs were 98% in 2018 and 97% in 2019 in Tanner, and 95% and 91% for 2018 and 2019, respectively, in Town Creek location.

Tanner Field Case

The variances explained by the first three principal components for each soil layer and dates in 2018 are shown in Figure 1.8. For the 2018 season, 96% of the total variance was explained exclusively by the first principal component. For all soil layers, PC1 was able to capture most of the variance of soil water content with little variation in the variance values. The

average variance value for 15, 30, and 60 cm were 0.95, 0.97, and 0.95, respectively. The PC2 and PC3, which together explained almost 2%, had a negligible contribution in the variance of volumetric water content for all the dates. PC2 showed low variances values with a maximum value of 0.1 considering all soil layers. The higher values of variances for PC2 were around Jun 15 until Jun 20 for the first two layers and the same period plus July 18 for the deepest layer. The period of Jun 15 to Jun 20 was the tasseling period for corn and it is considered the high-water demand period for this crop. PC2 even showing only 2% of the variance was able to capture the variability in soil water content during the most important period crop water use in all three depths.

The loadings of each PC for each soil layer and dates for the 2018 season are shown in Figure 1.9. The first principal component shows constant and positive loading values for all three soil layer depths. This stability in loadings values means that each date had the same importance in explaining the variance in this component and there is no effect of temporal variability that characterize this PC. Meanwhile, PC2 and PC3 showed differences in loadings values, positive and negatives, for different dates in the three soil layers. The loadings for this PC are different for each date and showed high negative loading values around 15 June for all three soil layer depths. As mentioned before, this period corresponded to the peak water demand for corn (tasseling). Even though the PC2 contributed with a little percentage of variance, it was important to capture the high peak of demand of water for all three layers as observed in the variances plot (Figure 1.8). The PC3 demonstrated different loading values for each date as PC2. The PC2 and PC3 seem to be related to temporal variability due to the differences in loadings values for different measurement dates.

Loading plots for every pairwise combination of the first three PCs, generated from the 2018 data collected at Tanner, were produced (Figure 1.10). Loadings of PC1 did not show variability in loadings values as showed in the loading plots (Figure 1.9) and this can also be visualized in Figure 1.10 that the loading plots for PC1 vs PC2 and PC1 vs PC3 are arranged along a vertical direction. The same behavior was observed by Martini et al., (2017) when the authors analyzed the spatiotemporal pattern of soil moisture and they concluded that it was caused by spatial variability. The loading plots of PC2 vs PC3 demonstrated that the loadings of each soil layer were able to group and separate from each other according to the soil depth. Martini et al., (2017) concluded that this effect is caused by temporal variability. Therefore, the factors controlling PC2 and PC3 might exhibit some temporal variability.

The score plots of each pairwise combination of the first three PCs are shown in Figure 1.11. The score plots also provided information to confirm that PC1 had influence of spatial variability. The score plots of PC1 vs PC2 and PC1 vs PC3 were forming clusters and separated from each other on the x-axes. Each soil sensor location that belonged to the same management zone were clustered together. This effect of clustering is related to the spatial variability, where sensors in the same zone demonstrated the same behavior when compared to sensors installed in another zone. Therefore, spatial variability was the main factor characterizing the PC1. Meanwhile, PC2 vs PC3 did not show a clear pattern of clustering the scores.

For the 2019 season, 97% of the total variance was explained by the first three principal components (Table 1.3). The PC1 was able to explain 93% of the total variance in the volumetric water content data, and PC2 and PC3 together explained 4% of the total variance. In the 2019 season, PC1 showed similar behavior of the 2018 season even the field being cultivated with cotton instead of the corn. The variances explained by each principal component at each soil

layer and date are shown in Figure 1.12. The PC1 alone explained almost the total variance for all soil layers and dates. The average variance value for the 15, 30, and 60 cm were 0.92, 0.95, and 0.91, respectively. The PC2 had a little contribution for the first two layers and a maximum variance values around 0.1 in the deepest layer. The PC3 had a negligible contribution for all soil layers and dates. The loadings values are shown in Figure 1.13. The same behavior of 2018 was observed during the 2019 season, with respect to the loadings of PC1. The first principal component demonstrated constant and positive values for all three soil layers. The PC2 demonstrated negative values for the 15 and 30 cm layers. The values for the 60 cm layer were the highest loading values, which means that this layer had the most influence in the PC, especially for the measurement dates in August where cotton was in high water uptake. The PC3 demonstrated positive and negative values for all three soil layers. High negative values of loadings in the first layer during the measurements in August (high water demand). The soil layer at 30 cm, the PC3 showed high values at the last five measurements and for the 60 cm layer, the high values were on the first dates. Loading plots for every pairwise combination of the first three PCs for 2019 were produced (Figure 1.14). The loading plots for PC1 vs PC2 and PC1 vs PC3 are arranged along a vertical direction as it was observed in 2018. The same behavior demonstrated that the PC1 in 2019 had an effect of spatial temporal that might be influenced by soil type or topographic features. Moreover, PC2 and PC3 also showed the same pattern observed in 2018, which was concluded that these two PCs had an effect of temporal variability instead of spatial. The score plots for each pairwise combination are shown in Figure 1.15. Similarly, results of 2018 were observed in 2019 for scores. The score plots of PC1 vs PC2 and PC1 vs PC3 were clustered together (same management zone) and separated from each other on

the x-axes. The PC2 vs PC3 did not show clear pattern of clustering the scores as it was noticed in 2018.

The results demonstrated that PC1 showed spatial variability, and PC2 and PC3 temporal distribution for both years. In addition, the spatial variability was responsible for 93% and 96% of the total variance of the volumetric water content.

Correlation analysis – Tanner Field

The Spearman's rank correlation between scores of the first three principal components, topographic indices and features, and soil electrical conductivity for 2018 and 2019 are shown in Table 1.5. For the 2018 corn growing season, the PC1 was positive, high, and significantly correlated with only the Topographic Position Index. The correlation value for TPI with the PC1 was 0.74. The PC1 was responsible for 96% of the variance of the entire data set and explained well the variance for the three soil layers. These results indicate that TPI could be used to explain PC1's spatial variability. The results demonstrated that the TPI explained most of the volumetric water content variability for the cornfield at Tanner with the weather conditions for the 2018 growing season. Even though the PC2 had a negligible contribution of 2% of the variance, this PC had high loadings during the high-water demand for corn (Tasseling). The PC2 demonstrated a significant correlation with elevation, slope, and TWI with correlation values of -0.62, 0.62, and -0.77, respectively. During the tasseling period, the corn roots are well distributed in the soil profile with most of the roots at 60 cm (Laboski et al.,1998). The correlation results for the PC2 evidenced that the volumetric water content variability was influenced by three different attributes. These results suggest that during the high crop water demand, all the topographic indices and the slope were significant to explain the water infiltration and uptake for all layers. The PC2 which demonstrated temporal variability showed that not only one index was

responsible to explain the variability in all the depths. Although in terms of importance, it can be concluded that TPI was already enough to explain the soil water content variability due to the high variance of PC1 for this field. Lastly, the PC3 did not demonstrate any significance with any topographic index and feature or soil electrical conductivity.

For the 2019 cotton season, the PC1 was also positive and highly correlated with the TPI. These results show that even having a different crop during 2019, the PC1 was able to explain 93% of the variance of the volumetric water content data set for all soil layers and it was correlated with TPI (0.72). The same conclusion for the 2018 season applies for 2019. The TPI was the topographic index that explained the spatial variability of the PC1. At the Tanner field, the soil showed little changes in texture, therefore it can be concluded that topography was the most factor that influenced the volumetric water content variability and TPI was the index that captured this variability. The PC2 did not show any significant correlation with any of the variables analyzed. However, the PC3 that explained only 1% of the variance, demonstrated correlation with slope and shallow (0-30 cm) and deep (0-90 cm) soil electrical conductivity.

The results demonstrated for both years, the PC1 was responsible to explain more than 93% of the variance of the entire volumetric water content data set and highly correlated to TPI. Spatial variability played an important role to explain the differences in the volumetric water content for this field. This information proved that different parts of the field demonstrated differences in volumetric water content according to the location where the sensors were installed. The uniform irrigations, which means applying the same irrigation rate, are the current irrigation method used by farmers. The results of this analysis demonstrated that farmers should consider variable rate irrigation to be able to modify the irrigation rate and meet the crop and soil water demand according to the spatial variability. Areas in the field where wet conditions are

common, due to the landscape position, should receive a different rate when compared to a dry area in the field. Delineating irrigation management zones that account for this variability will help farmers to increase water use efficiency (Sui and Yan, 2017) and avoid under or over-irrigation. Furthermore, the results could be a guidance for soil sensor placement to help farmers to be more effective in terms of irrigation scheduling.

Town Creek Field Case

The variances explained by the first three principal components for each soil depth in 2018 are shown in Figures 1.16. In 2018, the total variance of volumetric water content in the topsoil horizon (15 cm) was well explained by PC1 for almost all measurement dates with an average variance value of 0.87. The measurements of June 16, 17, 18, 19, 26, and 30 had the highest variance with values above 0.9. This period represents the high demand of water for the corn crop, which is the tasseling and silking growth stage. The other two PCs, PC2 and PC3, had a little contribution to the 15 cm layer with values below 0.10 for almost all the dates. For the soil layer of 30 cm, the PC1 had the highest variance values for all measurements except for the first date (Jun 3) which had a low value of 0.2. The average variance for PC1 in the 15 cm soil layer was 0.84. The PC2 demonstrated the highest variance value of 0.4 for the first measurement date, but for the other dates, the values were low. The PC3 had a negligible contribution to the second layer. The changes in soil water content at the 60 cm soil layer were explained by PC1 and PC2. The PC1 had the highest average values of 0.57 and PC2 of 0.33 over the total measurement dates. In the first six dates, the PC2 had the highest variance values in comparison to PC1. The last five measurement dates were well explained by a combination of PC1 and PC2. The dates from Jun 16 and Jun 30 was better explained by PC1 and PC2

demonstrated low values. For this layer, PC3 demonstrated low values for the first three dates and values close to zero for the other dates.

The loadings of the first three PCs for all depth and dates are shown in Figure 1.17. The PC1 demonstrated almost the same values of loadings for all measurement dates and soil layers. The loading values for the PC1 were all negative. Meanwhile, PC2 and PC3 showed negative and positive values for all three layers and dates. The highest loading values observed in the PC2 was found in the 60 cm layer. The Town Creek field had a similar behavior of PC2 and PC3 as observed in Tanner Field. The PC2 and PC3 appear to be more related to temporal variability based on the differences in loading values for different dates. The same behavior also can be observed in the pairwise combination of loadings showed in Figure 1.18. PC1 vs PC2 and PC1 vs PC3 formed the same vertical line as observed in the Tanner field. These results are related to the effect of spatial variability. The PC1 vs PC2 was also able to separate the loading values for 15 and 60 cm. This behavior represents the spatial variability as identified by Martini et al., (2017). The score plots of each pairwise combination of the first three PCs are shown in Figure 1.19. The score plots also confirmed that PC1 had the influence of spatial variability where the score plots of PC1 vs PC2 and PC1 vs PC3 were forming clusters and separated from each other on the x-axes, which proves that each management zone described a different behavior related to volumetric water content. Meanwhile, PC2 vs PC3 did not show a clear pattern of clustering the scores.

For the 2019 growing season, the variances explained by each principal component at each soil layer and date are shown in 1.20. The PC1 had the highest variances explained for all three layers and it was responsible for 76% of the variance of the entire data set. In the first soil layer, PC1 had the highest variance for all dates. The PC2 showed high values of variance at the

last five dates and PC3 had a negligible contribution. In the second layer, PC1 showed the highest values for most of the measurements with low values on Jun 20 and July 7. The PC2 and PC3 showed the highest values on the same dates (Jun 20 and July 7). In the bottom layer, PC1 showed high values for most of the dates. The PC2 had high values on July 23, 24, and 25 and the PC3 showed only values below 0.2. The loading values for each PC are shown in Figure 1.21. The loading values demonstrated the same behavior for PC1 as observed in 2018. The loading values for this PC were all negative and constants for all dates and soil layers. The PC2 and PC3 also showed the temporal effect based on the different loading values for each date in all depths. PC2 showed high values for all soil depth only at the last date and PC3 had high values only for the 60 cm soil layer. Figure 1.22 shows the vertical line formed by the pairwise combination of PC1 vs PC2 and PC1 vs PC3. These results confirmed the spatial influence affecting PC1 in 2019. The same result affecting PC1 was observed in Tanner for both years and in Town Creek. The PC1 for both locations were affected by spatial variability, and PC2 and PC3 by temporal variability. The pairwise combination of PC2 and PC3 were also able to separate 60 cm from the 15 and 30 cm. This indicates the temporal variability that affects PC2 and PC3. Lastly, the score plots for 2019 are shown in Figure 1.23. In the 2019 growing season, fewer sensors were available for the analysis, which hindered the visualization of clusters on the score plots. Even though it was clear that PC1 vs PC2 formed clusters for each sensor located in the same management zone and distant from the others.

The spatial and temporal effects are key information for irrigation, especially to understand the effect of water infiltration to deep layers. The soil water content in deep layers affected by the slope will also reflect in crop yield (Jiang & Thelen, 2004). These differences were explained by comparing two contrasting locations with soil sensors as shown in Figure 1.7.

Greater slopes will demonstrate a great chance of runoff and the water will not be able to infiltrate to deep layer. The use of VRI could help in this case by changing the rate of application in these areas to avoid runoff and consequently soil erosion. In addition, considering the size of each management zone for this field, the use of VRI could also help the farmer to decrease the amount of water applied during the growing season, saving water and energy, and consequently maximizing the profitability.

Correlation analysis – Town Creek Field

The Spearman's rank correlation between scores of the first three principal components, topographic indices and features, and clay, silt, and sand content for 2018 and 2019 are shown in Table 1.6. For the 2018 season, the scores of PC1 were positive, high, and significantly correlated with the Topographic Wetness Index (0.70) and negative, high, and significantly correlated with Slope (-0.71). This PC was also negatively correlated with the sand content (-0.46). The PC1, explained 77% of the entire volumetric water content data set, had high variance explained for all soil layers and was affected by spatial variability. The TWI, slope, and sand content explained the spatial variability for 2018. The PC2 which explained 15% of the data set and had high variances at the deep layer of 60 cm, demonstrated a negative correlation with Topographic Wetness Index (-0.45) and silt content (-0.68), and positive correlation with clay content (0.46). The correlation results for the PC2 showed that the clay and silt content associated with the TWI characterized the water infiltration process to the bottom layer. The PC3 did not show any significance with any of the terrain attributes and clay, silt, and sand contents. For the 2019 season, the scores of PC1 was negatively correlated with Topographic Position Index (-0.57). The PC1 explained 76% of the total variance of the volumetric water content data set, had high variance explained by each soil layer and affected by spatial variability. The PC1

did not show any significant correlation with clay, silt, or sand content in 2019. The difference in correlation between PC1 in 2018 and 2019 with terrain attributes could be related to the differences in rainfall distribution. In 2018, the month of June had a higher precipitation amount than 2019 and the historic average. In July, the 2019 season had significantly higher precipitation amount than 2018 and historic average. These differences were a factor that could influence the level of importance for different terrain attributes to explain the volumetric water content variability in each season. Fraisse et al., (2000) concluded that management zones vary from year to year and from crop to crop. The results of the correlation for this study proved the same concept as mentioned by Fraisse et al., (2000). The differences in weather from 2018 and 2019, resulted in a different index to explain the spatial variability of volumetric water content data set. Meanwhile, The PC2 demonstrated a positive correlation only with elevation (0.50). This PC explained 11% of the variance in the data set and demonstrated high loading values for the 15, 30, and 60 cm soil layers at the last dates. The PC3 showed significance with clay and silt content. The high loading values for PC3 were in the 60 cm soil layer. The water infiltration to deep layers could be associated with the clay and silt content as a result of the interpretation of PC3.

SUMMARY AND CONCLUSIONS

The use of principal component analysis showed to be an efficient method to analyze, interpret and to reduce the dimensionality of the spatial and temporal variability in volumetric water content data set. For both years and locations, three principal components were able to explain over 95% of the total variance of the original volumetric water content data set. Only the first principal component in Tanner was able to explain 93% and 96% of the variance in 2018 and 2019, respectively. For both locations and years, the PC1 demonstrated to be influenced by

spatial variability, and PC2 and PC3 by temporal variability. These results were important to identify the factors that affected each principal component and the relation between each component with terrain attributes and soil parameters. For the Tanner field for both years, the PC1 explained the maximum variance of volumetric water content for all soil layers. Moreover, the PC1 was only significantly correlated with the Topographic Position Index in 2018 and 2019. This result proved that TPI was the most important source of information to explain the volumetric water content variability in that field for both years and crops. The TPI, it could be considered the most effective source of information to be used to delineate irrigation management zones for Tanner field. For the Town Creek field, the PC1 also explained the maximum variance for all soil layers for both years and showed significance with TWI, slope and, sand content in 2018 and TPI in 2019. The differences related to which terrain attribute was significant can be related to the rainfall distribution for each year. The PC2 only explained the variances for the 60 cm layer in 2018 and for the last measurement dates in all layers in 2019 and had a significant correlation with TWI, clay, and silt in 2018, and elevation in 2019. For the Town Creek field, TWI, slope, and TPI can be considered as the most important terrain attributes to explain the variability of volumetric water content since both were correlated to PC1, which explained more than 76% of the data set for both years. Different topographic indices and topographic features were significant for both fields. These results proved that different field locations with different soil types, topography, weather conditions, and different crops, would result in different terrain attributes to explain the volumetric water content variability.

The results for this study showed that the topographic indices and slope were important to explain the volumetric water content variability. Delineating irrigation management zones using the indices and features determined in this study could help farmers to achieve higher crop yields

by avoiding runoff, nutrients leaching, and under or over-irrigation. These results also proved that variable rate irrigation is an important tool to help farmers to meet crop demand and soil water holding capacity based on the variability of the topography in the field. In order to increase irrigation efficiency and maximize the profitability, the terrain attributes analyzed could guide farmers on better decisions such as soil sensor placement, decide areas where it should receive irrigation first, and areas where the irrigation rate should increase or decrease.

Table 1.1. Average value of Topographic Indices (TPI and TWI), Topographic features (elevation and slope), and Apparent Soil Electrical Conductivity Shallow and Deep for each soil sensor location at Tanner Field

Sensor Number	Elevation (m)	TWI[1]	TPI[2]	Slope (%)	Shallow EC_a (dS/m)[3]	Deep EC_a (dS/m)[4]
3	185.49	3.82	-0.12	4.52	11.55	15.37
4	186.47	2.81	-0.93	5.92	9.89	16.49
5	188.42	2.58	1.19	4.21	9.78	16.11
6	185.83	2.32	0.67	6.85	9.88	15.32
7	183.72	2.59	-0.14	7.19	17.30	24.67
8	182.26	3.21	-1.17	7.31	9.73	20.89
9	183.90	3.42	-0.90	3.87	9.98	22.45
11	190.10	5.13	0.68	1.86	7.60	16.93
12	190.57	5.19	0.66	1.02	10.65	21.19
13	189.92	3.86	0.93	2.47	18.07	27.45
14	190.31	4.77	0.65	2.15	7.37	15.63
17	190.03	5.19	0.50	0.75	10.10	16.62
19	188.48	2.74	-0.53	3.16	12.80	21.31
20	190.26	4.16	0.29	2.16	12.15	21.33
21	189.82	4.40	0.56	2.19	12.91	25.70

[1]Topographic Wetness Index
[2]Topographic Position Index
[3]Shallow Apparent Soil Electrical Conductivity measured from 0 – 30 cm
[4]Deep Apparent Soil Electrical Conductivity measured from 0 – 90 cm

Table 1.2. Average value of Topographic Indices (TPI and TWI), Topographic features (elevation and slope), and clay, silt and sand content for each soil sensor location at the Town Creek Field

Sensor Number	Elevation (m)	TWI[1]	TPI[2]	Slope (%)	Clay (%)	Silt (%)	Sand (%)
1	172.66	11.60	-1.24	1.23	53.7	19	27.3
2	172.94	11.15	-0.73	2.22	37.5	39.3	23.2
4	173.78	9.76	-0.91	2.64	28.1	53.5	18.4
6	174.02	10.72	-0.31	1.55	43.5	44.8	11.7
7	174.54	11.43	-0.16	1.74	23	50.7	26.3
8	174.21	9.63	-0.08	0.98	23	50.7	26.3
9	173.39	11.30	-0.09	0.57	43.5	44.8	11.7
10	173.19	10.21	-0.45	0.56	43.5	44.8	11.7
11	173.31	9.58	-1.19	2.03	37.5	39.3	23.2
12	174.08	8.24	0.10	4.31	37.5	39.3	23.2
15	172.81	7.06	2.43	8.50	44.2	32.1	23.7
18	174.86	7.37	3.24	4.44	35.2	32.9	31.9
19	174.39	6.85	2.98	4.79	35.2	32.9	31.9
22	174.46	8.58	0.74	3.41	47.3	28.2	24.5
24	173.86	11.24	-0.66	0.50	41.1	36.1	22.8
26	174.03	7.81	0.91	3.81	47.7	23.5	28.8
28	173.09	8.44	-1.20	0.90	49.6	42.8	7.6
30	173.69	8.49	-0.52	5.13	28.5	41.5	30

[1]Topographic Wetness Index
[2]Topographic Position Index

Table 1.3 Eigenvalues, proportion of variance, and cumulative proportion for the first three principal components in the Tanner field (2018 and 2019).

Tanner - 2018			
	PC1	PC2	PC3
Eigenvalues	68.91	1.33	0.64
Proportion of Variance	0.96	0.02	0.01
Cumulative Proportion	0.96	0.98	0.98
Tanner - 2019			
	PC1	PC2	PC3
Eigenvalues	80.85	2.52	1.22
Proportion of Variance	0.93	0.03	0.01
Cumulative Proportion	0.93	0.96	0.97

Table 1.4 Eigenvalues, proportion of variance and cumulative proportion for the first three principal components in the Town Creek field (2018 and 2019).

Town Creek - 2018			
	PC1	PC2	PC3
Eigenvalues	39.08	7.81	1.39
Proportion of Variance	0.77	0.15	0.03
Cumulative Proportion	0.77	0.92	0.95
Town Creek - 2019			
	PC1	PC2	PC3
Eigenvalues	52.19	7.31	3.34
Proportion of Variance	0.76	0.11	0.05
Cumulative Proportion	0.76	0.86	0.91

Table 1.5 Spearman's correlation between the scores of the first three principal components, terrain attributes and soil texture at Tanner Field for 2018 and 2019.

	2018			2019		
Terrain Attributes	PC1	PC2	PC3	PC1	PC2	PC3
Elevation	0.42	-0.62**	0.18	0.47	0.06	-0.50
Slope	-0.29	0.62**	-0.23	-0.22	0.01	0.74**
TPI[1]	0.74***	-0.06	-0.32	0.72***	0.14	-0.07
TWI[2]	-0.07	-0.77***	0.23	-0.34	0.04	-0.48
Shallow EC_a [3]	-0.03	-0.21	0.31	0.22	-0.17	-0.74**
Deep EC_a [4]	-0.39	-0.31	0.32	-0.17	-0.27	-0.78***

[1]Topographic Position Index
[2]Topographic Wetness Index
[3]Shallow Apparent Soil Electrical Conductivity measured from 0 – 30 cm
[4]Deep Apparent Soil Electrical Conductivity measured from 0 – 90 cm
*significant $p<0.1$
**significant $p<0.05$
***significant $p<0.01$

Table 1.6 Spearman's correlation between the scores of the first three principal components, terrain attributes, and soil electrical conductivity at Town Creek Field for 2018 and 2019.

	2018			2019		
Terrain Attributes	PC1	PC2	PC3	PC1	PC2	PC3
Elevation	-0.19	0.07	-0.08	0.23	0.50*	-0.01
Slope	-0.71***	0.29	-0.21	-0.47	0.42	-0.03
TPI[1]	-0.19	0.22	-0.28	-0.57**	0.30	0.14
TWI[2]	0.70***	-0.45*	0.28	0.32	-0.43	-0.14
Clay	0.18	0.46*	0.09	0.09	-0.44	-0.64***
Silt	0.41	-0.68***	-0.06	0.07	0.31	0.74***
Sand	-0.46**	0.29	-0.27	-0.29	0.37	-0.34

[1]Topographic Position Index
[2]Topographic Wetness Index
*significant p<0.1
**significant p<0.05
***significant p<0.01

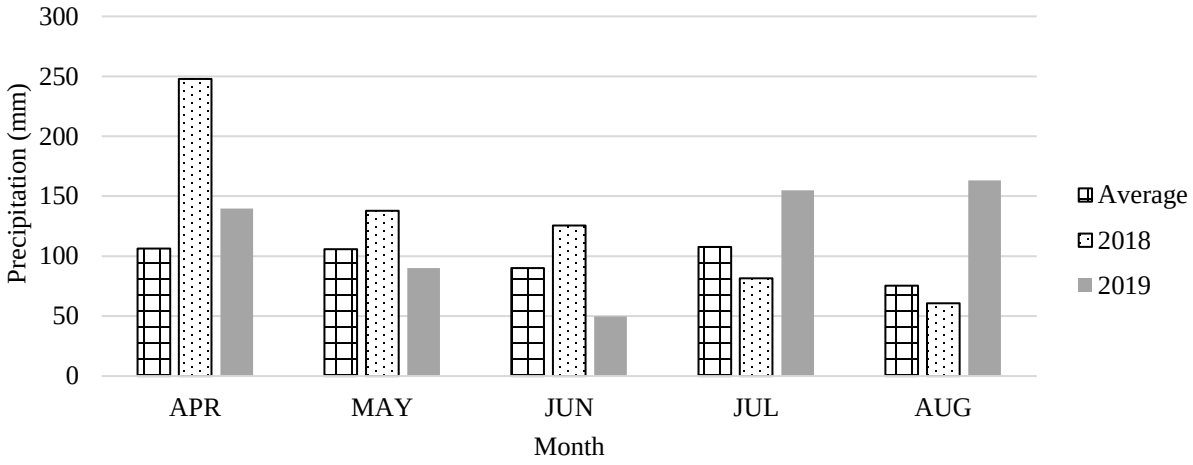

Figure 1.1 Total precipitation (Average from 1999 - 2019, 2018 and 2019) during the corn growing season at the Tanner field.

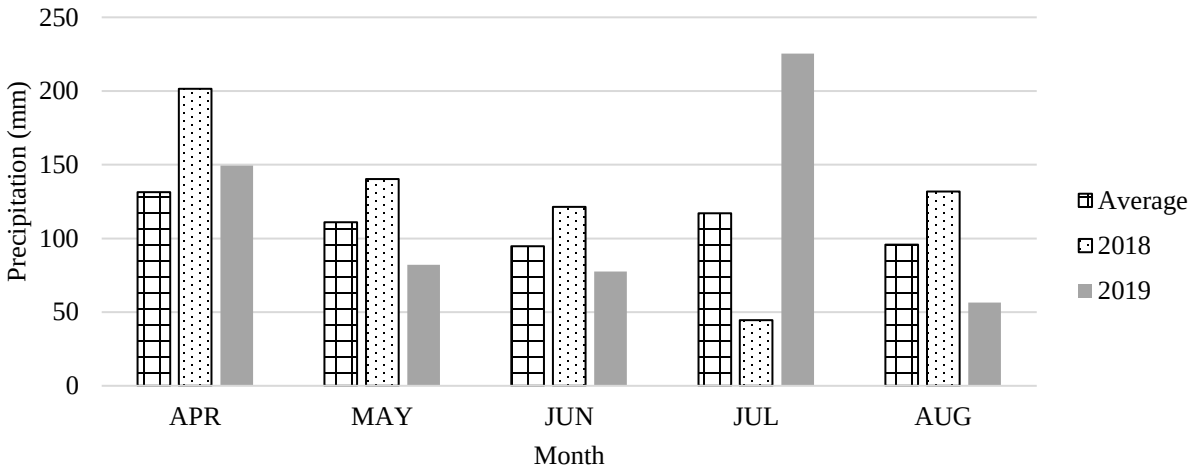

Figure 1.2 Total precipitation (Average from 1999 - 2019, 2018 and 2019) during the growing season at the Town Creek field

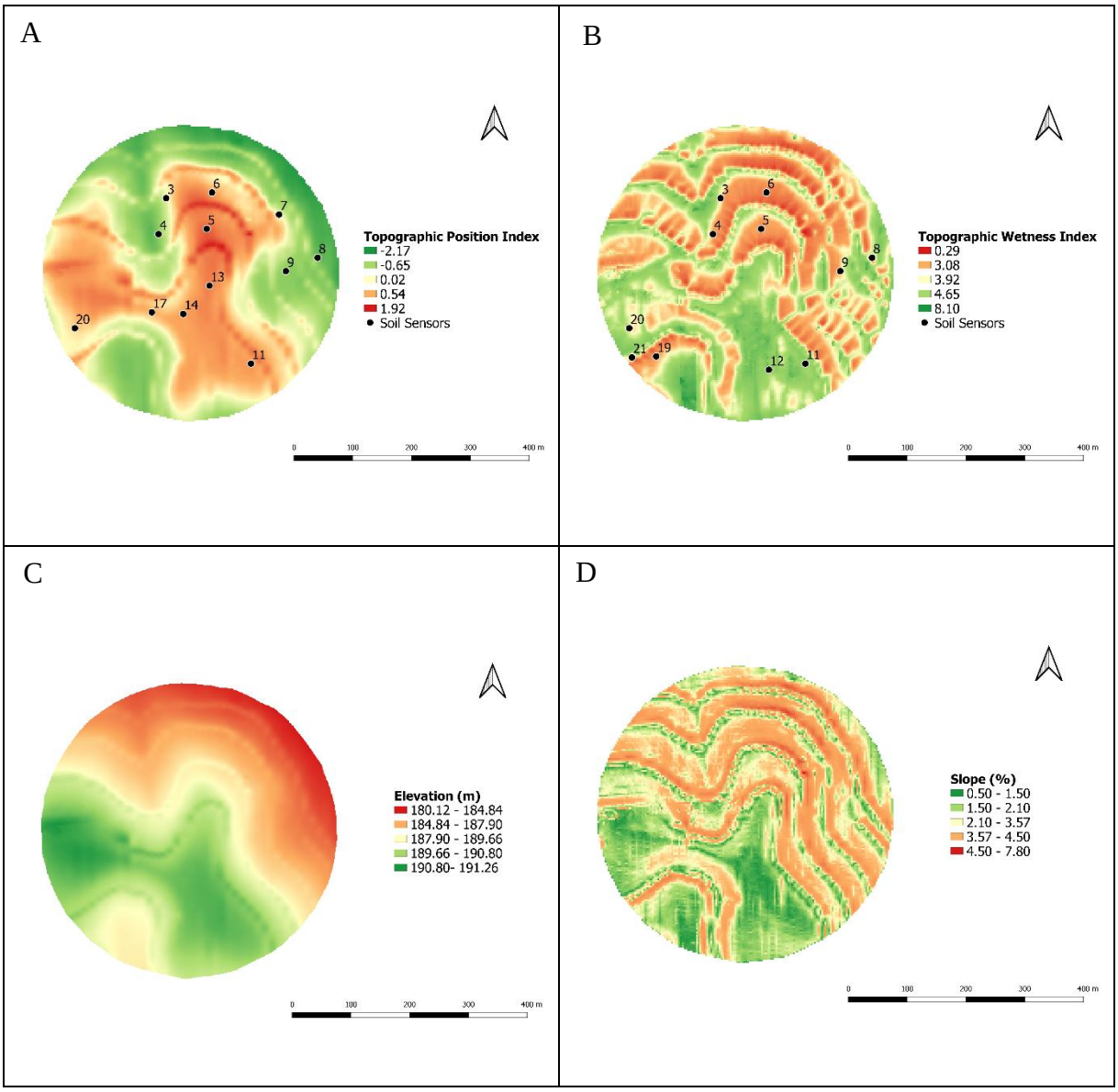

Figure 1.3. Topographic indices (TPI and TWI), topographic features, and soil sensor location for 2018 and 2019 at Tanner Field. A- Topographic Position Index and soil sensor locations during the 2018 growing season. B- Topographic Wetness Index and soil sensor locations during the 2019 growing season. C- Field elevation in meters. D. Field slope in percentage.

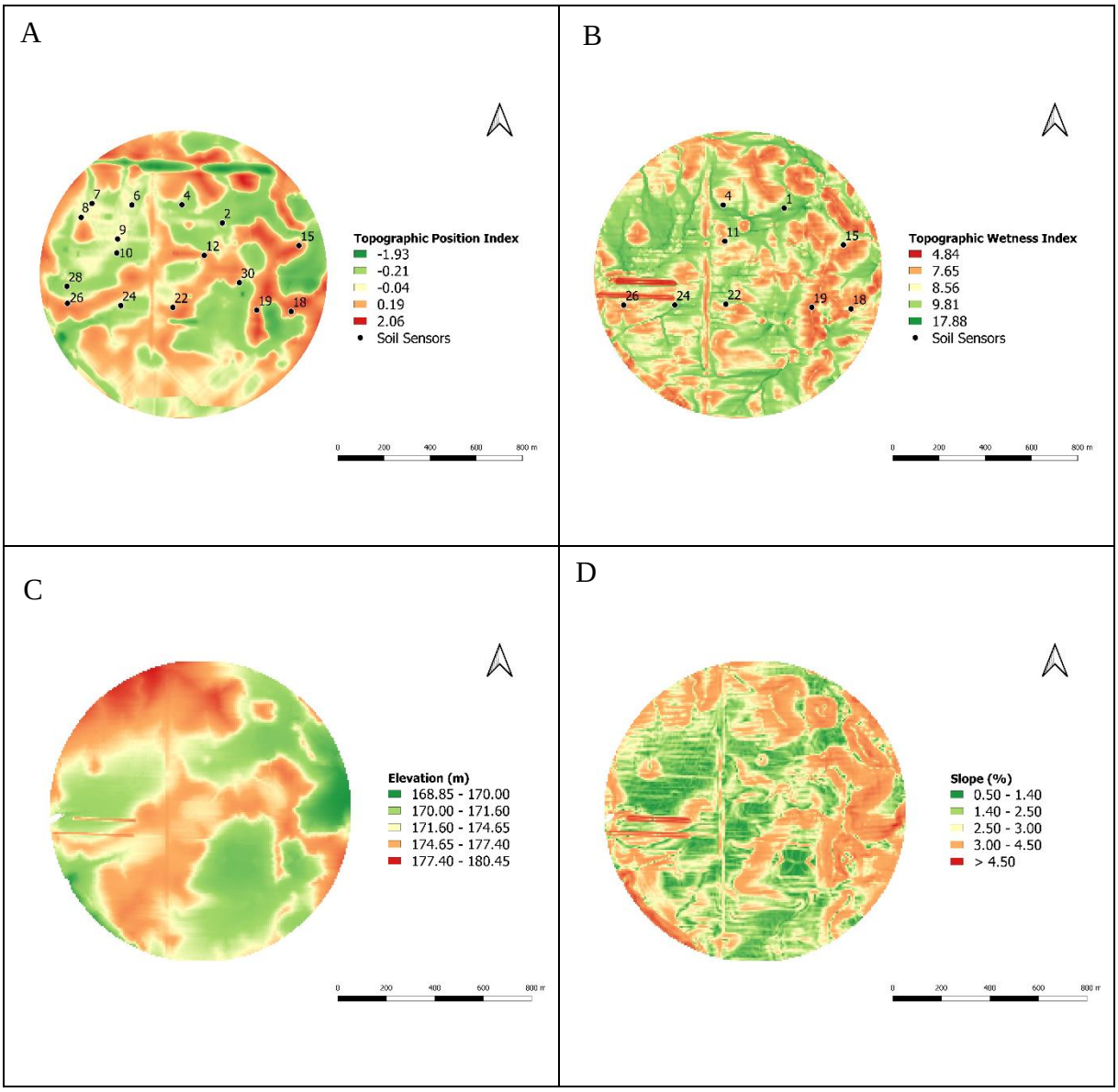

Figure 1.4. Topographic indices (TPI and TWI), topographic features, and soil sensor location for 2018 and 2019 at Town Creek Field. A- Topographic Position Index and soil sensor locations during the 2018 growing season. B- Topographic Wetness Index and soil sensor locations during the 2019 growing season. C- Field elevation in meters. D. Field slope in percentage.

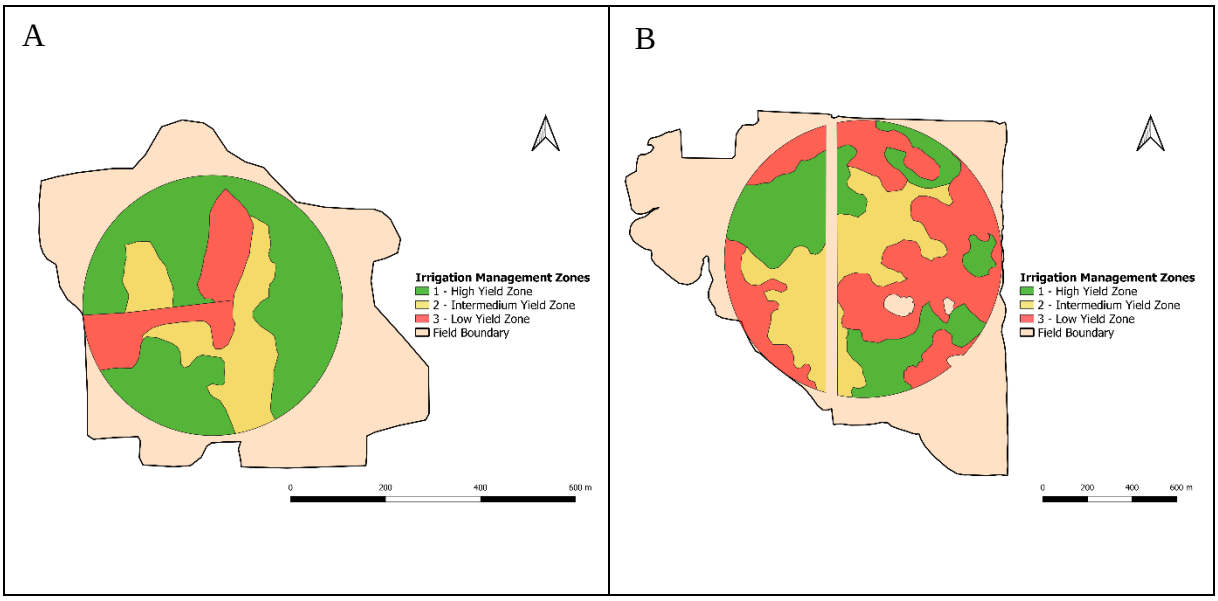

Figure 1.5. Irrigation management zones for both fields in 2018 and 2019. A- Tanner Field. B- Town Creek field

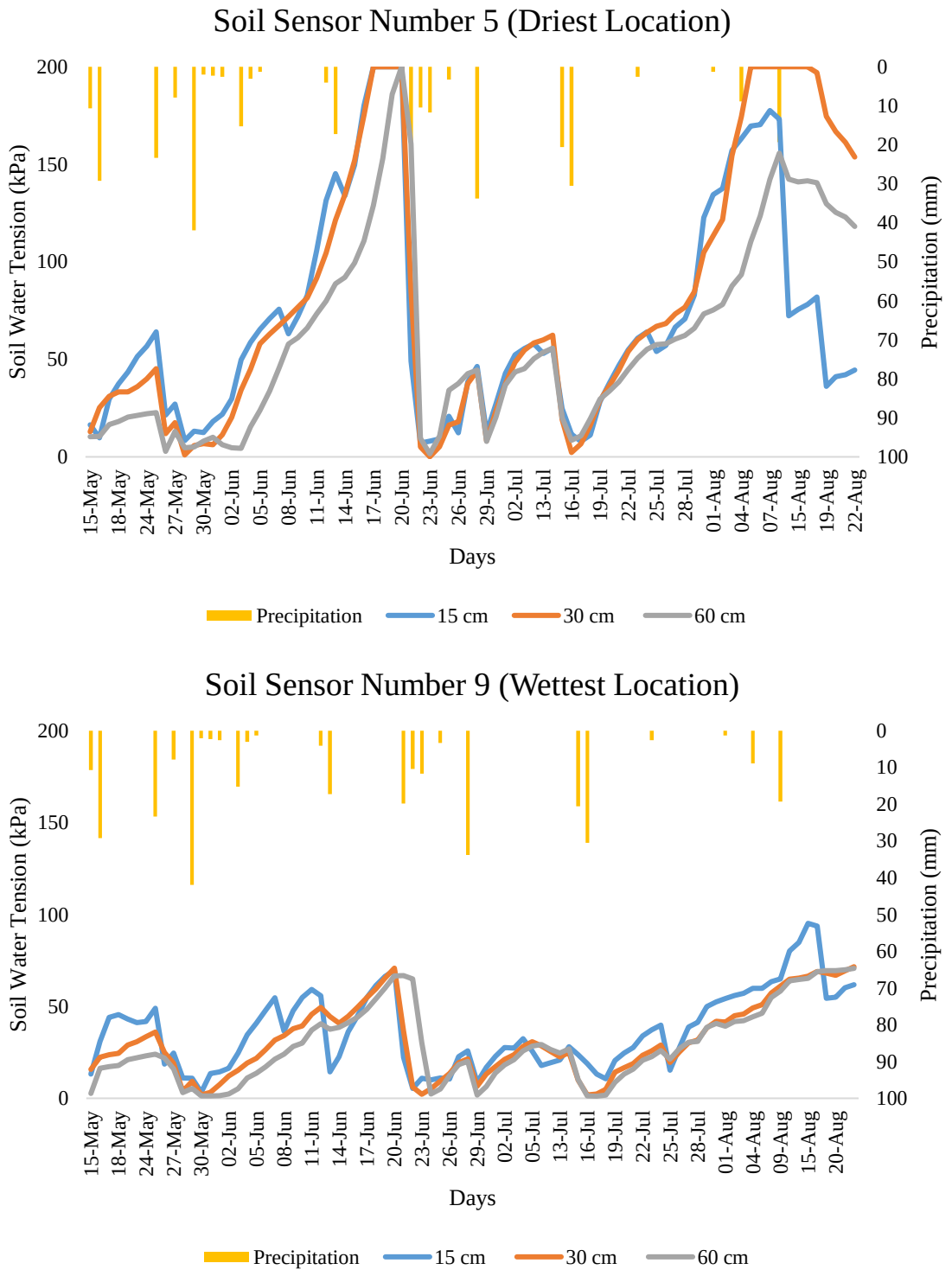

Figure 1.6. Soil water tension changes from sensors five and nine installed at two contrasting locations in the Tanner Field during the 2018 growing season

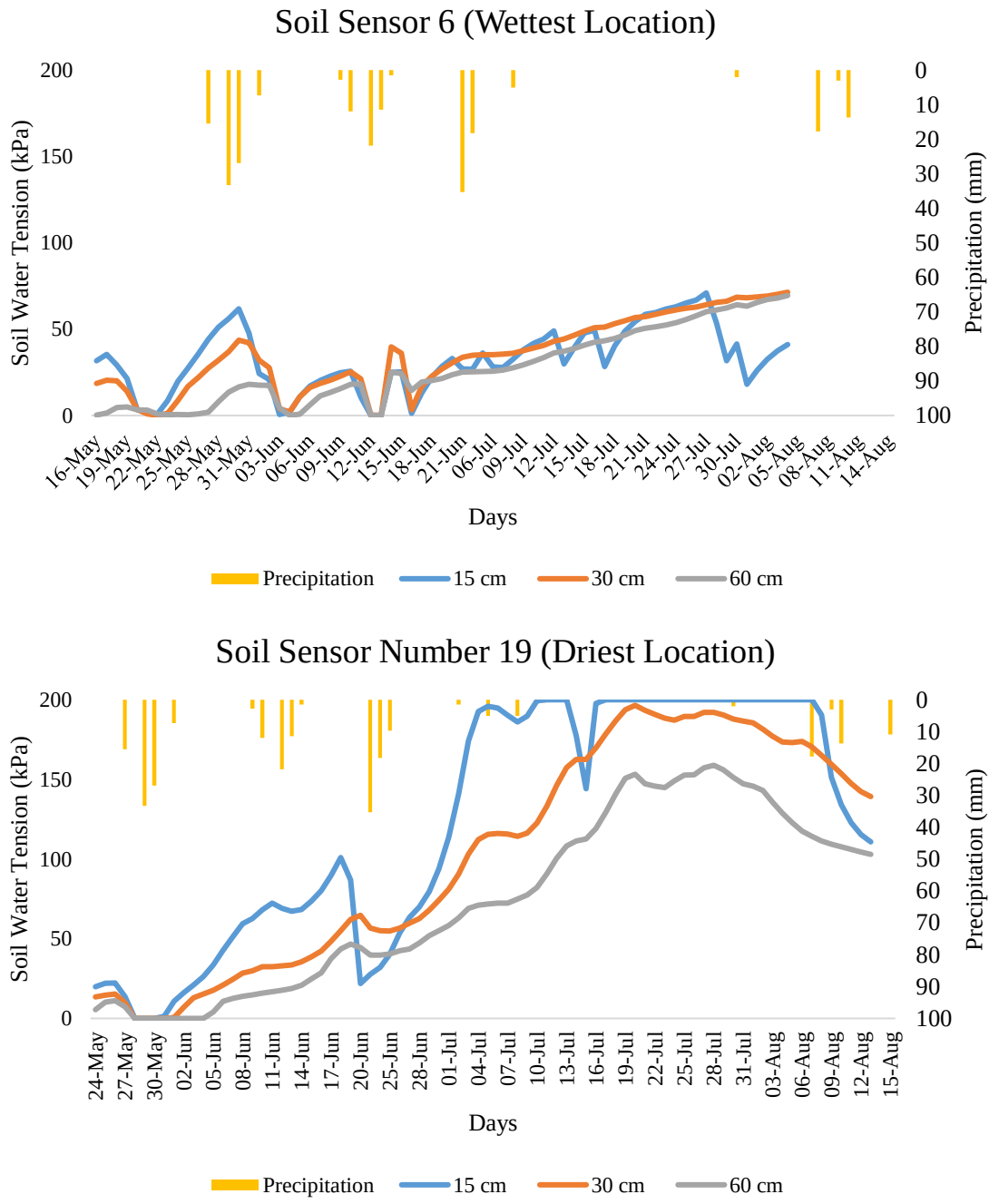

Figure 1.7. Soil water tension changes from sensors six and 19 installed at two contrasting locations in the Town Creek Field during the 2018 growing season

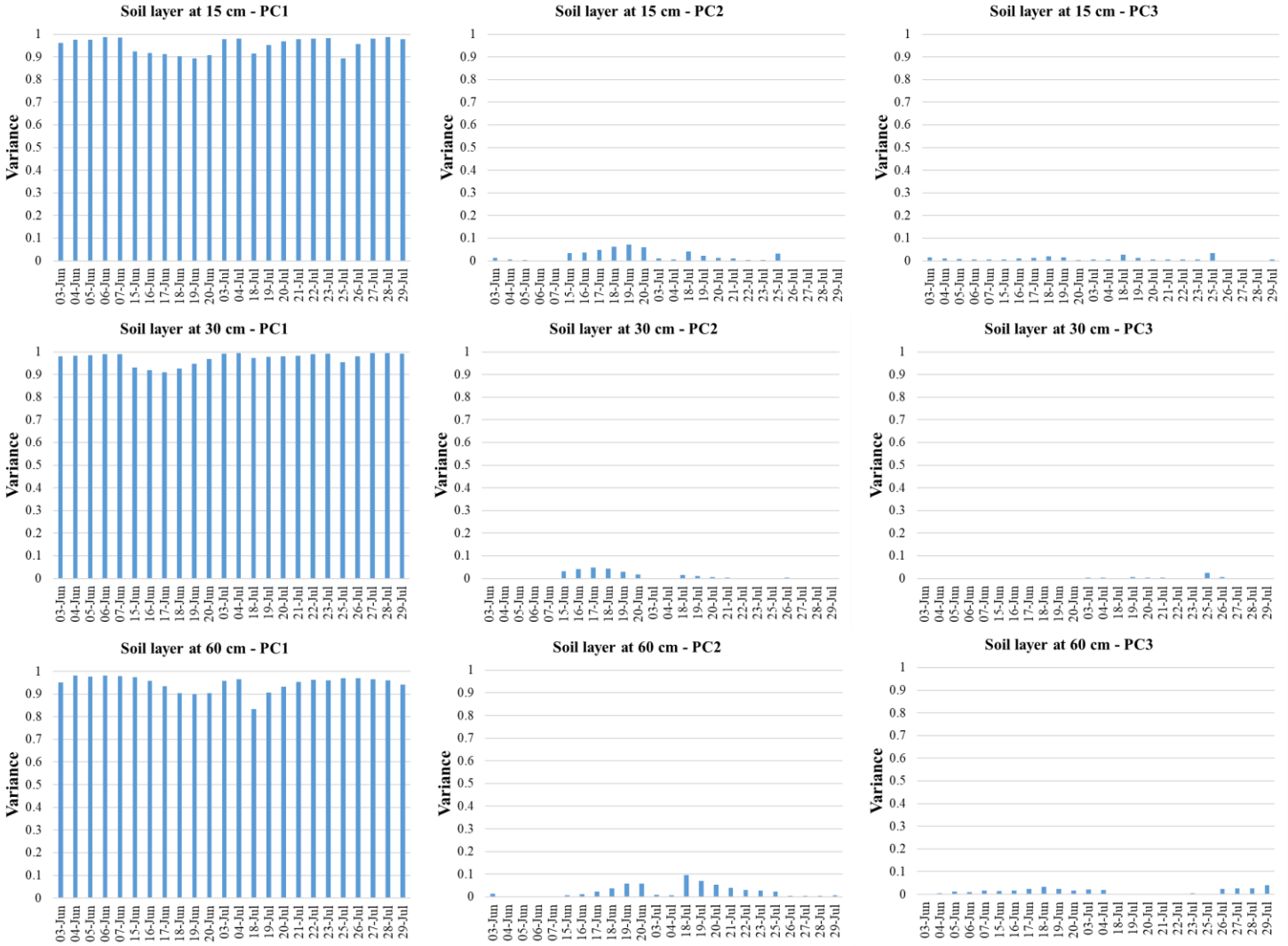

Figure 1.8. Bar plots of the spatial variance of daily volumetric water content explained in 2018 by the first three principal components (PC1, PC2, PC3) for each measurement date and soil depth (15, 30, 60 cm) at the Tanner field. From left to right, each column represent a different PC, from top to the bottom represent the variance of volumetric water content at depth of 15, 30 and 60 cm. Each bar represent a different measurement date from June to July 2018.

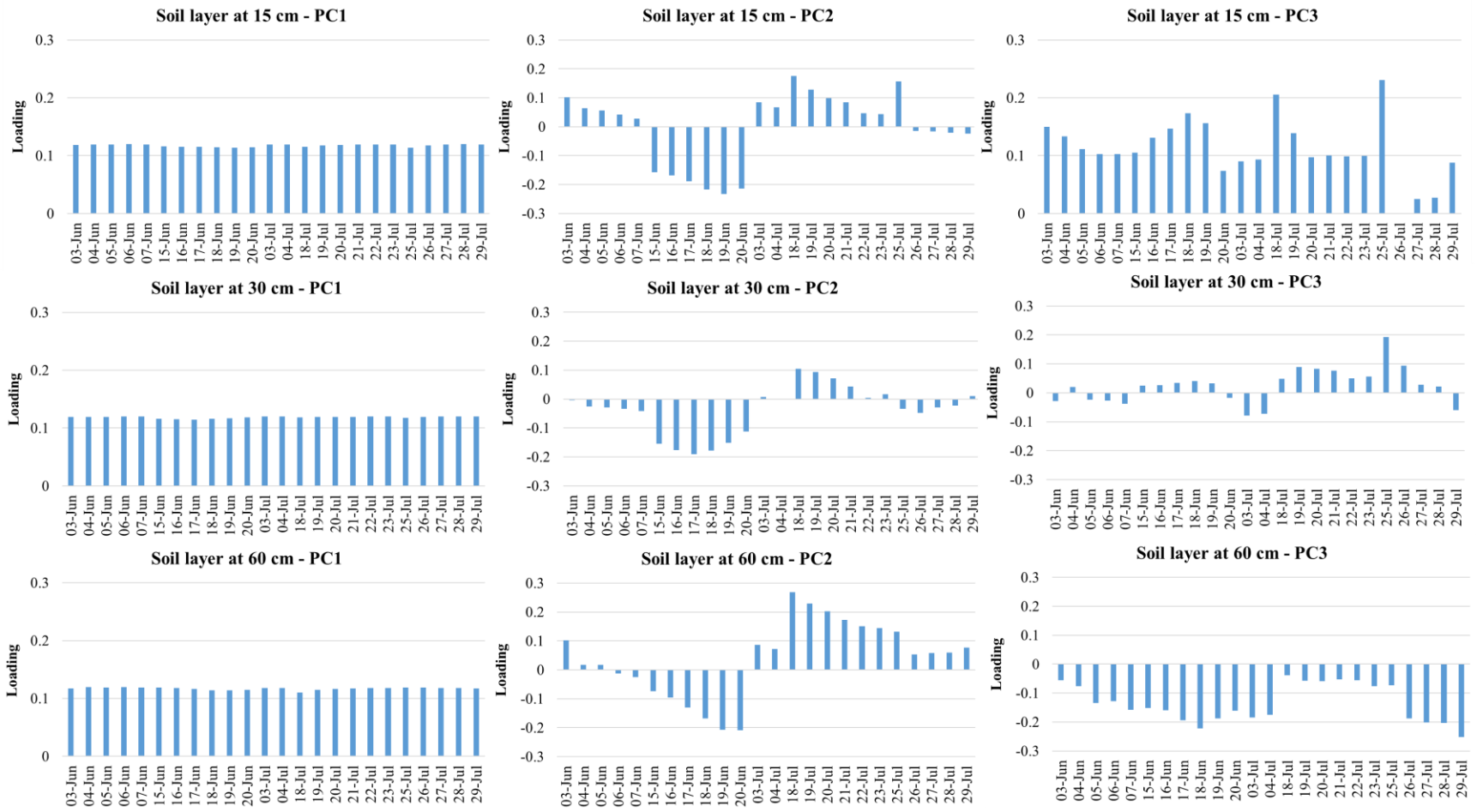

Figure 1.9. Bar plots of the loadings of the first three principal components (PC1, PC2, PC3) identified from the 2018 data for each measurement date and soil depth (15, 30, 50 cm) at the Tanner field. From left to right, each column represent a different PC, from top to the bottom, represent the loadings at each soil depth of 15, 30 and 60 cm. Each bar represent a different measurement date from June to July 2018.

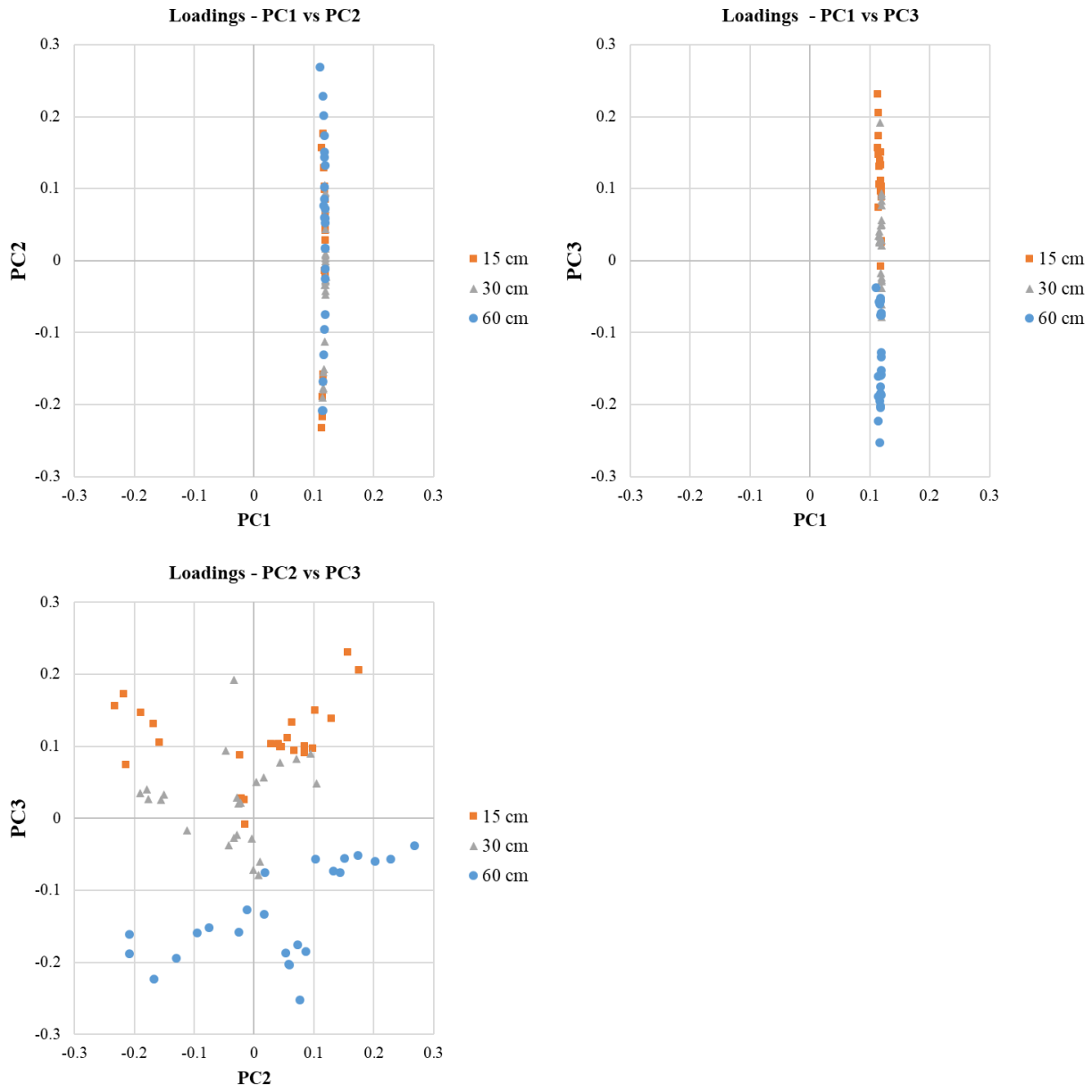

Figure 1.10. Loadings plots of PC1 vs PC2, PC1 vs PC3, and PC2 vs PC3 for the Tanner field in 2018. For each loading plot, every point represents daily mean volumetric water content measured at depths of 15, 30, and 60 cm.

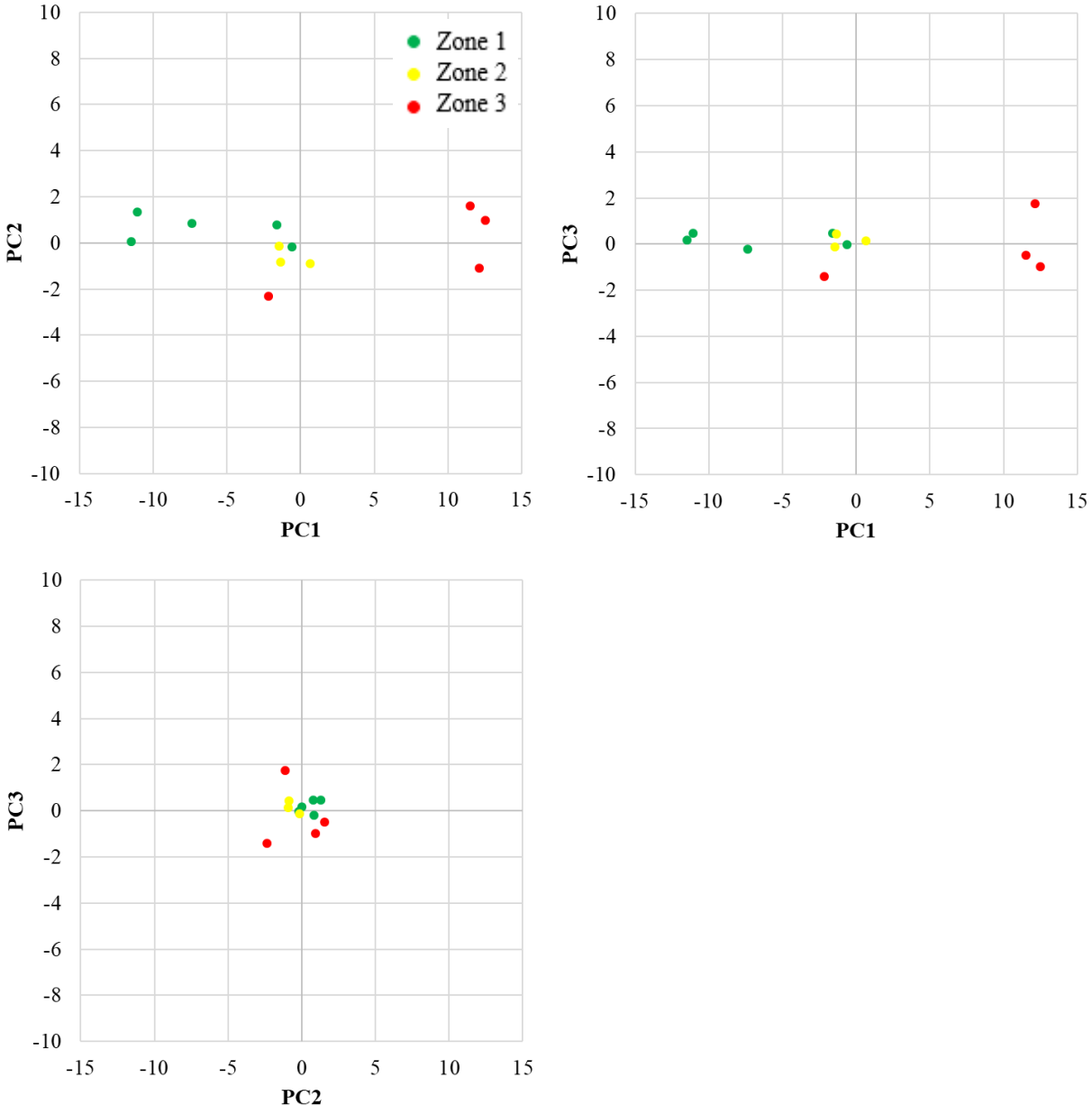

Figure 1.11. Score plots of PC1 vs PC2, PC1 vs PC3 and PC2 vs PC3 for the Tanner field in 2018. Each color refers to a different irrigation management zone where the sensors were installed.

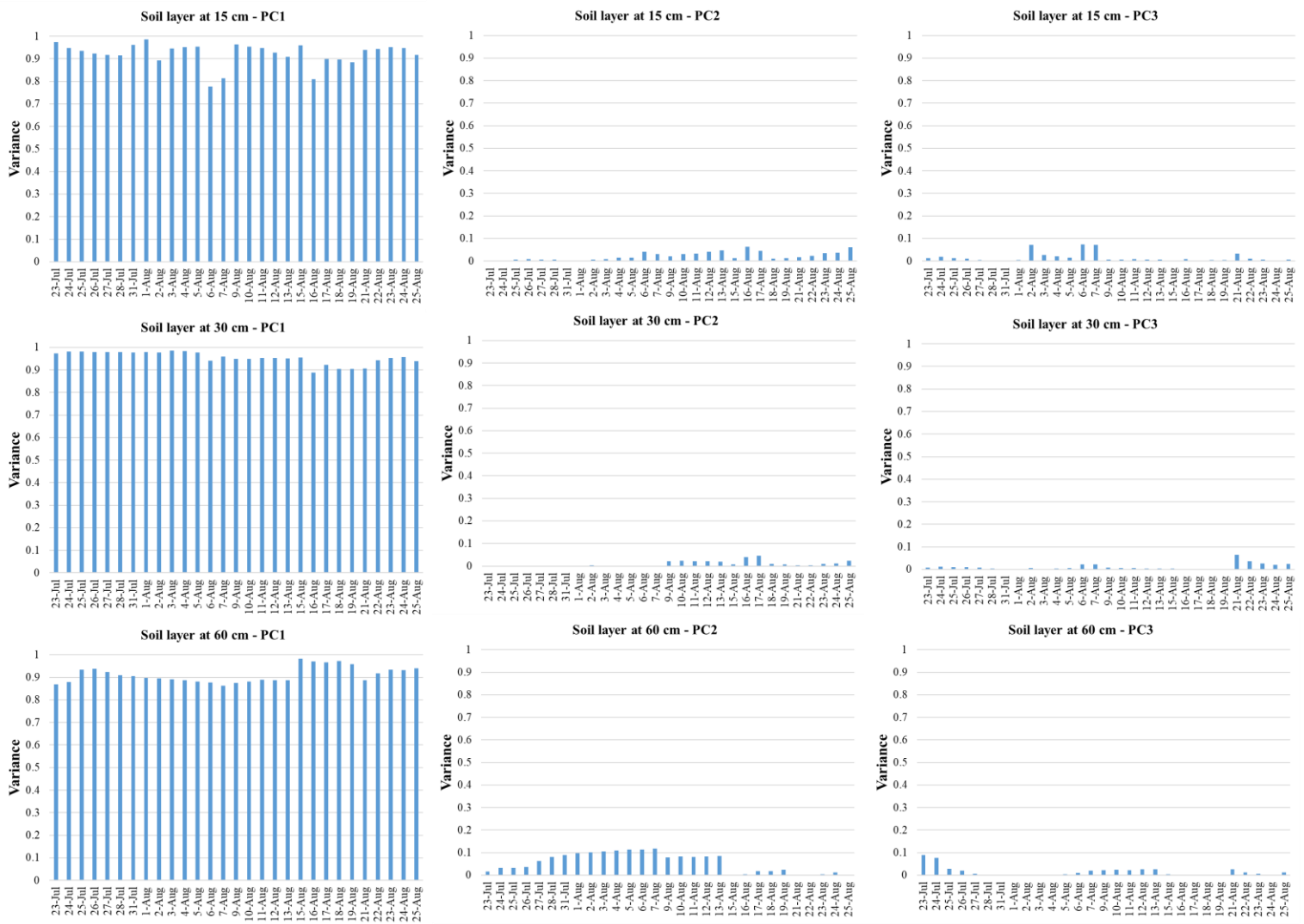

Figure 1.12. Bar plots of the spatial variance of daily volumetric water content explained in 2019 by the first three principal components (PC1, PC2, PC3) for each measurement date and soil depth (15, 30, 60 cm) at theTanner field. From left to right, each column represent a different PC, from top to the bottom represent the variance of volumetric water content at depth of 15, 30 and 60 cm. Each bar represent a different measurement date from July to August 2019.

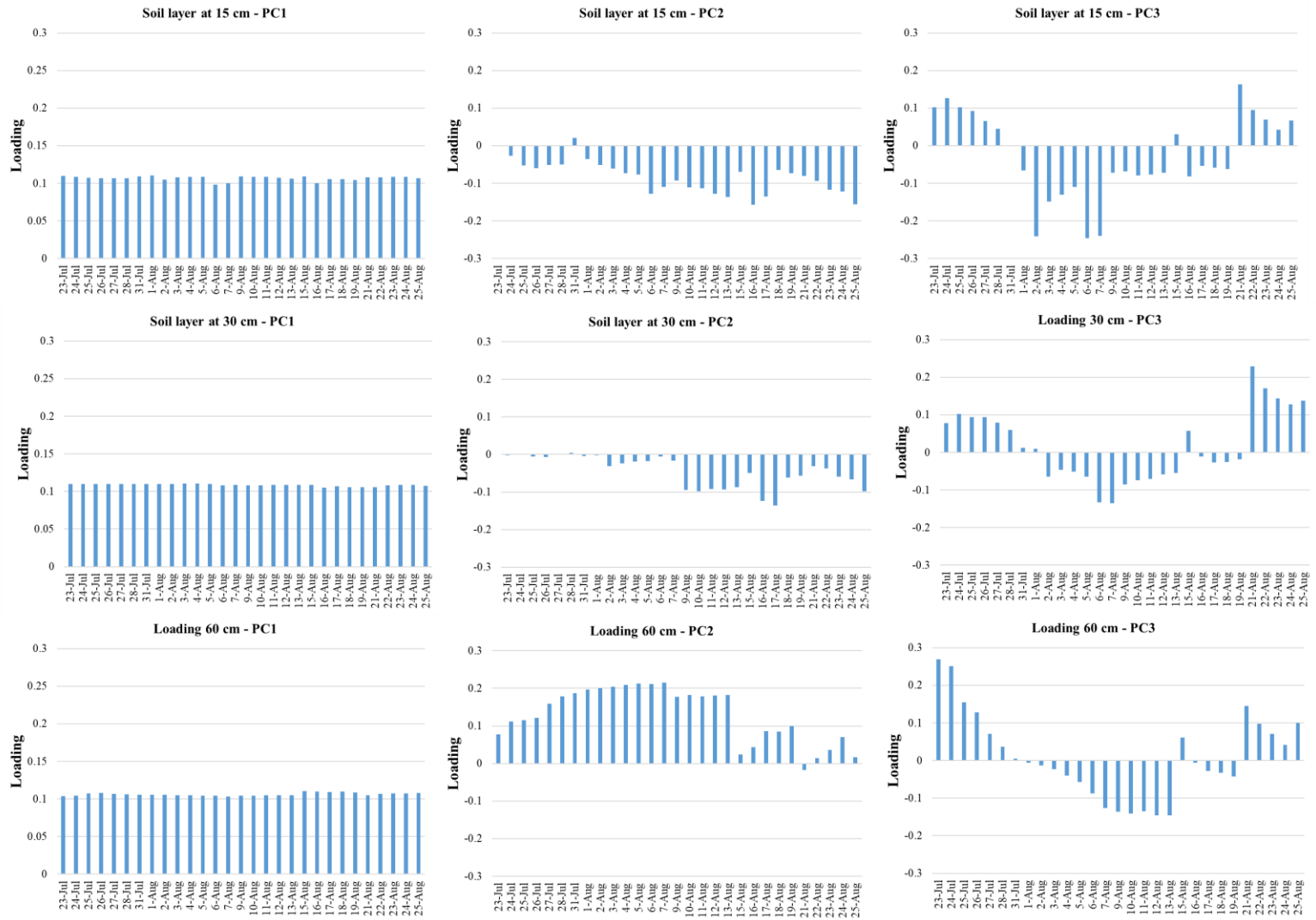

Figure 1.13. Bar plots of the loadings of the first three principal components (PC1, PC2, PC3) identified from the 2019 data for each measurement date and soil depth (15, 30, 50 cm) at the Tanner field. From left to right, each column represent a different PC, from top to the bottom, represent the loadings at each soil depth of 15, 30 and 60 cm. Each bar represent a different measurement date from July to August 2019.

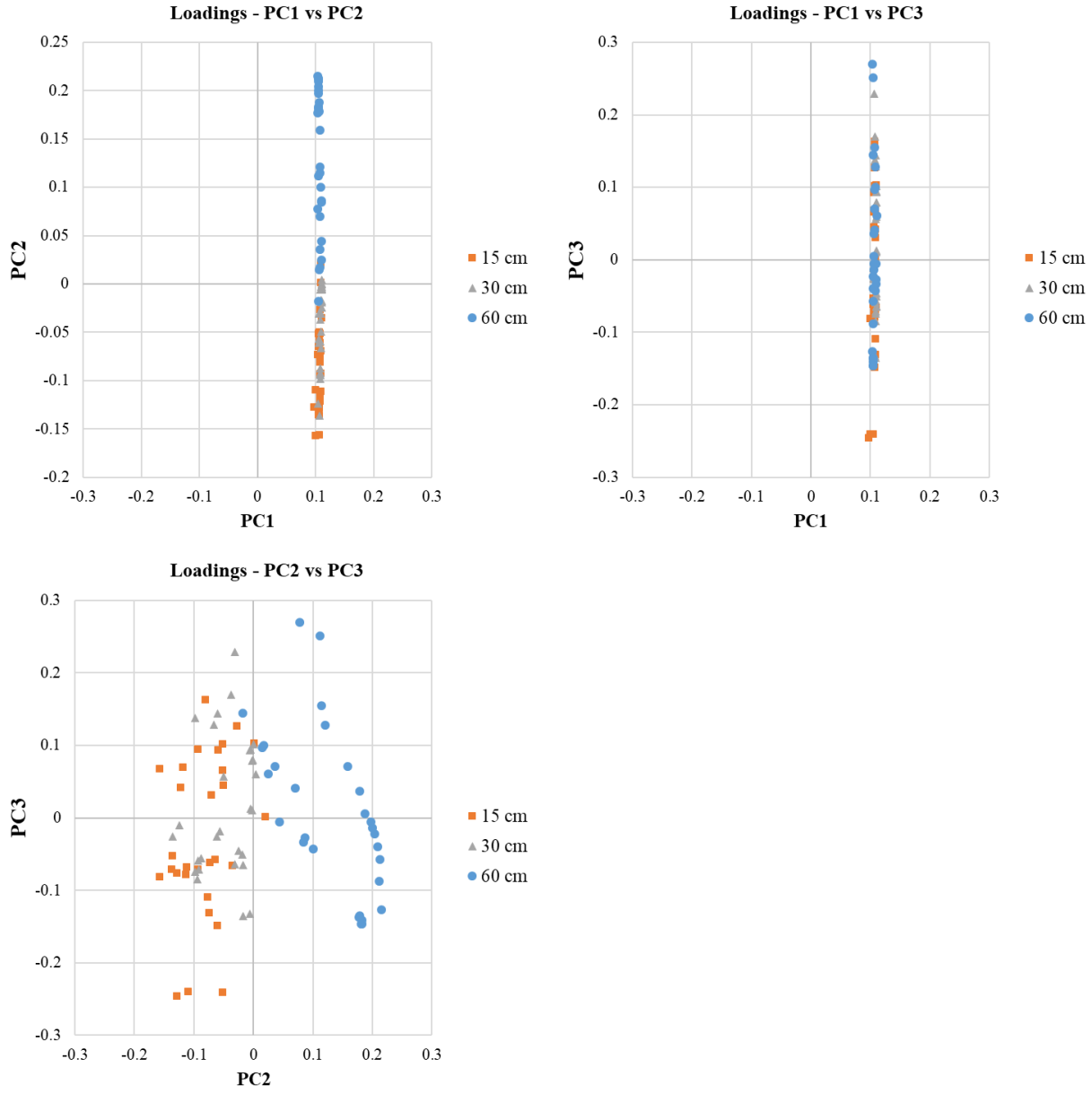

Figure 1.14. Loadings plots of PC1 vs PC2, PC1 vs PC3, and PC2 vs PC3 for the Tanner field in 2019. For each loading plot, every point represents daily mean volumetric water content measured at depths of 15, 30, and 60 cm.

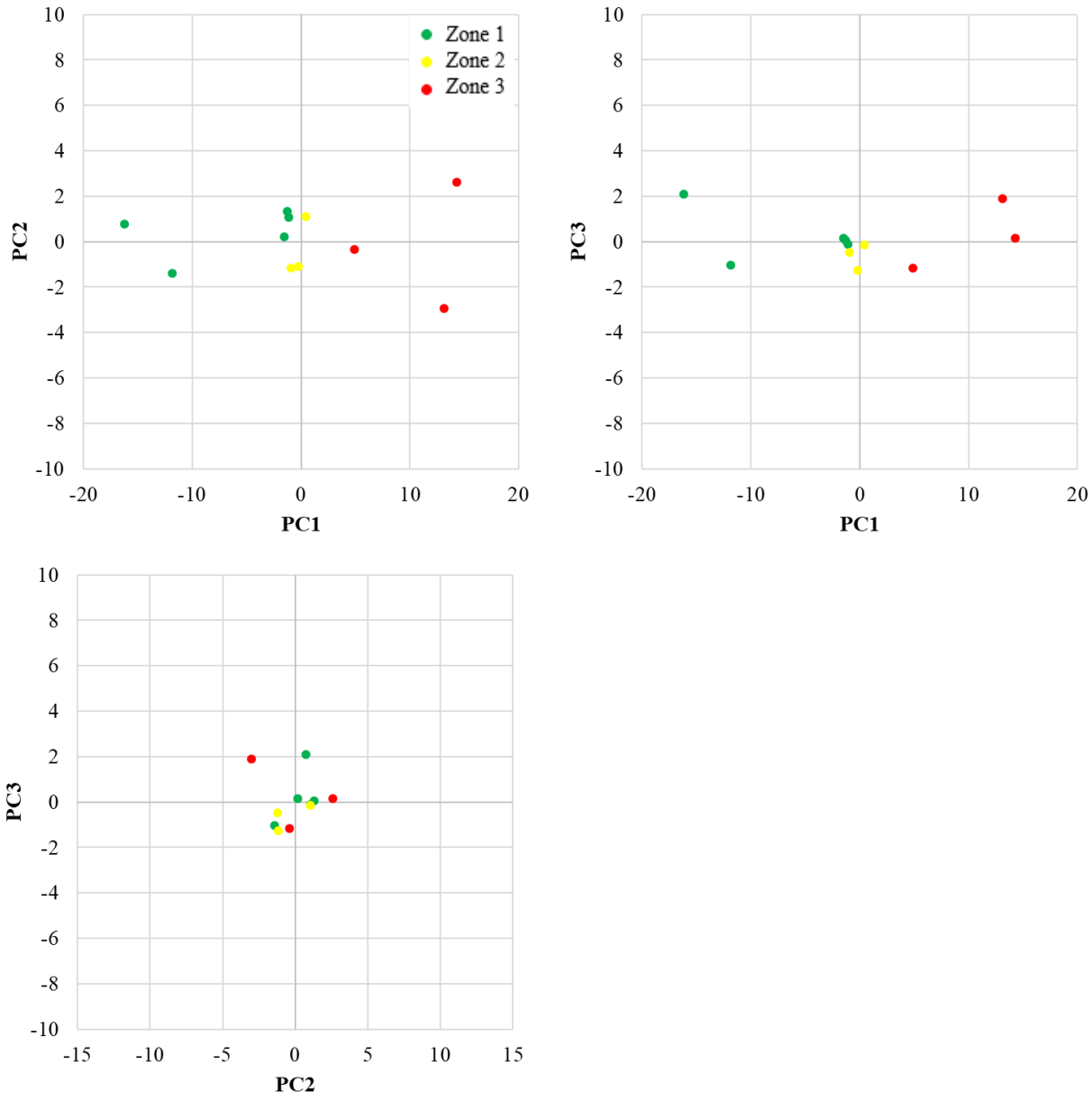

Figure 1.15. Score plots of PC1 vs PC2, PC1 vs PC3 and PC2 vs PC3 for the Tanner field in 2019. Each color refers to a different irrigation management zone where the sensors were installed

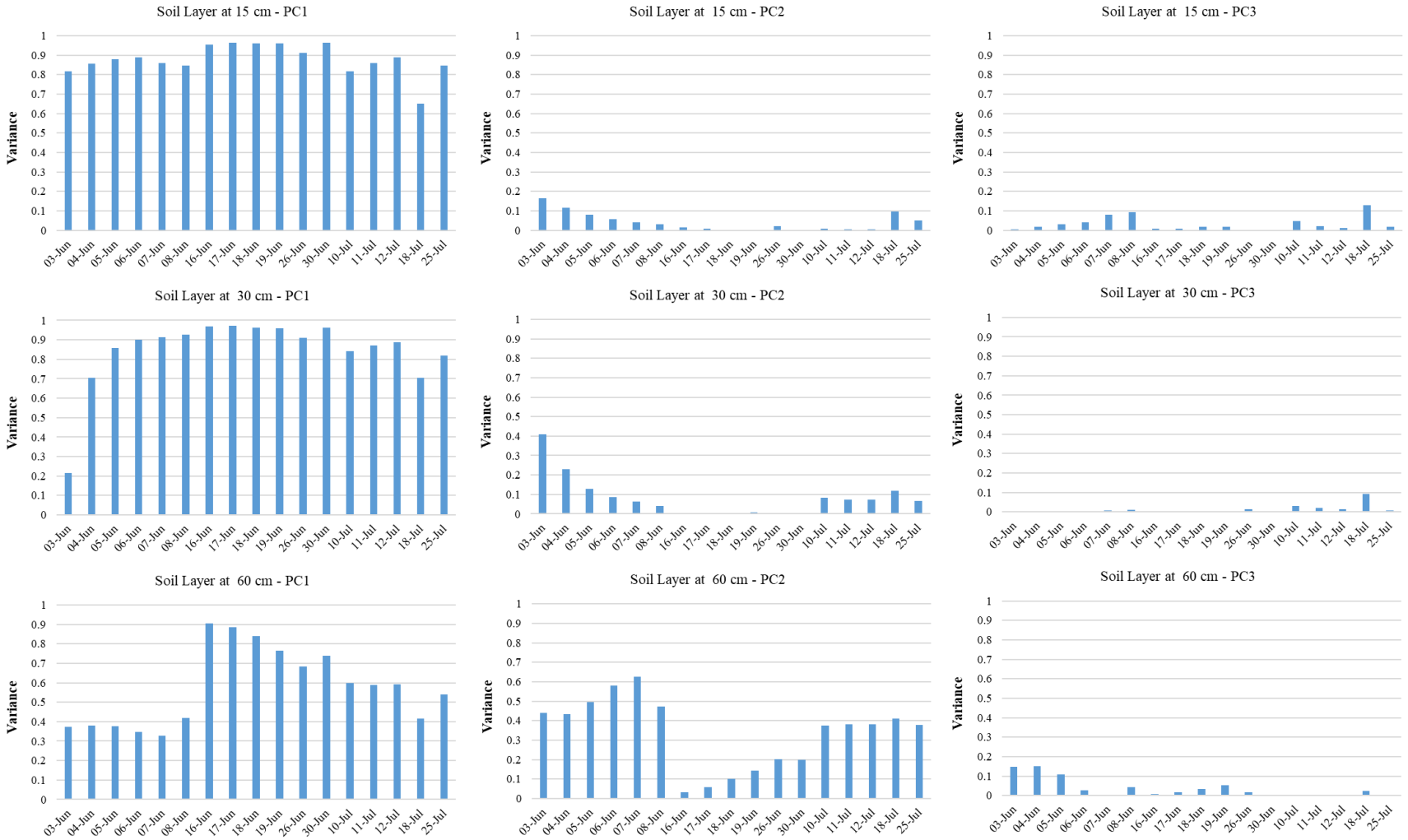

Figure 1.16. Bar plots of the spatial variance of daily volumetric water content explained in 2018 by the first three principal components (PC1, PC2, PC3) for each measurement date and soil depth (15, 30, 60 cm) at the Town Creek field. From left to right, each column represent a different PC, from top to the bottom represent the variance of volumetric water content at depth of 15, 30 and 60 cm. Each bar represent a different measurement date from June to July 2018.

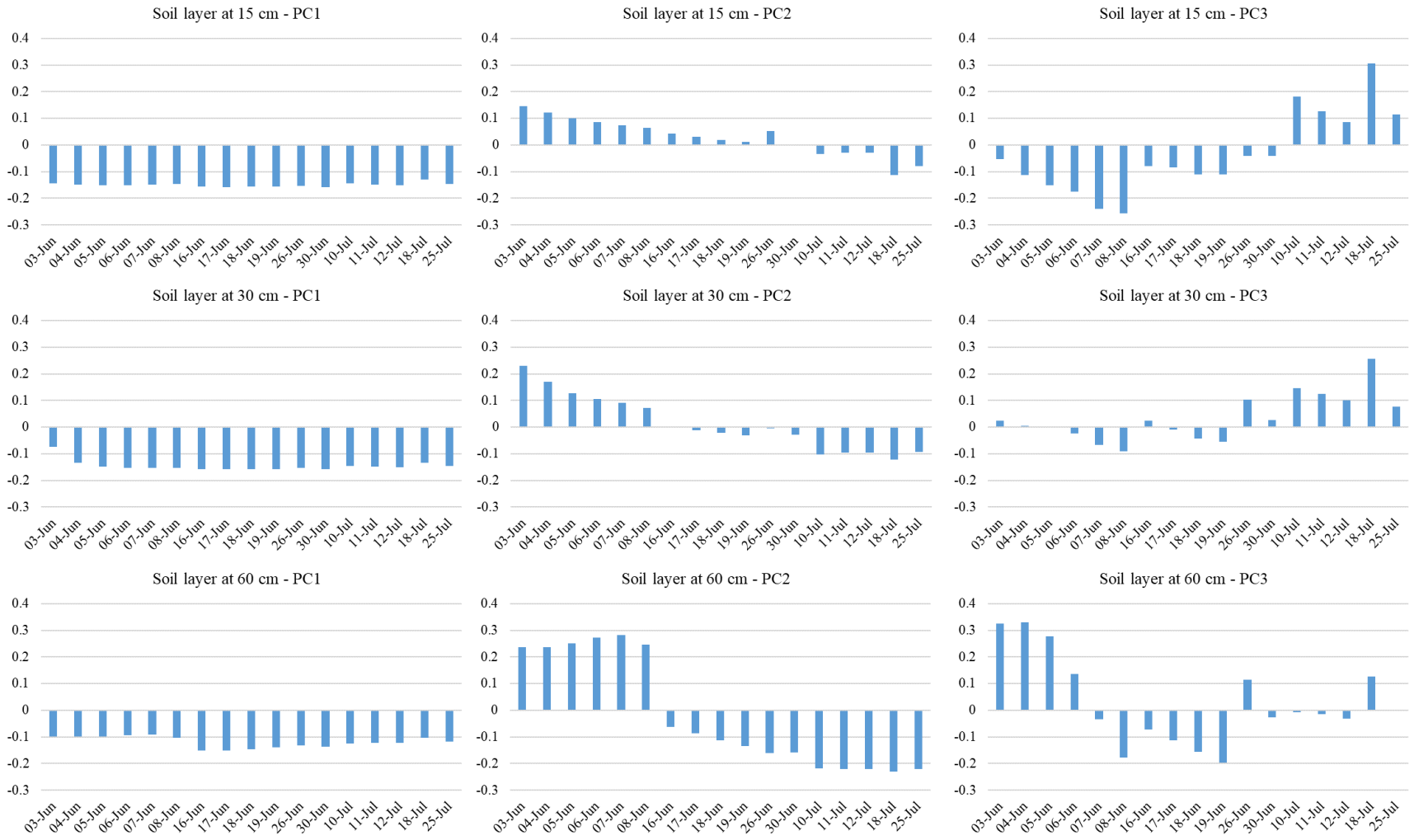

Figure 1.17. Bar plots of the loadings of the first three principal components (PC1, PC2, PC3) identified from the 2018 data for each measurement date and soil depth (15, 30, 50 cm) at the Town Creek field. From left to right, each column represent a different PC, from top to the bottom, represent the loadings at each soil depth of 15, 30 and 60 cm. Each bar represent a different measurement date from June to July 2018.

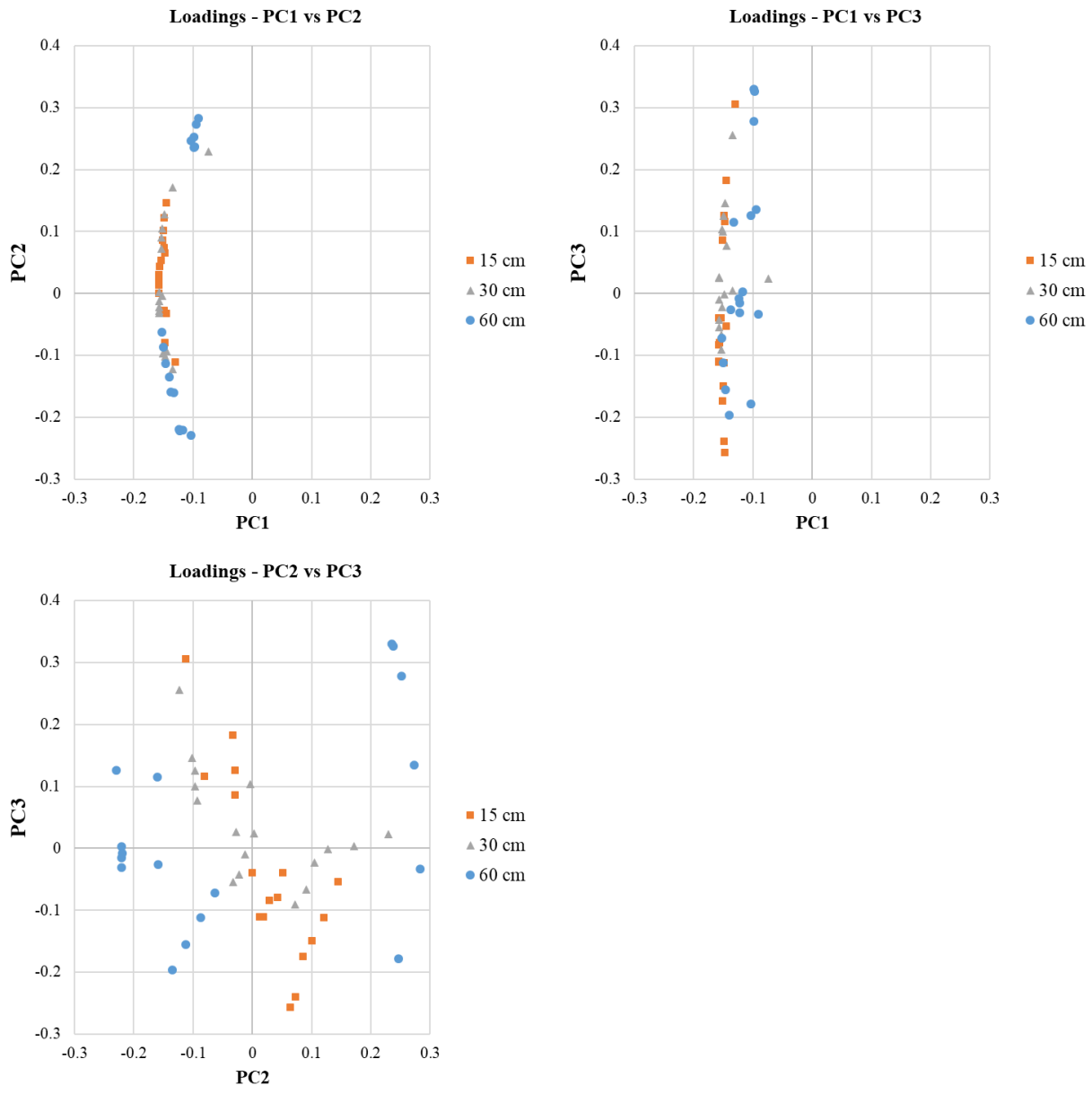

Figure 1.18. Loadings plots of PC1 vs PC2, PC1 vs PC3, and PC2 vs PC3 for the Town Creek field in 2018. For each loading plot, every point represents daily mean volumetric water content measured at depths of 15, 30, and 60 cm.

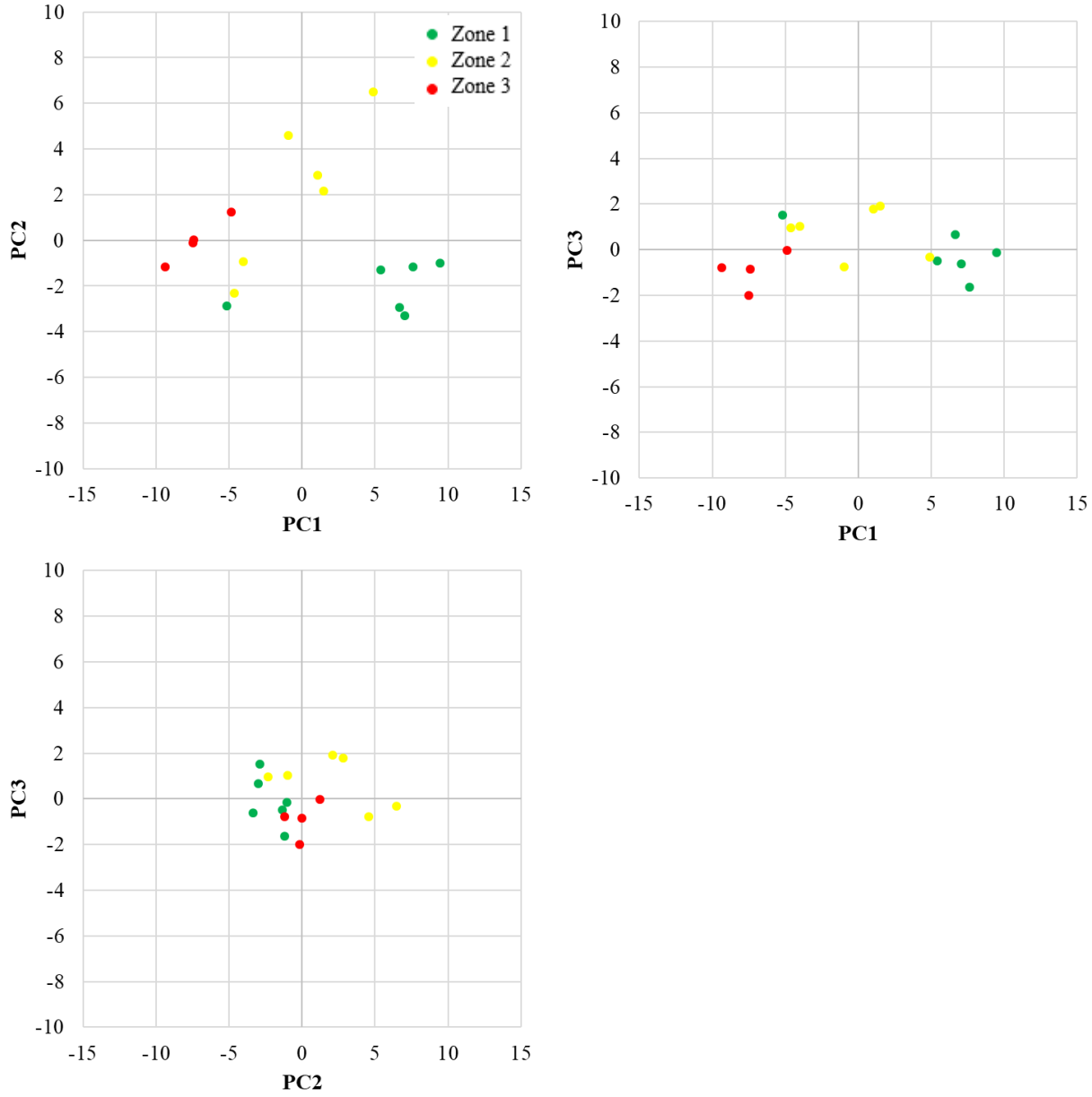

Figure 1.19. Score plots of PC1 vs PC2, PC1 vs PC3 and PC2 vs PC3 for the Town Creek field in 2018. Each color refers to a different irrigation management zone where the sensors were installed.

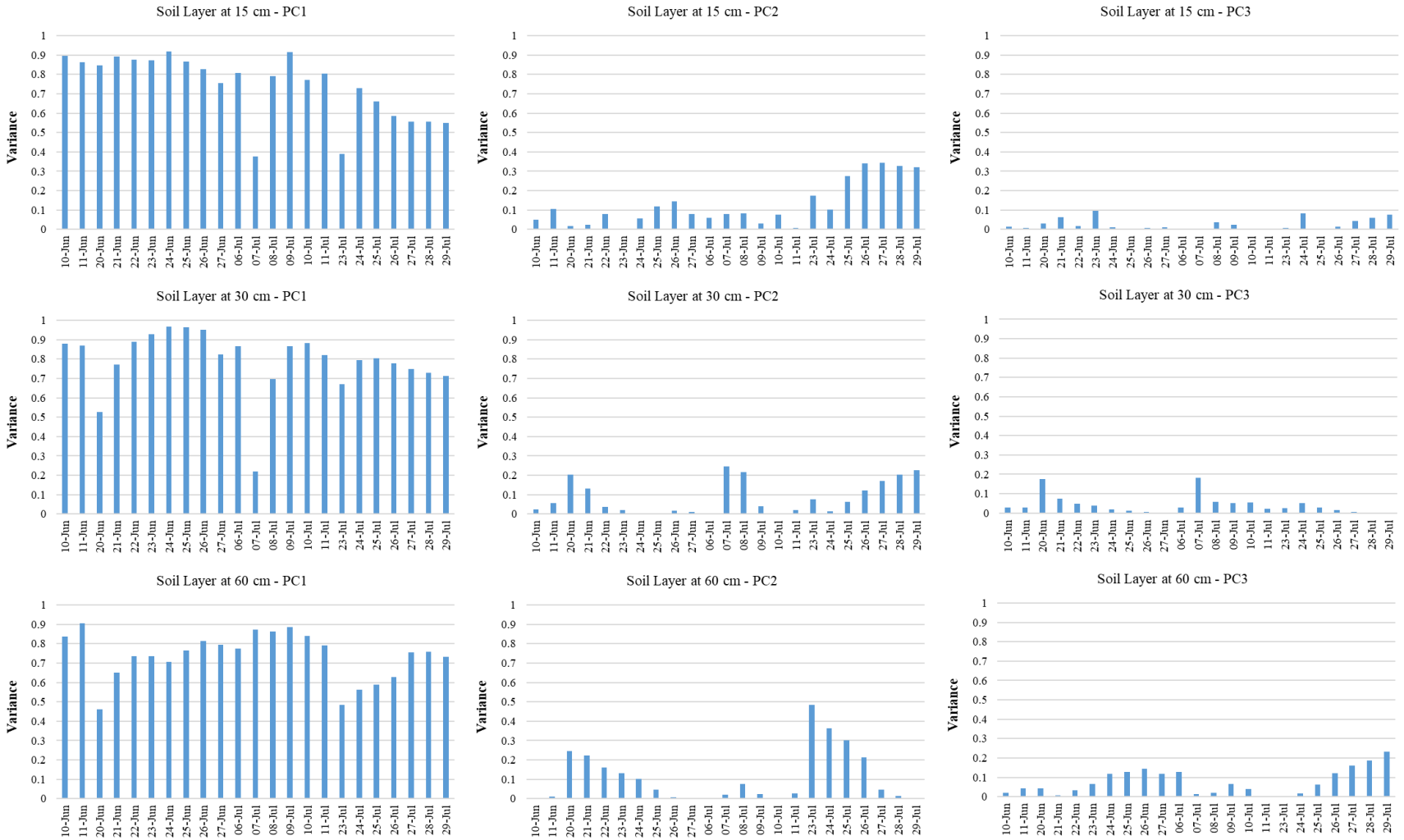

Figure 1.20. Bar plots of the spatial variance of daily volumetric water content explained in 2019 by the first three principal components (PC1, PC2, PC3) for each measurement date and soil depth (15, 30, 60 cm) at the Town Creek field. From left to right, each column represent a different PC, from top to the bottom represent the variance of volumetric water content at depth of 15, 30 and 60 cm. Each bar represent a different measurement date from June to July 2019.

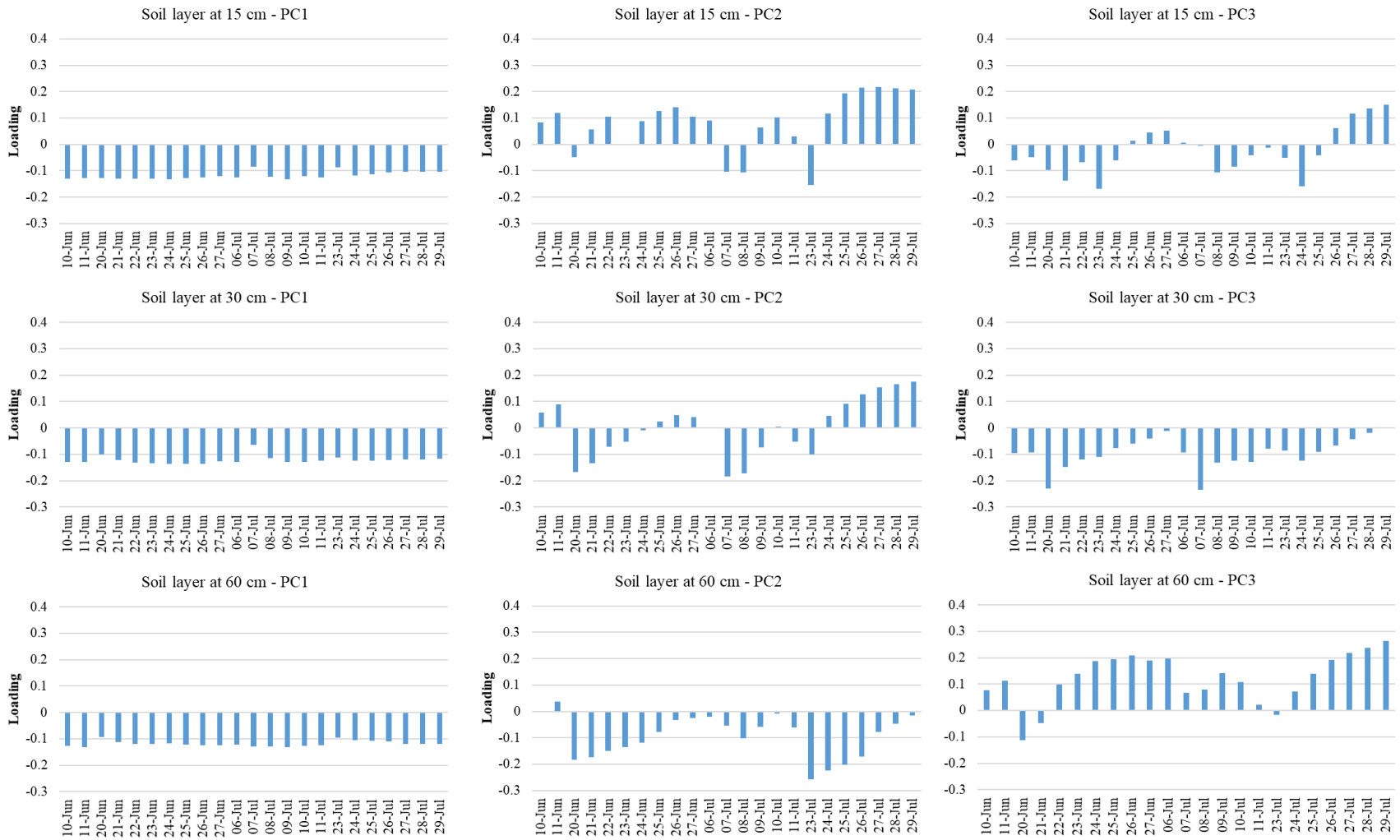

Figure 1.21. Bar plots of the loadings of the first three principal components (PC1, PC2, PC3) identified from the 2019 data for each measurement date and soil depth (15, 30, 50 cm) at the Town Creek field. From left to right, each column represent a different PC, from top to the bottom, represent the loadings at each soil depth of 15, 30 and 60 cm. Each bar represent a different measurement date from June to July 2019.

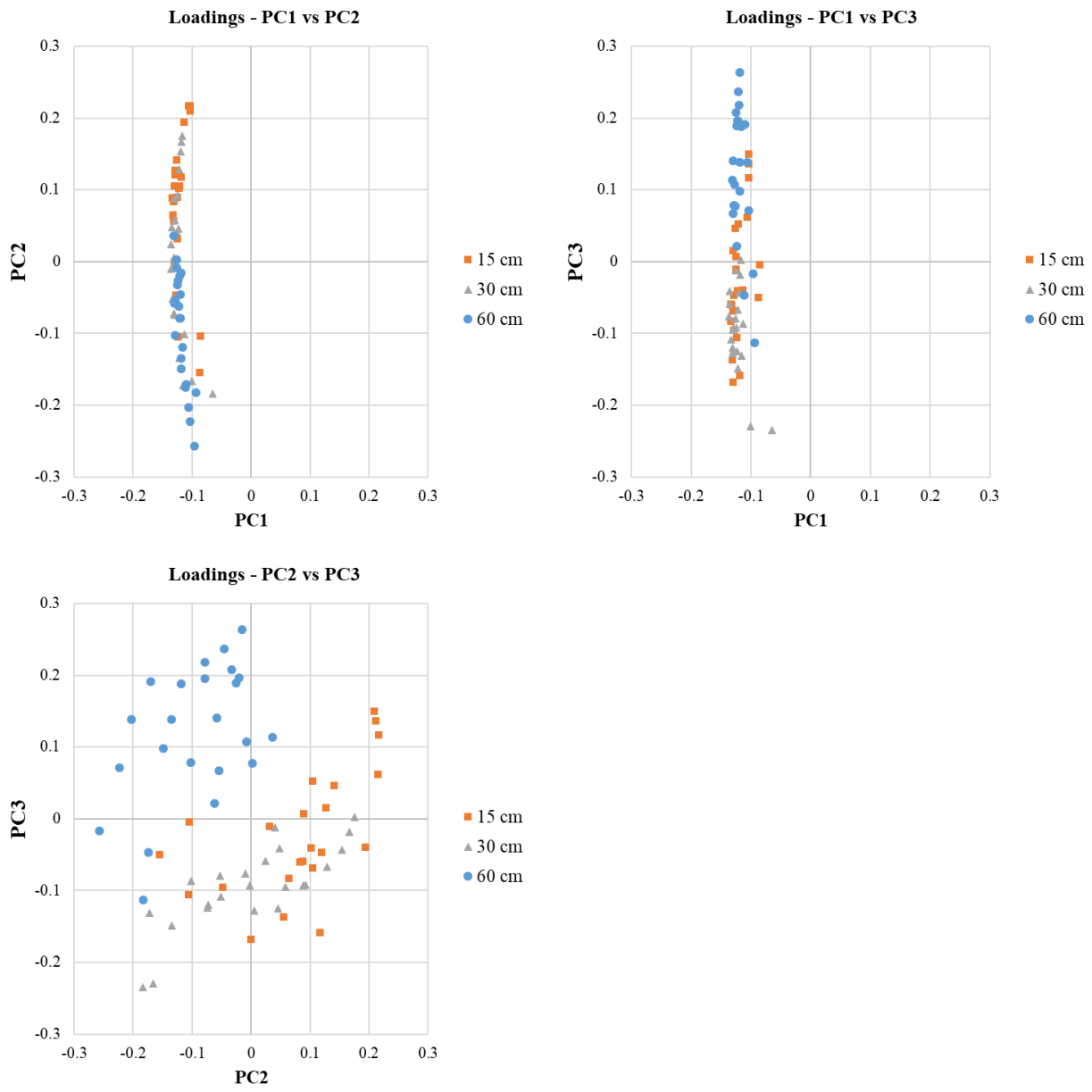

Figure 1.22. Loadings plots of PC1 vs PC2, PC1 vs PC3, and PC2 vs PC3 for the Town Creek field in 2019. For each loading plot, every point represents daily mean volumetric water content measured at depths of 15, 30, and 60 cm.

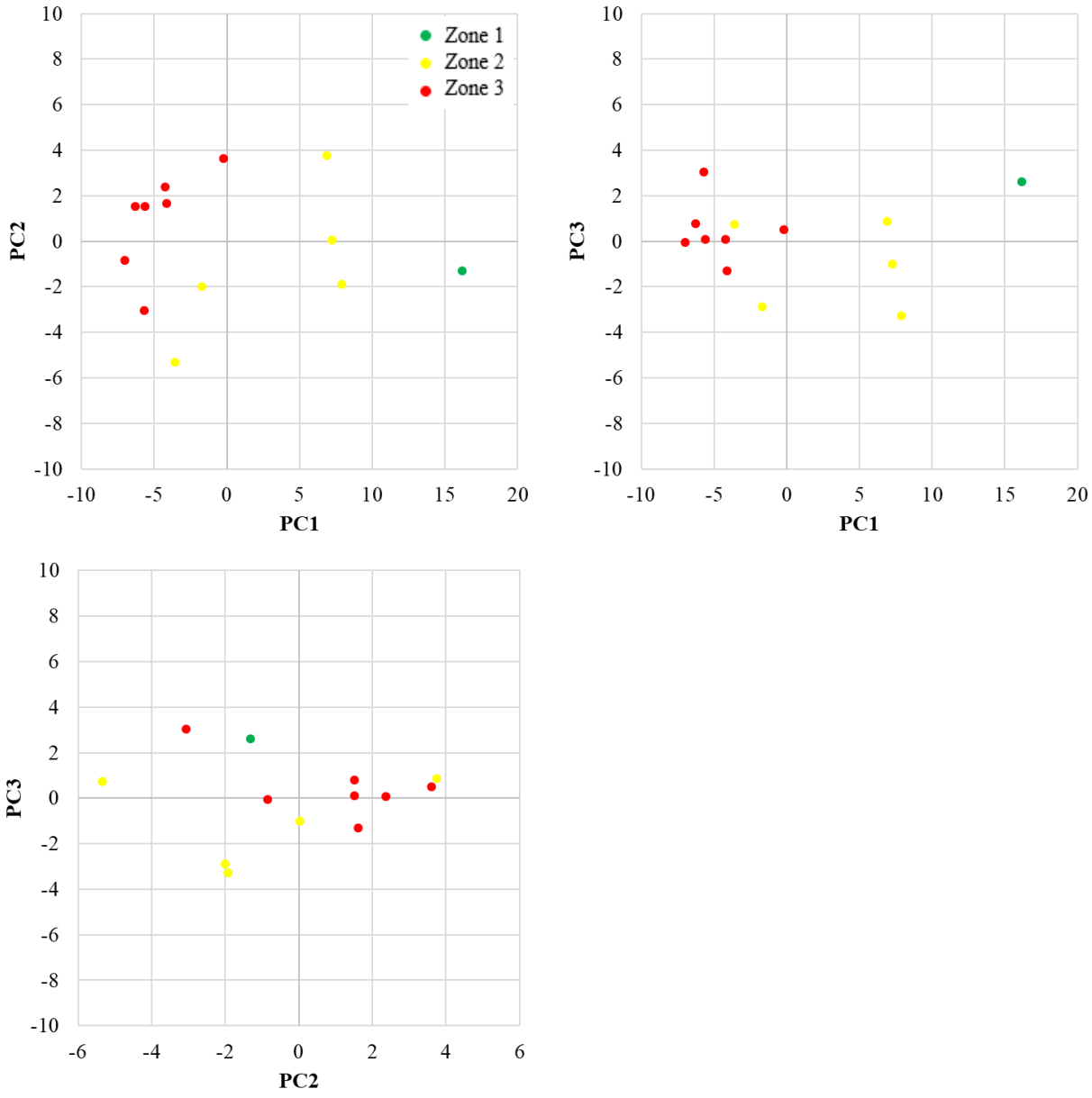

Figure 1.23. Score plots of PC1 vs PC2, PC1 vs PC3 and PC2 vs PC3 for the Town Creek field in 2018. Each color refers to a different irrigation management zone where the sensors were installed.

III. EVALUATION OF DEFICIT IRRIGATION SCENARIOS FOR CORN IN ALABAMA USING CROP GROWTH SIMULATION MODELING

Abstract

Irrigation scheduling is a powerful tool for farmers to increase water use efficiency and to meet crop water demand. Determining the soil moisture threshold to initiate irrigation is one of the most challenging decisions that farmers deal with every season. The objectives of this study were (1) to calibrate and validate the CERES-Maize model in DSSAT v.4.7.5 under the conditions of a 120 hectares irrigated corn field in Town Creek, Alabama, (2) to identify the soil water content threshold, percentage of soil water depletion, to initiate irrigation and irrigation rate for maximizing net returns and irrigation efficiency. Data of leaf area index, volumetric water content, crop yield, and aboveground biomass collected during the 2019 growing season was used for model calibration. The soil type in the field study was a Decatur silty clay loam, which is the predominant soil type for the region where the study field was located. The model was validated using crop yield data during the 2018 growing season. Crop growth simulation of various deficit irrigation strategies was conducted using the seasonal analysis tool in DSSAT using 36 years of weather data (1984-2019). The deficit irrigation strategies tested in this study started from triggering irrigation at 20%, 30%, 40%, 50%, 60%, 70%, 80% and 90% of soil water depletion. The criteria do determine the best deficit irrigation strategy was analyzing the mean-Gini dominance which identify the best strategy in terms of net return and lower risks.

The percent soil water depletion treatment that maximized net returns was used to evaluate irrigation rate treatments required to refill the soil back to field capacity (full rate). The irrigation treatments evaluated were fix water rates of 12.7, 19, 25.4 mm. The results demonstrated that the calibrated model was able to predict well the crop yield with RMSE = 69 kg ha^{-1} (0.5%). The phenology was well predicted with same simulated and observed dates for the anthesis and two days of difference for the physiological maturity. Results from model validation showed

simulated crop yield with RMSE = 450 kg ha^{-1} (3.5%). Simulation results showed that triggering irrigation at 70% of soil water depletion maximized net returns compared to initiating irrigation at greater soil water content. The second step simulated different fixed amounts with the 70% of soil water depletion threshold. Results from this analysis showed that applying a fix irrigation rate of 25.4 mm when the soil reaches 70% soil water depletion increased the net returns. These results could help farmers growing corn under the conditions on a silt loam soil use these thresholds and rates to maximize net returns. The results of this study will help Alabama farmers to manage better irrigation decisions related to irrigation timing and rate to help them increase irrigation water use efficiency, achieve higher yield and improve the profitability.

INTRODUCTION

Irrigation is one of the most important crop management practices used by farmers to achieve high crop yields. Due to the lack or well distributed precipitation during a crop growing season, USA farmers are increasing irrigation adoption as a type crop insurance or way to increase crop yield. Total irrigated land in the United States is about 22.5 million hectares. More specifically, in Alabama, the irrigation has increased by 25% between 2012 and 2017, and the state has a total irrigated farmland of 58,000 hectares (USDA - NASS, 2017). The state is one of the main producers of cotton and peanuts in the country, ranking as number sixth and second producer, respectively. Corn (*Zea mais L.*) production has shown a substantial increase in Alabama in the past years, with 103,200 hectares cultivated in 2018 from which 13% were irrigated (USDA – NASS, 2018). This area indicates then that corn is the second most irrigated row crop in the state. This crop consumes around 600 mm of water during the growing season (Kranz et al., 2008) and irrigation is required to meet water demand preventing crop water stress during a shortage of precipitation.

A local survey conducted with farmers in North Alabama in the 2018 and 2019 growing seasons showed that most of the needs regarding irrigation were related to irrigation scheduling, especially determining irrigation amount and timing. By implementing the technology-based irrigation practices, farmers could improve water use efficiency, soil conservation, sustainably, and profitability. Farmers around the world require more training and information regarding different irrigation scheduling methods and benefits (Howell, 2001). Several irrigation scheduling methods are available for farmers such as the use of soil sensors (Sui, 2017), checkbook method (Harrison, 2012; Melvin & Yonts, 2009), smartphone apps (Vellidis et al., 2014), and others. Each irrigation scheduling method has its advantages and disadvantages

related to costs, implementation, data analysis and liability (Harrison, 2012; Broner, 2005). The majority of farmers still use the crop condition or the feel of the soil as an irrigation scheduling method (USDA – NASS, 2018), which is concerning. These methods provide low accuracy, do not account for field variability, and are time-consuming, especially when the farmer has multiple irrigated fields to manage. Technologies that provide remote and easy access to available information are a good strategy for farmers to be assertive in irrigation decisions. As an example, there are many commercial soil sensors available for farmers that provide accurate information about soil water status and recommend irrigation rates that are useful for irrigation scheduling. However, farmers and crop consultants still lack knowledge of how to use and interpreted soil sensors data, and how to identify the best irrigation management strategy that maximizes yield and, consequently, the net returns (Kisekka et al., 2015).

Crop simulation models have been used in the past to simulate crop responses under different environmental scenarios. More specifically, crop models such as Agricultural Production Systems Simulator (APSIM) (Holzworth et al., 2014), Root Zone Water Quality Model (RZWQM) (Fang et al., 2010), AquaCrop (Raes et al., 2018), and Decision Support System for Agrotechnology Transfer (DSSAT) have been used to evaluate the effect of deficit irrigation strategies on crop yield. The DSSAT group of models have been largely used for simulating plant growth, plant development, and yield for over 42 different crops (Hoogenboom et al., 2019). The CERES-Maize model is integrated within the DSSAT software which uses soil parameters (texture and chemical), weather conditions (precipitation, maximum and minimum temperature, solar radiation, wind speed), and agronomic practices (planting data, row spacing, plant population, seed depth, and management practices) to simulate maize crop developments during a desired growing season (Soler et al., 2007). DSSAT's soil water balance accounts for

irrigation applications, precipitation, infiltration, drainage, soil evaporation and plant water uptake (Ritchie et al., 1998). In addition, DSSAT includes routines that consider the costs of different irrigation strategies as well total irrigation events, total amount applied, and crop yield to determine irrigation strategies that maximizes net returns (Hoogenboom et al., 2004). Kisekka et al. (2015) evaluated different soil water depletion thresholds to trigger irrigation in Kansas and concluded that 50% of plant available water maximized the net returns over different corn price scenarios. Saseendran et al. (2008) also simulated different soil water depletion levels in Northeastern Colorado and observed that triggering irrigation at 80% of soil water depletion optimized the benefits related to corn yield return, total water applied, and the number of irrigations. Even though several studies that simulated different irrigation strategies have been conducted, a site-specific research is needed to identify the best irrigation strategy due to the differences in soil texture, climate conditions, water availability, commodity prices, and field size among different regions of the country.

In North Alabama, soil types vary from clay to silty clay and South Alabama soils mainly represent coarse soiltextures. These significant differences in soil characteristics change substantially soil water holding capacity and plant available water values, suggesting the need for different irrigation management strategies per soil type. Few studies related to irrigation thresholds have been conducted in Alabama. The main objectives of this study were (1) to calibrate and validate CERES-Maize for a specific corn hybrid, soil type, and Alabama weather conditions; (2) to apply the calibrated model to identify the best deficit irrigation strategy to initiate irrigation that maximizes net returns; and (3) to identify the best irrigation amount required for each irrigation application based on the best deficit irrigation strategy to maximize net returns.

MATERIAL AND METHODS

Experimental Field

The study was conducted at a corn field located in Town Creek, Alabama (34º 43’ 6.67” N, 87º 23’ 13.52” W, 181 m above sea level) during the 2018 and 2019 crop growing seasons. The site location is classified as humid subtropical (Cfa) according to Peel et al. (2007) with average annual precipitation of 1,380 mm. The historic average precipitation during the corn growing season, from March to August, is 520 mm. The field has a total of 160 hectares with 120 hectares irrigated by a 12-span Reinke© center pivot system of 623 meter length. The predominant soil type of this field is a Decatur silty clay loam with 2% to 10% slope variation and elevation changes from 169 to 180 meters. In both years, the field was cultivated with the corn hybrid Dekalb® DKC 66-97 of 116 days relative maturity. The field was planted using 0.76 meters row spacing and a plant population of 84,000 seeds per hectare. The agronomic practices such as planting date, fertilization, irrigation events, and harvest are given in Table 2.1.

The experimental field was part of a soil sensor-based irrigation scheduling and variable rate irrigation demonstration study. The field was divided into three different irrigation management zones (MZ) (Figure 2.1). Yield maps from ten years of corn, soybean, and wheat rotation, soil texture, apparent soil electrical conductivity, terrain elevation, and satellite images were analyzed to evaluate the field variability and to delineate the irrigation MZs. The management zone one (MZ1) was designated as the high yielding zone, small changes in slope, and high soil water holding capacity. Management zone two (MZ2) exhibits intermedium yield with slight changes in slope and management zone three (MZ3) is the low yielding one where greater changes in slope occur and soil water holding capacity is the lowest. For this modeling study, the characteristics and data from MZ1 have only being considered was considered due to

the high yield potential and its soil type, one of the most common soil types in the North Alabama region.

Soil Data and Weather

Even though the soil of the experimental site is classified as Decatur Soil Clay Loam based on the National Cooperative Soil Survey (SSURGO), soil cores were collected from several locations within field for soil type, texture, and organic carbon determination (Table 2.2). For the surface layer at 10 cm, soil pH and basic soil fertility parameters were also assessed. For the deeper layers, only soil texture and total nitrogen were analyzed. Each soil core was divided into sections of 15 cm each starting at the soil surface and up to 160 cm depth and sample sections were sent to commercial soil testing laboratory for analysis. Soil water retention curves (SWRC) were generated from undisturbed soil samples at soil depths of 15, 30, and 60 cm. The undisturbed soils were analyzed using a Hydraulic Property Analyzer (HYPROP 2, Meter Group, Inc., Pullman, WA, USA) which determines the relationship between soil matric potential and volumetric water content. This equipment only measures the soil water tension up to 0.085 MPa. The estimation of volumetric water content at higher tensions required use of a dew poring hygrometer equipment (WP4C, Meter Group, Inc., Pullman, WA, USA). Using HYPROP-FIT (Version 4.1.0.0, Meter Group, Inc., Pullman, WA, USA), the Hyprop and WP4 data were fitted using Van Genuchten model (van Genuchten, 1980). The tension value for field capacity was considered 0.033 MPa and 1.5 MPa for the permanent wilting point. Using the same undisturbed soil samples, the soil bulk density was calculated as the weight of dry soil (oven-dried at 105°C) divided by the volume of the undisturbed ring collected (250 cm^3). The SWRC parameters were needed to determine the upper and lower limit volumetric water content of each soil layer, total plant available water, and to convert soil water tension values into volumetric water content for

the soil water balance calibration in DSSAT.

The weather data for the 2018 and 2019 growing seasons was obtained from a Davis Vantage Pro 2 Weather Station (Davis® Instruments, Hayward, California, USA) installed outside the experimental field. The weather station collected data of solar radiation, precipitation, maximum and minimum temperature, wind speed, relative humidity, and dew point temperature at a 15 minutes interval. The weather data for the period of 1984 to 2019 used for the seasonal analysis was obtained from NASA Langley Research Center Atmospheric Science Data Center Surface meteorological and Solar Energy (SSE) web portal supported by the NASA LaRC POWER Project (Stackhouse, 2020). The average precipitation, solar radiation, and maximum and minimum temperature from 1984 to 2019 are given in Figure 2.2.

Plant Measurements

The corn growth stages were recorded during the growing season from vegetative stages to crop physiological maturity. The most important dates for model calibration were anthesis and physiological maturity dates. Growth stages during the vegetative stage were determined using the collar method which considers the number of leaves with visible collars (McWilliams et al., 1999). Tasseling stage was determined when tassel was visible and the silking stage was determined when more than 50% of the plants had the silks outside of the husks. Physiological maturity was determined with the presence of the black layer by sampling five different corn ears.

Volumetric water content (prior to planting) and previous crop residues were collected and the values were inputted as initial conditions in the model. Three days before planting, the volumetric water content was collected at 15 cm and 30 cm soil depth from two different locations within MZ1. Soil samples for volumetric water content were collected using 250 cm^3 rings. The weight (wet) each soil sample was recorded from before the samples were placed

into the oven (105°C) and after samples achieved constant dry weight. The volumetric water content was calculated as the ratio between the mass of water and sampling volume. Crop residue biomass was assessed by collecting all residue of a 1 m^2 from two different locations within MZ1. The collection of crop reside biomass was performed at the planting and represented the amount of crop residue left from the previous planted crop that could potentially become of source of nitrogen. Samples were oven dried at 70°C and weighted until they achieved constant mass. Total weight was used to estimate the crop residue in kilogram per hectare. The dry crop residue samples were sent to a commercial laboratory to determine their nitrogen and phosphorus content.

Above-ground corn biomass were collected during the 2019 growing season at 35, 64, and 92 days after planting (DAP) and at harvest (154 DAP) by sampling four-meter rows. For each sample, leaves, husks, ears, and stems were separated and then oven-dried at 70°C until they reached a constant mass. Leaf area index (LAI) was collected at 57, 72, 92 and 128 DAP only during the 2019 growing season using a LAI-2200 instrument (LI-COR, Inc., Lincoln, NE, USA). The LAI was measured from four different locations within MZ1 with five replications for each location.

Yield at harvest was recorded from six different locations within MZ1. Six-meter rows of whole plants were harvested manually and then separated into components (leaves, steam, ear, and husk) and hand harvested from each sampling location during the 2018 and 2019 growing seasons. The biomass components were oven dried following the same procedure for the within-season above-ground biomass determination. A total of 20 ears were selected from each sample to determine the number of grains per ear. For kernel moisture determination and grain weight, a total of 2,000 seeds were considered. The kernels were weighed, and yield was corrected to 0%

moisture.

Volumetric water content

The soil volumetric water content in 2018 and 2019 were assessed using Watermark® soil sensors. Soil sensor probes with three Watermarks located at 15, 30 and 60 cm were installed in the field at 30 DAP, and hourly data were recorded until the crop reached physiological maturity. For the model calibration of soil water balance of this study, 72 and 88 days of data were used in 2018 and 2019, respectively.

The Watermark sensor measures the electrical resistance by two electrodes inside of the sensor. The resistance is converted to soil matric potential value (or soil tension) expressed in kilopascal (kPa) using the equation developed by Shock et al. (1998):

$$\Psi(\Omega) = -\frac{(4.093 + (3.213 * k\Omega))}{1 - (0.009733 * k\Omega) - (0.01205 * T_s)} \quad (1)$$

where $\Psi(\Omega)$ is the soil matric potential in kPa, $k(\Omega)$ is the resistance value, and T_s is soil temperature in ºC.

Data from three soil sensor probes installed at MZ1 were used for the soil water balance calibration in 2019. For each soil depth, the daily average of soil water tension values was considered. The soil water tension values were converted into volumetric water content using the van Genuchten method and SWRC parameters, as given below:

$$\theta(\psi) = \theta_r + \frac{\theta_s + \theta_r}{[1 + (\alpha|\psi|)^n]^m} \quad (2)$$

where $\theta(\psi)$ is the soil volumetric water content (cm^3/cm^3), θ_r is residual water content ($cm^3\ cm^{-3}$), θ_s is saturated water content ($cm^3\ cm^{-3}$), α is related to the inverse of the air entry suction (cm^{-1}), $|\Psi|$ is suction pressure (cm of water), and *m* and *n* are the empirical shape-defining parameters (dimensionless).

Model Calibration and Evaluation

Cultivar Coefficients

The data collected from the 2019 growing season was used for the CERES-Maize model calibration. Since the corn hybrid (DKB 66-97) used in this study was not available in the CERES-Maize model database, a similar hybrid (PIO 31P42) was used as a basis for starting the genetic coefficients calibration of the new hybrid (Isasmendi, 2013). This hybrid was already calibrated for Alabama conditions in a previous study. The Generalized Likelihood Uncertainty Estimation (GLUE) tool was used for cultivar coefficient estimation with a total of 50,000 runs. After running GLUE, the sensitivity analyses tool was used to estimate the cultivar coefficients value that minimized the error between simulated and measured values of phenology dates (anthesis and physiological maturity), biomass (leaf, stems, tops weight, LAI), crop yield (grain weight), and yield components (kernels per m^2 and unit grain weight). There are six cultivar coefficients that are used for corn calibration and are described in Table 2.3. The calibration process was divided into two parts. The first part was the plant development and life cycle calibration. This was performed by calibrating P1, P2, P5, and PHINT values. The second part consisted on calibration of parameters that affected crop yield and plant growth (G2 and G3).

Different statistical parameters were used to evaluate each iterative step of model calibration. The parameters considered were root mean square error (RMSE) and the Index of Agreement (*d-stat*) proposed by Willmott, 1982. For RMSE, the closer the value is to zero, the better the relationship between simulated and observed values. In contrast, the Index of Agreement varies from zero to one, with values close to one indicating the best agreement

between simulated and observed values. The index of agreement works best with time series of data. Equations 3 and 4 were used to calculate RMSE and *d-stat*, respectively.

$$RMSE = \left[N^{-1} \sum_{i=1}^{n} (P_i - O_i)^2 \right]^{0.5} \quad (3)$$

$$d - stat = \left[\frac{\sum_{i=1}^{n} (P_i - O_i)^2}{\sum_{i=1}^{n} (|P_i'| + |O_i'|)^2} \right], 0 \leq d \leq 1 \quad (4)$$

where N is the number of observed values, P_i is the predicted observation, O_i is the measured observation, P'_i is the prediction observation minus the mean observed variable, O'_i is the measured observation minus the mean observed variable.

Soil Water Balance

The soil sensors probes used in the study measured changes in soil water content at soil depths of 15, 30 and, 60 cm. As the soil layers were divided every 15 cm in DSSAT (Table 2.2), the layers considered for the soil water content measurements were soil layers two (10 to 25 cm), three (25 to 40 cm) and five (55 to 70 cm). The soil parameters collected included lower limit (LL, $cm^3\ cm^{-3}$) where plants are not able to extract water, drained upper limit or field capacity (DUL, $cm^3\ cm^{-3}$), saturated water content (SAT, $cm^3\ cm^{-3}$), saturated hydraulic conductivity (KSAT, cm h^{-1}), bulk density (g cm^{-3}), and root growth factor were first generated by SBuild Program of DSSAT Version 4.7.5 (Hoogenboom et al., 2019). Changes in LL, DUL, SAT, KSAT and growth factor were necessary to match the simulated and observed, minimize the root mean square error, and maximize the Index of Agreement. The values for the runoff curve number (73), soil drainage factor (0.4) and soil albedo (0.13) were generated with SBuild program based on soil texture, slope, and drainage for the experimental site. These values were not changed during the calibration process.

Model Validation

The data collected during the 2018 growing season were used for the model validation. The data considered for model validation were crop yield, grain unit weight, kernel number per square meter, and volumetric water content over 72 dates. For the validation, only the RMSE was used to evaluate crop yield and yield components.

Evaluation of Deficit Irrigation Strategies

After calibrating and evaluating the CERES-Maize model for simulating corn growth, development and yield, the model was used to study the effect of different deficit irrigation scenarios were assessed to identify the best irrigation threshold needed to initiate irrigation, so it maximizes crop yield and net returns. Different soil water depletion scenarios representing various plant available water thresholds were evaluated to trigger irrigation. Eight different soil water depletion of plant available water treatments were tested using historical weather data from 1984 to 2019. The seasonal analysis tool in DSSAT allows simulation of crop yield under the same management strategy over multiple years of weather data (dry, wet, and average climate years) (Hoogenboom et al., 2019). The agronomic practices (rates, timing, operations) used in the seasonal analysis were the same as in the 2019 growing season. For all deficit irrigation strategies evaluated in this study, it was considered nitrogen fertilization of 67 kg N ha^{-1} at planting and 201 kg N ha^{-1} at side-dress application. The irrigation efficiency of the center pivot was considered as 88%, with a plant population of 7.7 plants m^{-2}, and row spacing of 0.76 cm. This analysis allowed evaluation of possible interaction between irrigation management and weather conditions on crop growth and yield. This type of analysis helps in identification of the optimal crop management strategies either across all weather scenarios or specific ones.

Treatment 1 on this analysis was defined as irrigation initiation when the plant available water level reached 20% of depletion, as subsequent treatments from two through eight 10% of depletion increment each (Table 2.4). The soil water depletion of plant available water was calculated based on the total soil water holding capacity of the soil after calibrating the soil water balance. The plant available water (PAW) and soil water depletion were calculated using equations 5 and 6:

$$PAW = DUL - LL \tag{5}$$

$$Soil\ water\ depletion = \left[\frac{(DUL - WC_i)}{(DUL - LL)}\right] * 100 \tag{6}$$

where DUL is the volumetric water content at the drained upper limit or field capacity, LL is the volumetric water content at the lower limit or permanent wilting point and, WC_i is the measured volumetric water content at a specific time.

For each one of the soil water depletion scenarios evaluated, the irrigation amount was calculated based on the total amount of water required to bring the soil back to field capacity. The model was set to automatically irrigate when the soil water depletion reached the target for each soil water depletion treatment in the top 60 cm. The simulation on different soil water depletion percentage levels resulted on different irrigation amounts required to refill the soil back to field capacity for each treatment. The center pivot efficiency was also included in the irrigation calculation. The efficiency of the study field center pivot was 88%. The 88% irrigation efficiency was determined by assessing the uniformity of water application running a catch can test prior the 2019 planting season. The soil depth of 60 cm was considered on these analyses of

the irrigation trigger and irrigation amount calculation because about 60% of corn roots are located at the soil depth (Laboski et al., 1998). Corn roots can achieve deep layers, but the 60 cm soil profile represents the zone where most of corn water uptake occurs and therefore it is the depth used for irrigation scheduling calculations (Kranz et al., 2008).

Identification of the best deficit irrigation strategy and best irrigation rate

The identification of the most efficient irrigation threshold that maximizes net returns was performed using the mean-Gini dominance (MGD) analysis tool in DSSAT (Hoogenboom et al, 2019; Kisekka et al., 2015). The MGD compares two possible risks scenarios related to the net return ($ ha^{-1}), A and B, scenario A is better than B by MGD if:

$$E(A) \geq E(B) \tag{7}$$

$$\text{and } E(A) - G(A) \geq E(B) - G(B) \tag{8}$$

where E(.) is the mean, and G(.) is the Gini-mean difference of distributions A and B.

The MGD analysis assumes that the decision maker is averse to risk and then, it provides support to make an assertive management decision. The Gini coefficient is a measurement of statistical dispersion and it is calculated as expressed in equation 9:

$$G = \frac{\sum_{i=1}^{n}\sum_{j=1}^{n}|x_i - x_j|}{2n^2\mu} \tag{9}$$

where $|x_i - x_j|$ is the absolute difference of a randomly selected pair of values of a random variable, and μ is the arithmetic mean.

After the best treatment was identified using MGD tool, this treatment was used for a second run of analysis. This analysis used the same historical weather data (1984 to 2019) and three different irrigation rates were considered and tested using MGD tool. The irrigation rates simulated were 12.7, 19, and 25.4 mm, and full rate (48 mm). It is important to emphasize that

most farmers, especially in North Alabama where heavy soils are found, do not apply irrigation rates over 25.4 mm because of potential runoff, therefore the greatest fix irrigation rate selected for the analysis was 25.4 mm. The 48 mm rate was also added to simulate the effect of full rate on net return but instead one application of 48 mm, it was considered this rate divided in two irrigation applications.

This analysis required production and irrigation cost data as input. The corn price considered in this analysis was \$0.14 kg^{-1}, based on the average corn price for the last four years. Cost for irrigation was considered as \$0.027 mm^{-1}, seed costs, fertilizers and based costs were considered for a target of corn yield of 15,700 kg/ha. The costs were obtained from the "Irrigated Corn Budget" developed by Runge et al. (2019).

RESULTS AND DISCUSSION

The historical monthly average precipitation (1984-2019), and the 2018 and 2019 monthly growing season records are shown in Figure 2.3. During the 2019 growing season, dataset year used for model calibration, monthly precipitation values were below the historic records in March, May, June, and August, and above the historical average in April and July. In 2018, accumulated monthly precipitation was below the historical average in March and July, whereas higher numbers were observed in April, May, June, and August. During both years, corn production could have been impacted by precipitation below historic average values in July 2018 and May-June 2019. These periods correspond to corn reproductive growth stages from tasseling to grain filling, which are most sensitive to water deficit conditions. The lack of precipitation was supplemented by irrigation events to avoid crop water stress and to maintain the high yield potential. Irrigation dates and amounts are presented in Table 2.1.

Model Calibration and Validation

Cultivar Coefficients

The cultivar coefficients were estimated based on crop growth, yield components, crop yield, biomass and phenology. The coefficients were adjusted for the corn hybrid DKC 66-97 utilized in this study. Table 2.3 shows the final values for each of the six cultivar coefficients calibrated. The hybrid PIO 31P42 that was used a basis for the calibration was modified by changing the cultivars coefficients to match the yield, grain unit weight, LAI, and biomass measured values of the new hybrid. Table 2.3 shows the values for each cultivar coefficients for both hybrids. The DKC 66-97 hybrid used in this study compared to the PIO 31P42 hybrid had higher values for P1, G2, G3 and PHYNT and lower values for P2 and P5. These differences between both hybrids could be explained by the differences in growing hybrid cycle and their own genetic characteristics. However, using a previously calibrated hybrid for Alabama as a basis helped to improve and to calibrate the hybrid selected for the study.

The simulated phenology dates after calibration shown in Table 2.5 were in a good agreement with observed values. For the anthesis date, both the model and the observed data were found to be the same (78 DAP). The physiological maturity date was two days late compared to the observed data.

Soil water content

The volumetric soil water content was calibrated by adjusting the values of DUL, LL, SAT, KSAT, and root growth factors for each soil depth to match simulated with observed values. Table 2.6 shows the calibrated values for each soil depth and variable. The calibration process started by changing DUL and LL values from the estimated soil water retention curves. The changes started in the top layer and continue through to the bottom of the soil profile and the

RMSE and *d-stat* were evaluated in order to identify the values that best approximate the simulated to the observed values. The DUL values varied from 0.3 $cm^3\ cm^{-3}$ to 0.425 $cm^3\ cm^{-3}$. The shallow soil layers showed lower values of DUL and the deeper soil layers the greatest DUL values. The same pattern was observed on the LL values with the first layers showing lower values when compared to deeper layers, varying from 0.190 $cm^3\ cm^{-3}$ to 0.264 $cm^3\ cm^{-3}$. In addition, values of KSAT, SAT, and root growth factors were modified to increase the agreement between simulated and observed values. The root growth factor was adjusted to decrease RMSE and increase *d-stat* for the simulated yield, biomass, LAI, and soil water content variables. Changes on the root growth factor values for this study were considered until the layer 100-115 cm. Since minimal changes in volumetric water content in the deeper layers were found, it was assumed that the roots system did not reach soil depth beyond 115 cm. Figure 2.4 shows the daily changes on soil water content after calibration for each soil depth where soil sensors were measuring daily soil water changes. For all the three measured layers (10-25, 25-40, and 55-70 cm), low RMSE values and *d-stat* values close to one were recorded. Layer 10-25 cm showed RMSE of 0.026 $cm^3\ cm^{-3}$ which represent 9% of difference between observed and simulated and *d-stat* of 0.875. Both RMSE and *d-stat* values indicated stronger agreement between observed and simulates values for the two deeper layers. The layer at 25-40 cm demonstrated a RSME of 0.022 $cm^3\ cm^{-3}$ (6%) and *d-stat* of 0.899, and RMSE of 0.015 $cm^3\ cm^{-3}$ or 5% and *d-stat* of 0.957 for the 55-70 cm layer. RMSE was low for all three layers and *d-stat* values higher than 0.87, showing a strong agreement between observed and simulated values for all soil depth evaluated.

Leaf Area Index and Above-Ground Biomass

After model calibration, simulated LAI values followed the trend of observed values. The time series of observed and simulated LAI data for the study hybrid is presented in Figure 2.5. In general, the LAI increased until it reached the maximum value at the end of the vegetative period and then started to decrease due to leaf senescence towards the end of the growing period. The maximum LAI value for the simulated was 4.25 $m^2 m^{-2}$ and the observed was 4.13 $m^2 m^{-2}$ (Table 2.5). The simulated LAI reached the maximum value before the observed values and, by the end of the season, simulated LAI was about 0.7 $m^2 m^{-2}$ lower than the observed LAI. The statistic values for the LAI measurements demonstrated a RMSE of 0.585 $m^2 m^{-2}$ and *d-stat* of 0.88.

The simulated above-ground biomass values at maturity was compared to the observed value (Table 2.5). The final observed value was 24,232 kg ha^{-1}, while simulated was 22,955 kg ha^{-1}, which was only 5% lower than the observed value. The first two above-ground biomass samples collected at 35 DAP and 64 DAP showed a perfect match with the simulated values (Figure 2.6). Even though the last two measurements at 92 DAP and 154 DAP showed a small difference between values measured and simulated, a small RMSE value (kg ha^{-1}) and a high d-stat value (0.99) were found, indicating an agreement between the simulated and observed for above-ground biomass (Figure 2.6).

Yield and Yield Components

Yield components and final crop yield were well predicted by the model after calibrating soil parameters, soil water balance, and cultivar coefficients (Table 2.5). The unit grain weight at maturity was equal to 0.337 g $unit^{-1}$ and had RSME of 0.001 g $unit^{-1}$, suggesting that the simulated value was the same as the observed. The number of grains per square meter value at maturity was also well predicted. The simulated value was 3,563 grains m^{-2} and the observed 3582 grains m^{-2}, which corresponded to a RMSE = 19 grains m^{-2}, which corresponds to 0.5%

error. The final simulated crop yield showed good agreement with the observed value. The RMSE was 69 kg ha^{-1}, which corresponded to 0.5% error, showing strong yield prediction after the model calibration.

Model Validation

The crop yield and yield components data measured during the 2018 growing season were used model validation. During the 2018 growing season, higher precipitation amounts and more evenly distributed were registered compared to the 2019 growing season, which could explain the high records of crop yield. The final yield was well predicted by the CERES-Maize model in 2018 season as shown in the Table 2.7. The simulated yield was 12,155 kg ha^{-1} and the observed 12,605 kg ha^{-1} which results in a RMSE of 450 kg ha^{-1} (3.5%). For the yield components, the model simulations showed a strong agreement with observed values. For the unit grain weight, the number of kernels per unit at maturity, and the number of grain per square meter RMSE values were 0.01 g $unit^{-1}$ (3.5%), 15.9 kernel $unit^{-1}$ (3%), and 593 grains m^{-2} (14%), respectively.

Best Soil Water Depletion Threshold to Trigger Irrigation

The calibrated and validated model was used to identify the best irrigation deficit strategy to trigger irrigation using net returns and crop yield as selection criteria. The results from a seasonal analysis with 36 years of historical weather data of crop yield changes with respect to the different soil water depletion treatment evaluated are shown in Figure 2.7. The box plot shows a large yield interquartile range for all eight soil water depletion treatments evaluated. This wide range of crop yield could be explained by the variability of precipitation among 36 growing seasons included in the study (1984-2019). Figure 2.8 shows the precipitation during the

growing season for each year considered in the seasonal analysis (1984 – 2019). A total of 19 out of 36 years analyzed demonstrated precipitation below the historical average. These differences in precipitation strongly influenced crop yield as it is shown in the Figure 2.7. The 25-percentile showed an average of values of 9,575.75 kg ha^{-1} and the 75-percentile 12,270.95 kg ha^{-1} considering all treatments. The differences are not only related to precipitation but also temperature and solar radiation. High temperatures can also decrease the yield, especially linked with poor distribution of precipitation. The high temperatures are associated with low pollination and therefore decrease the crop yield (Naveed et al., 2014). There were small differences in the average yield of most soil water depletion treatments, especially between the range of 20% to 70% soil water depletion (Figure 2.7). The yield difference between the 20% and the 70% soil water depletion was 31 kg ha^{-1}. These yield differences showed that triggering irrigation using lower soil water depletions will not significantly increase crop yield. The same results were found by Kisekka et al. (2015) in Kansas, where the authors tested different deficit irrigation strategies to initiate irrigation in a silt loam soil and found small changes yield changes resulted from triggering irrigation with lower soil water depletion values compared to greater depletion values.

Yield reduction was only observed when irrigation was triggered using soil water depletion of 80% or greater (Figure 2.7). The yield difference between the 70% to the 80% and 90% thresholds were 189 kg ha^{-1} and 642.5 kg ha^{-1}, respectively. The corn price plays an important role in the decision of the best irrigation threshold. The differences in crop yield between triggering irrigation in two different soil water depletion need to be large enough that justify the costs to pay one more irrigation event. In this study, triggering irrigation at 70% of soil water depletion is more profitable than 60% because the crop yield is similar but triggering

at 70% requires less irrigation, and therefore, less money spent which result in a maximization of net returns.

Every time that the soil water depletion reached the plant available water trigger level for irrigation, an automatic irrigation was applied to refill the soil profile back to field capacity. The number of irrigations and the total amount of water applied to each soil water depletion treatment are shown in Figures 2.9 and 2.10, respectively. Treatment 1, 20% soil water depletion, showed the greater number of irrigation events, with 12 irrigation events were recorded on average. This result was expected since it takes a shorter period for the soil water level to be depleted at 20% compared to greater soil water depletion values. This treatment also reduces the chance of a precipitation event increasing soil water level, which could reduce the need for irrigation as shown for the other treatments. The number of irrigation applications decreased as soil water depletion increase from 20% to 90% soil water depletion. The average irrigation application for the treatments from 20% to 90% soil water depletion were 6.2, 4.3, 3.1, 2.3, 1.8, 1.4, 1.0, and 0.7 respectively. In addition, there are some years where no irrigation application was required due to a high precipitation during the growing season. This means that for wet years, or years with a good distribution of precipitation, the soil profile does not reach the soil water depletion target and irrigation is not needed. The seasonal analysis demonstrated that irrigation application is highly dependent on weather conditions for each specific year and changes from year to year. The goal of determining the best irrigation threshold is to guarantee the maximum yield with the minimum irrigation applications required to avoid crop stress. Another important aspect that can be used to identify the best irrigation threshold is to check the average of the total irrigation amount applied during the seasons (Figure 2.10). As mentioned before, the treatment of 20% soil water depletion showed the greatest amount applied due to the high number of irrigation

applications. For each treatment, a different irrigation rate was necessary every time irrigation was triggered as a result of a specific soil water depletion level. The total amount required to refill the soil back to field capacity per treatment and per irrigation application are shown in Table 2.8. The treatment with 90% of soil water depletion, for example, 90% replenishment of soil water depleted from a depth of 1.6 m soil profile, required 60 mm of water in one irrigation application compared to other treatments. Meanwhile, the treatment of 20% soil water depletion only needed 20% replenishment of soil water resulting on 19 mm per irrigation to refill the soil to a depth of 0.6 m soil profile. This information is an important factor to decide the best irrigation threshold. The number of irrigation applications and the total amount applied affect the goal of maximizing net returns. If more irrigation applications and high irrigation rates are required, irrigation costs increase. Center pivot irrigation systems require more time to complete a full irrigation cycle if irrigation rate increase, which means more hours to finish a single pivot revolution. A situation like this could result in higher costs of electricity or diesel depending on the energy source under which the pivot operates.

In order to determine the best irrigation deficit strategy, the MGD analysis was used to identify the treatment that maximizes efficiency and reduces the risk for lower net returns. Table 2.9 shows the results of the MGD analysis for all treatments evaluated. The selection of the best treatment was based on the highest $E(x)$ and $E(x) - G(x)$, which consider the highest return per hectare with the low risk. The results showed that the treatment with 70% of soil water depletion was the most effective in terms of the number of irrigation applications, total amount applied and crop yield. This analysis suggests that the most cost-effective threshold for irrigation occurred was when the soil water content reaches 70% soil water depletion and the irrigation amount necessary to replenish that deficit was 48 mm (Table 2.8). The irrigation amount of 48 mm is too

high to be applied in only one single irrigation application. This amount, especially for the silty clay loam soil found at the experimental site, cannot be applied in a single irrigation event due to the high chances of runoff. This amount (48 mm) needs to be applied in, at least, two irrigation applications, which will cause an increase in the number of irrigation applications, costs, and making this irrigation management less profitable.

Determining the best irrigation rate

The irrigation rate is an important factor that directly affects the number of hours a center pivot irrigation system needs to work to complete a revolution. The higher the rate, the lower the pivot speed, and the higher the number of hours required to complete a revolution. The previous analysis showed that the best irrigation threshold was triggering irrigation at 70%. Greater soil water depletion might result in higher irrigation rates that if applied on fine soil texture soils could exceed soil infiltration rate resulting in water runoff. In this analysis, the irrigation threshold of 70% soil water depletion was tested with three irrigation fixed amounts, 12.7, 19, and 25.4 mm, as well as full irrigation rate need to refill the soil water level back to field capacity.

Figure 2.11 shows the simulated crop yield for each treatment with fix irrigation amounts. There was no difference in crop yield among treatments. These results showed that it is possible to reduce the irrigation amount instead of applying the total amount to refill the entire soil profile back to field capacity without reducing the crop yield. By reducing the irrigation amount, irrigation costs could be reduced, resulting in profitability increase. Every time a higher rate of irrigation is applied, the center pivot irrigation system will run for a greater number of hours which might reduce the benefit of rainfall events replenishing soil profile between irrigation events. If the soil water content is at field capacity, the water from precipitation will

either infiltrate to deeper layers or runoff might occur. These possible scenarios might also lead to nutrient leaching or soil erosion.

The number of irrigation applications simulated for each irrigation application are shown in Figure 2.12. The fixed amount of 12.7 mm required more irrigation applications, with an average of four applications and a maximum number of 13 applications. Meanwhile, the fixed amount of 25.4 mm resulted in a smaller number of irrigation events among all irrigation amounts evaluated, with an average of two applications and a maximum of seven applications. Overall, the 25.4 mm fixed irrigation amount treatment had the same crop yield as the other treatments but required less irrigation applications when compared to the other two fixed amount rates.

The MGD analysis was used to determine the best fixed amount of irrigation using the 70% soil water depletion as an irrigation threshold. Table 2.10 shows the results for the MGD analysis. The treatment using the fixed amount of 25.4 mm showed to be the most effective strategy that maximize net returns ($E(x)$) and had the lowest risk that can lower the net returns ($E(x) – G(x)$).

The results demonstrated that 70% of soil water depletion with a fixed rate of 25.4 mm was the best irrigation strategy. Triggering irrigation using the soil water depletion concept is challenging at times because of the balance between crop water stress, yield losses, soil water infiltration and soil water availability. These crop simulation results shows that under the conditions of silty clay soil in Town Creek, AL, a farmer should not let the soil water depletion decrease more than 70%. This information is key to determine when to initiate irrigation; however, other factors such as crop type, crop growth stage, weather conditions and irrigated land size might place an important role on irrigation initiation. At the study field, the center pivot

irrigation system of takes four days to complete a revolution by applying the fixed rate of 25.4 mm. The soil water depletion can go from 40% to 70% in three days if the corn is at the peak of water demand (tasseling and silking), which means that the last day of the irrigation, part of the field will demonstrate soil water depletion higher than 70% and crop yield losses will happen.

SUMMARY AND CONCLUSIONS

The CERES-Maize model in DSSAT-CSM v4.7.5 showed a good prediction of yield, phenology, and biomass for corn cultivated at North Alabama. The simulated yield had an error of 0.5% in 2019 and 3.5% in 2018 when compared with the observed yield, demonstrating a high accuracy in yield prediction. This agreement between simulated and observed values indicates that the model can be used as a decision support tool to assess different irrigation deficit strategies that provide the maximum net return with lower risks. The results showed that among the 20% to 70% soil water depletion levels evaluated, no average corn yield differences existed using 36 years of historical weather data. The differences between the treatments were related to the number of irrigations required and total amount applied, which influenced the total net returns. The irrigation threshold that maximized net returns triggered irrigation when soil water depletion reached 70%. The irrigation amount required to replenish 70% of soil water depletion was 48 mm, but in practice, this amount cannot be applied in a single irrigation event due to the potential of runoff and even pumping capacity. Additional evaluations of different fixed amounts of irrigation showed that decreasing the irrigation rate could maintain the same crop yield but decrease the number of irrigation applications and increase the net return. The irrigation rate that maximized net returns every time the soil water depletion reached 70% was 25.4 mm per irrigation application. Weather conditions will influence irrigation timing and rate. Seasonal analyses results showed that the number of irrigations can be as high as seven applications, two

applications on average, or no need for irrigation. Depending on the crop growth stage and weather conditions, irrigation should be triggered before soil water depletion reaches 70% to avoid crop water stress and yield losses, especially because of the number of days required for the pivot finish a full circle. Further studies are required to simulate different irrigation deficit strategies and rates for each corn growth stage to improve the water use efficiency, yield, net returns and to decrease risks.

Table 2.1 Main agronomic practices for 2018 and 2019 growing seasons.

Agronomic Practices	2018	2019
Planting	April 10	March 26
Fertilizer at planting	16 kg N ha^{-1} , 45 kg P ha^{-1}, 45 kg K ha^{-1}	67 kg N ha^{-1} , 44 kg P ha^{-1}, 44 kg K ha^{-1}
Side Dress Fertilizer	150 kg N ha^{-1} (May 20)	201 kg N ha^{-1} (May 05)
Irrigation Events	June 8 (10.2 mm), July 2 (12.7 mm), July 12 (19 mm), July 21(15.2 mm)	May 31 (15.2 mm), June 13 (25.4 mm), Jun 29 (25.4mm)
Harvest	September 3	August 29

Table 2.2 Description of soil properties for the experimental field located in Town Creek, Alabama.

Depth	Soil Layer	Clay (%)	Silt (%)	Sand (%)	Soil Texture	Organic Carbon (%)
0-10	1	24.8	52.8	22.4	Silt Loam	1.02
10-25	2	29.2	59.2	11.6	Silty Clay Loam	1.02
25-40	3	31.2	57.2	11.6	Silty Clay Loam	0.94
40-55	4	32	60	8	Silty Clay Loam	1.02
55-70	5	32	60.4	7.6	Silty Clay Loam	1.08
70-85	6	38	54.8	7.2	Silty Clay Loam	1.43
85-100	7	44	52.8	3.2	Silty Clay	1.55
100-115	8	44	44.8	11.2	Silty Clay	2.03
115-130	9	42	47.2	10.8	Silty Clay	1.29
130-145	10	46	43.2	10.8	Silty Clay	1.09
145-160	11	46	43.2	10.8	Silty Clay	1.09

Table 2.3 Cultivar coefficients of the corn hybrid Dekalb 66-97 in the CERES-Maize model – DSSAT-CSM v4.7.5

Cultivar Coefficients	Legend	Unit	Initial Values	Final Values
Thermal time from emergence to end juvenile phase	P1	Degree Days	240	247.4
Photoperiod sensitivity coefficient	P2	Days	0.60	0.436
Thermal time from silking to physiological maturity	P5	Degree Days	927.0	915.7
Maximum possible number of kernels per plant	G2	Unitless	780.0	786.0
Kernel filling rate during linear grain filling/optimum conditions	G3	mg d^{-1}	8.10	9.10
Phyllochron interval (degree days required for a leaf tip to emerge)	PHINT	Degree days	41.50	47.50

Table 2.4 Different irrigation deficit strategies used to trigger irrigation in a seasonal analysis

Treatment	Soil Water Depletion	%PAW
1	20%	80%
2	30%	70%
3	40%	60%
4	50%	50%
5	60%	40%
6	70%	30%
7	80%	20%
8	90%	10%

Table 2.5 Simulated and observed data for the model calibration using 2019 growing season data at Town Creek, Alabama.

Variable	Simulated	Observed
Anthesis day (DAP)	78	78
Physiological maturity day (DAP)	130	128
Yield at Harvest Maturity (kg[dm]/ha)	11969	12038
Number at maturity (nº/m2)	3563	3582
Unit weight at maturity (g [dm]/unit)	0.336	0.337
Number at maturity (nº/unit)	508.9	453.7
Tops weight at maturity (kg [dm]/ha)	22,955	24,232
Leaf area index, maximum	4.25	4.13

Table 2.6 Soil properties calibrated for the experimental field at Town Creek, Alabama

Depth	Lower Limit (LL) (cm^3 cm^{-3})	Drained Upper Limit (DUL) (cm^3 cm^{-3})	Saturation (SAT) (cm^3 cm^{-3})	Bulk Density (g cm^{-3})	Saturated Hydraulic Conductivity (KSAT)(cm h^{-1})	RGWF[1]
0-10	0.190	0.300	0.400	1.33	0.15	1
10-25	0.195	0.300	0.400	1.33	0.15	1
25-40	0.220	0.320	0.400	1.33	0.16	1
40-55	0.220	0.300	0.400	1.38	0.16	0.6
55-70	0.240	0.360	0.400	1.38	0.16	0.35
70-85	0.213	0.386	0.452	1.38	0.15	0.25
85-100	0.252	0.420	0.442	1.41	0.09	0.10
100-115	0.251	0.414	0.467	1.34	0.09	0.05
115-130	0.238	0.404	0.467	1.34	0.09	0
130-145	0.264	0.425	0.467	1.34	0.09	0
145-160	0.264	0.425	0.467	1.34	0.09	0

[1]Root Growth Weighting Factor

Table 2.7 Simulated and observed data for the model validation using the 2018 growing season data at Town Creek, Alabama

Variable	Simulated	Observed
Anthesis day (DAP)	74	71
Physiological maturity day (DAP)	123	126
Yield at Harvest Maturity (kg[dm]/ha)	12,155	12,605
Number at maturity (nº/m2)	3,663	4,256
Unit weight at maturity (g [dm]/unit)	0.331	0.320
Number at maturity (nº/unit)	523.2	539.1

Table 2.8 Irrigation amount required per application for different soil water depletions thresholds for a silty clay loam soil type at Town Creek, Alabama

Treatment	Soil Water Depletion	Irrigation amount (mm)
1	20%	19
2	30%	25
3	40%	31
4	50%	37
5	60%	43
6	70%	48
7	80%	54
8	90%	60

Table 2.9 Net returns for different soil water depletion thresholds over 36 years of weather data at Town Creek, Alabama

Treatment	Soil Water Depletion	*E(x)*	*E(x) – G(x)*
1	20%	275.5	150.9
2	30%	302.4	172.8
3	40%	328.7	197.5
4	50%	347.4	215.7
5	60%	361.8	233.6
6	70%	372.7	244.9
7	80%	361.9	235
8	90%	329.4	188

E(x) corresponds to the expected value ($ ha^{-1}), and *G(x)* is the Gini-mean difference ($ ha^{-1}).

Table 2.10 Net returns for different irrigation fixed amounts over 36 years of weather data at Town Creek, Alabama

Treatment	Fixed Amount	*E(x)*	*E(x) – G(x)*
1	12.7 mm	320.1	178.5
2	19 mm	352.9	221.6
3	25.4 mm	372.7	244.9
4	Field Capacity	355	221.8

E(x) corresponds to the expected value ($ ha^{-1}), and *G(x)* is the Gini-mean difference ($ ha^{-1}).

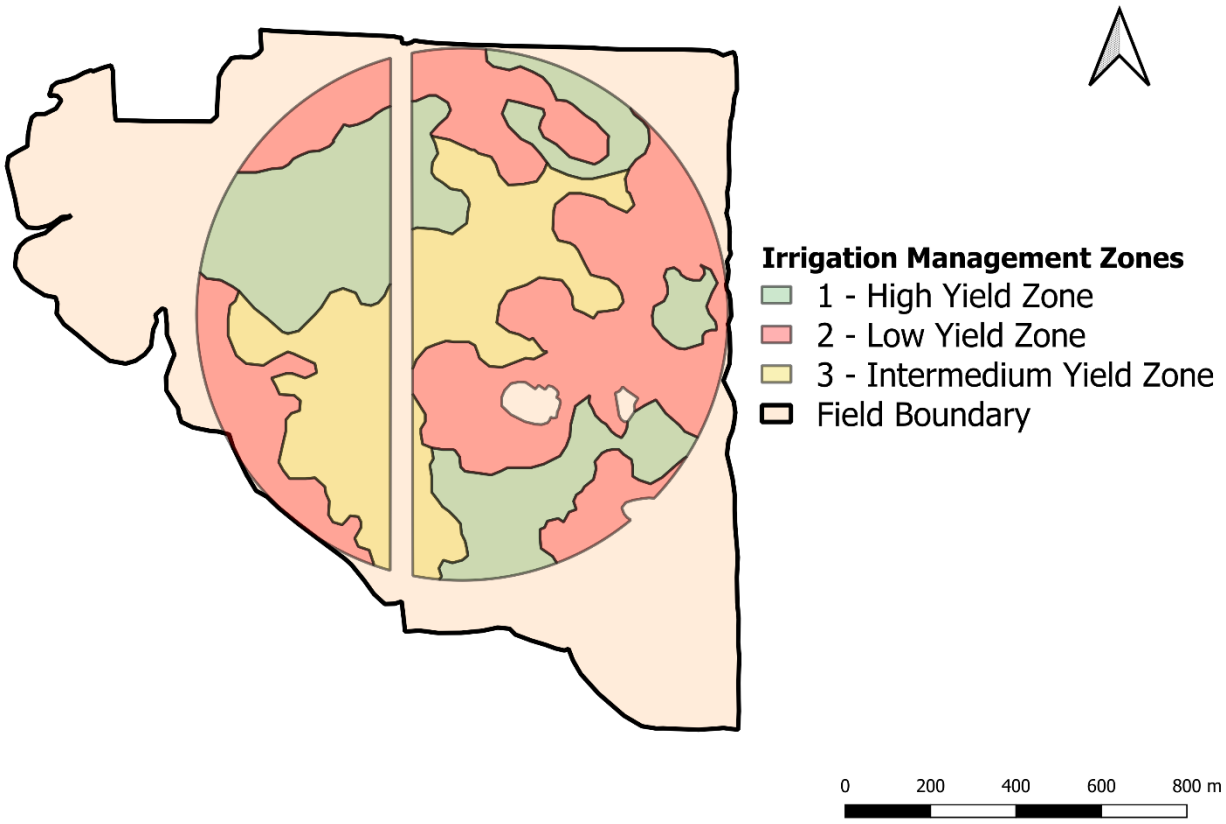

Figure 2.1 Irrigation Management Zones for Town Creek field for 2018 and 2019 growing season

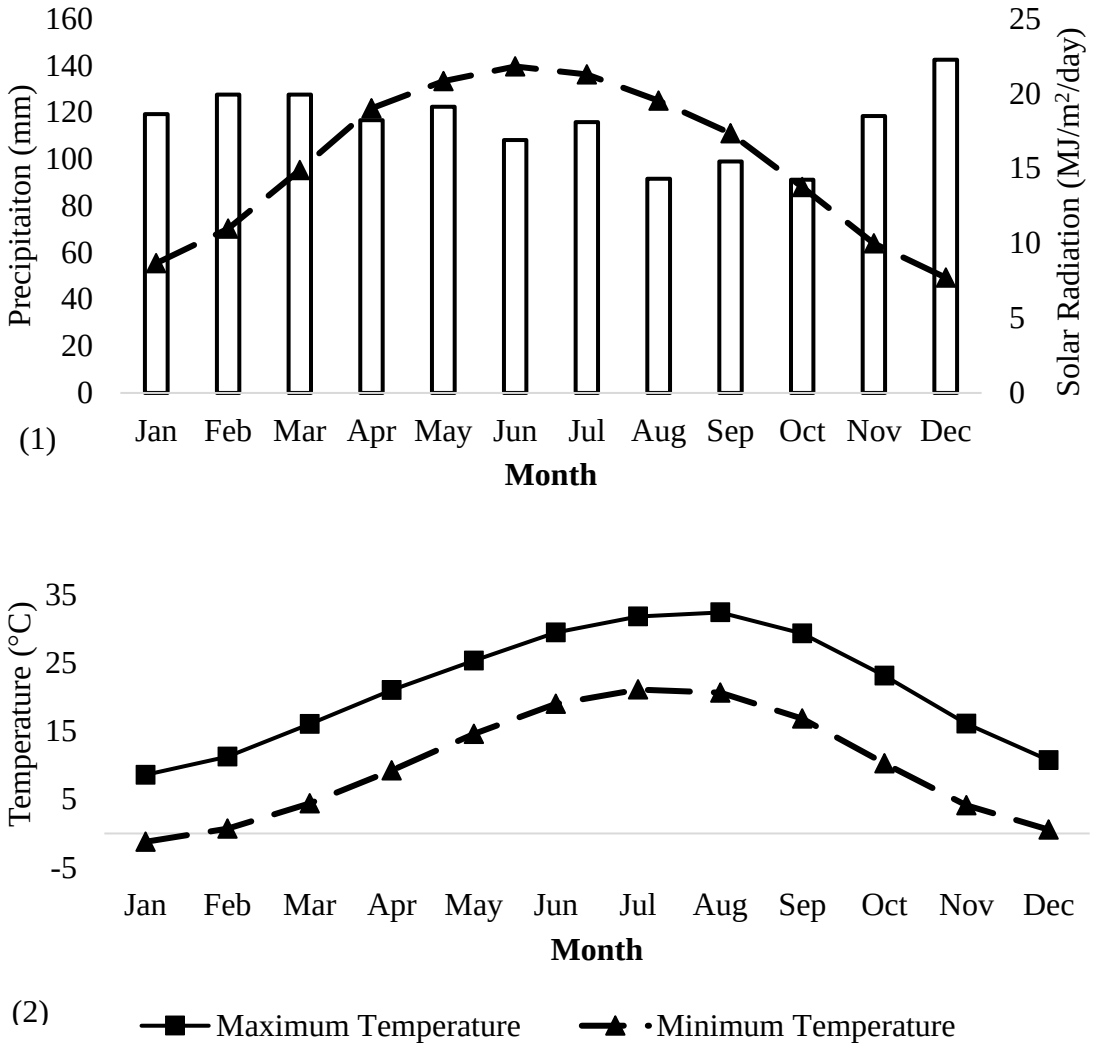

Figure 2.2 Historic weather conditions (1984-2019) for Town Creek, Alabama, United States. (1) average monthly precipitation and average daily solar radiation: (2) maximum and minimum air temperature.

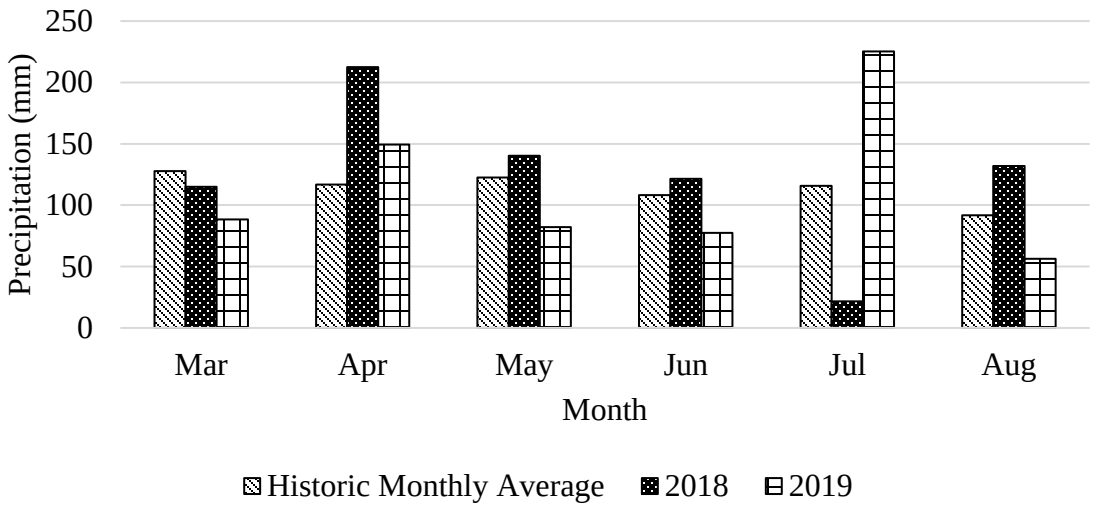

Figure 2.3 Comparison of precipitation records of historic monthly average (1984-2019) and growing seasons 2018 and 2019.

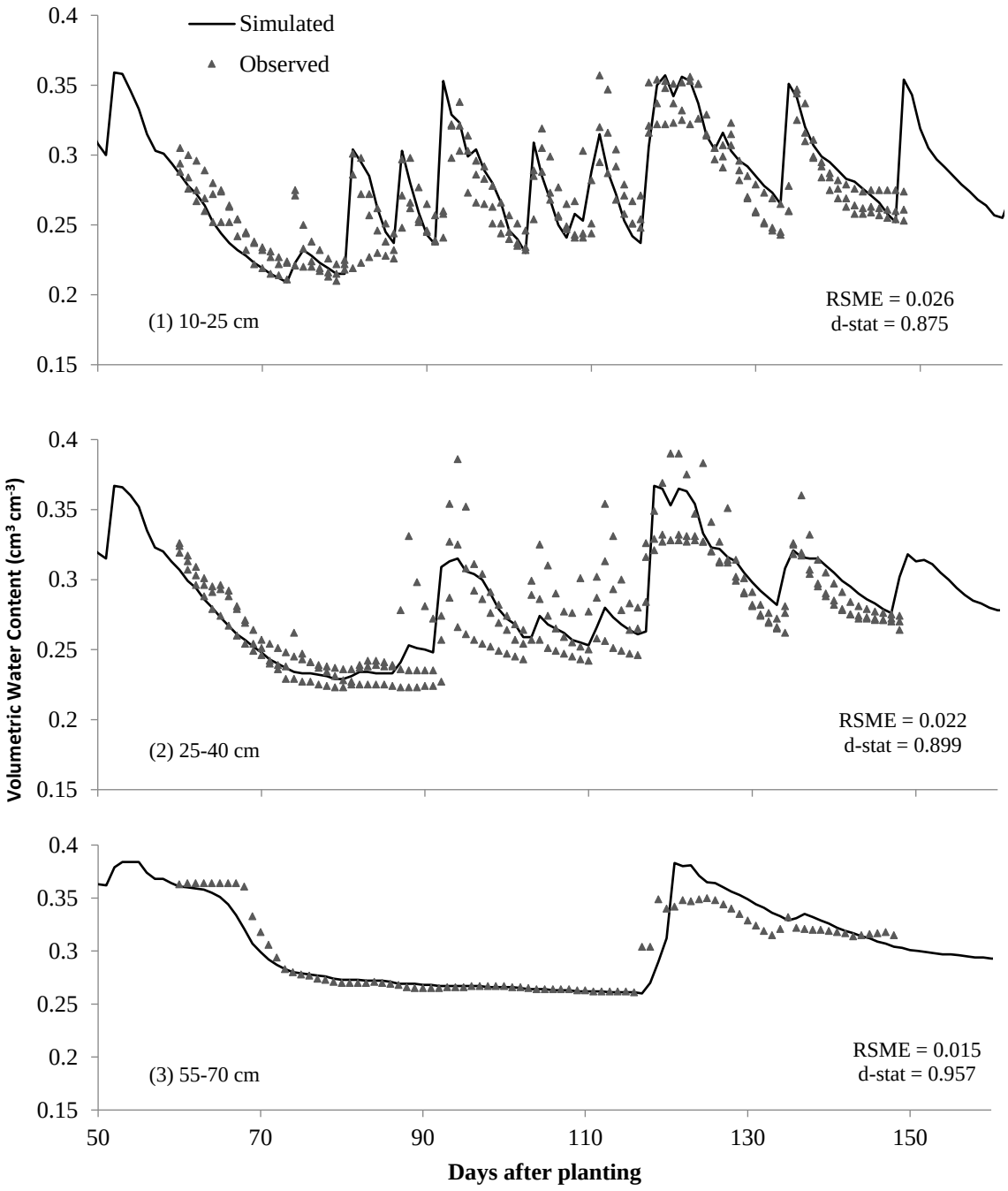

Figure 2.4 Simulated and observed volumetric water content at the depths of 1-25 cm (1), 25-40 cm (2) cm, and 55-70 cm (3).

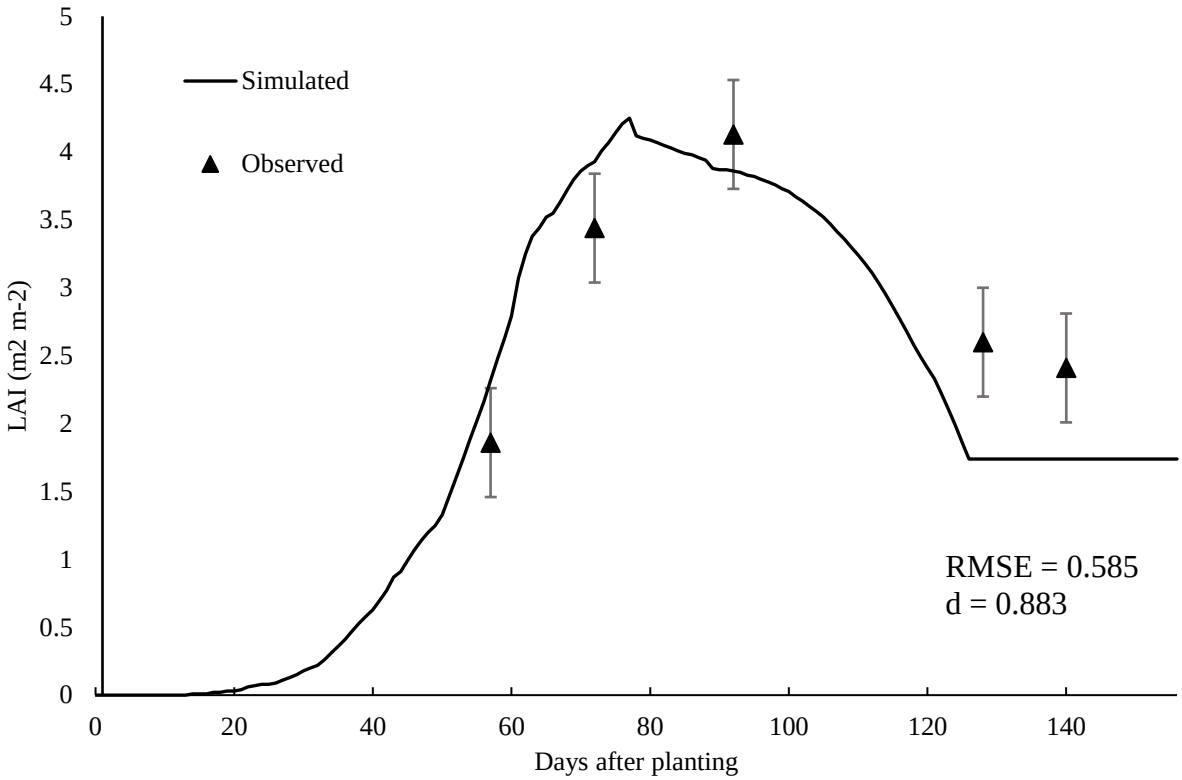

Figure 2.5 Observed and simulated leaf area index for the Dekalb 66-77 corn hybrid under irrigation in 2019 at Town Creek, Alabama

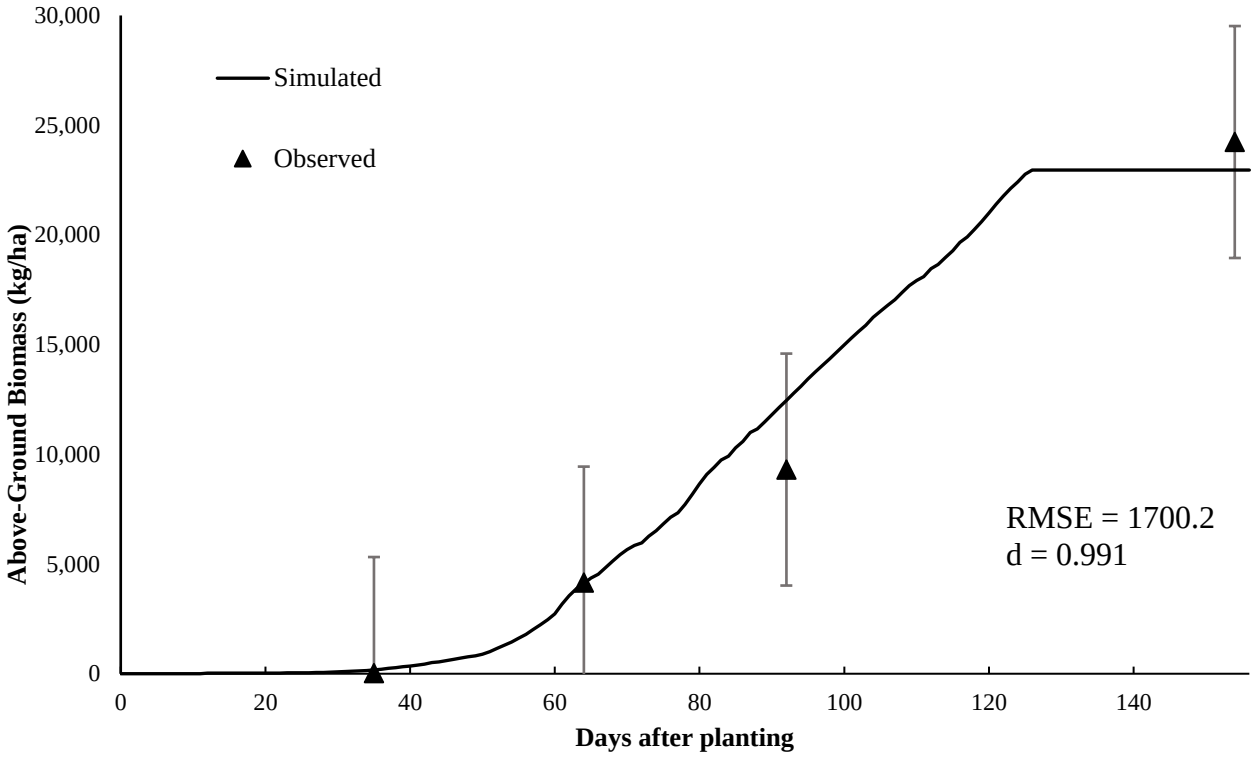

Figure 2.6 Observed and simulated above-ground biomass for a corn hybrid under irrigation in 2019 at Town Creek, Alabama

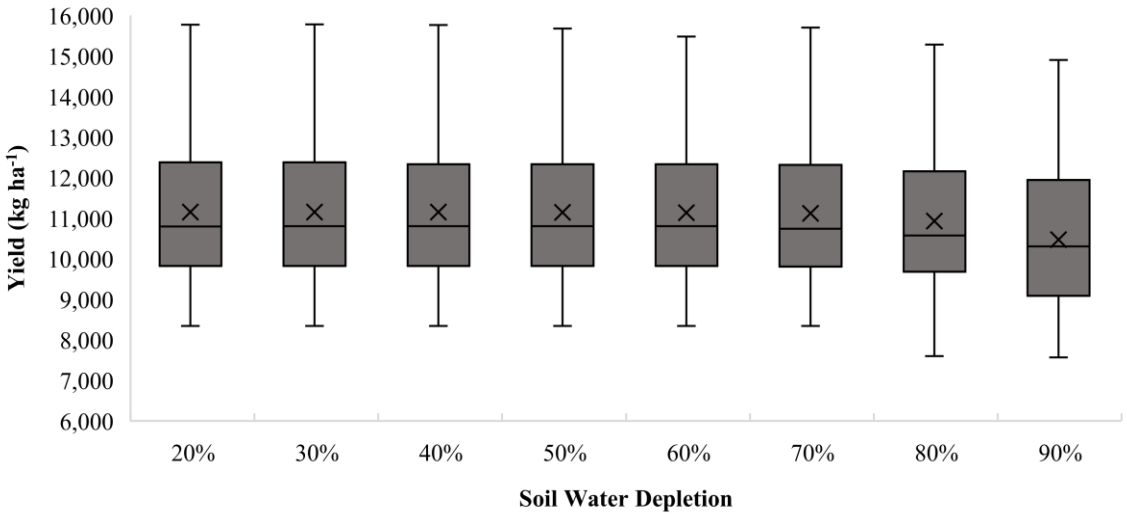

Figure 2.7 Box plot of simulated corn yield by different soil water depletion thresholds. Thresholds range from 20% to 90% depletion from plant available water. Results from seasonal analysis using 36 years (1984-2019) of weather data at Town Creek, Alabama

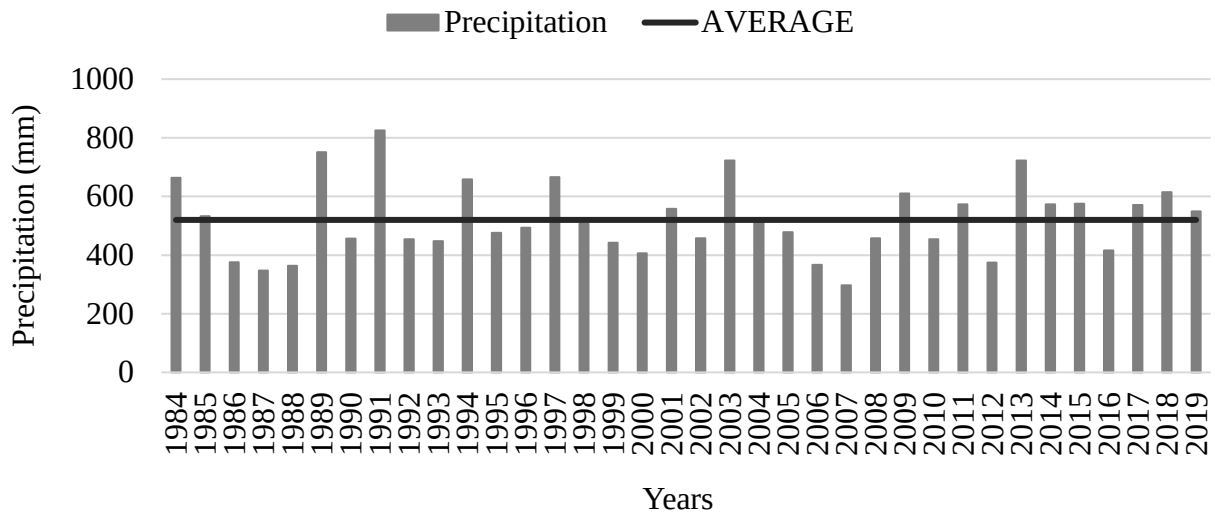

Figure 2.8 Total precipitation during the growing season (March to August) for each year from 1984 to 2019 used in the seasonal analysis.

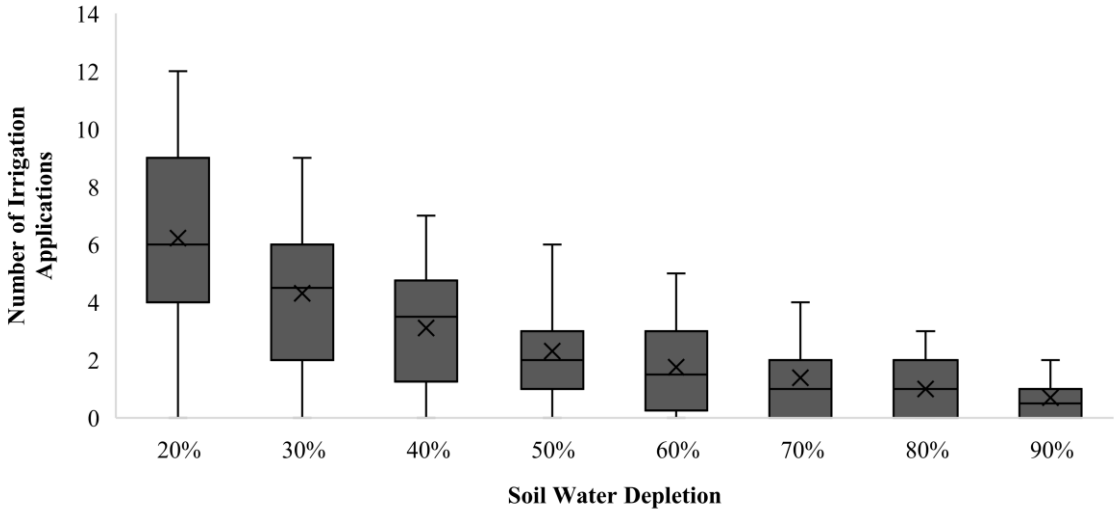

Figure 2.9 Box plot of simulated number of irrigation applications for different soil water depletions thresholds. Thresholds range from 20% to 90% depletion from plant available water. Results from seasonal analysis using 36 years of weather data at Town Creek, Alabama

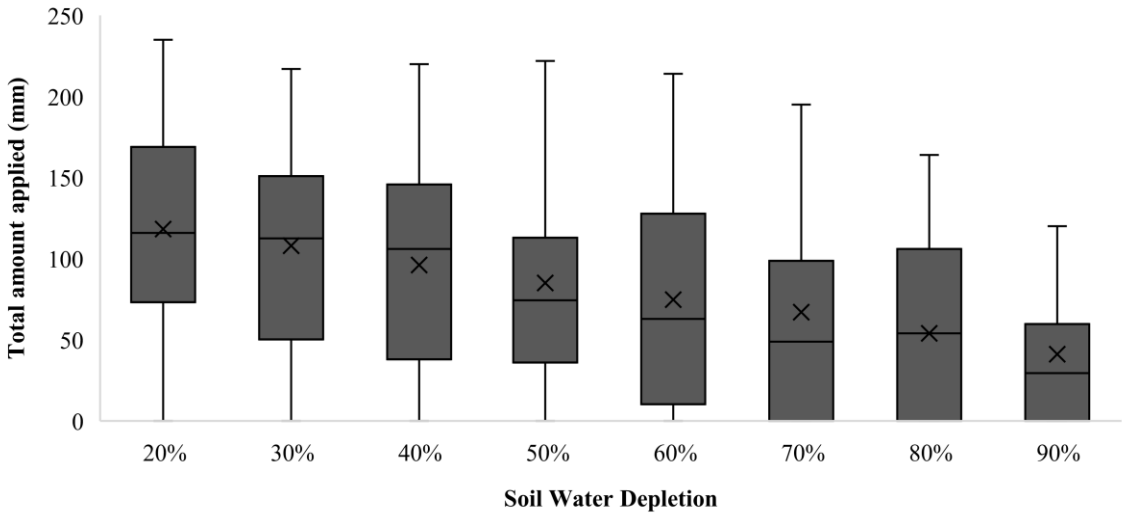

Figure 2.10 Box plot of simulated of the total amount (mm) applied for different soil water depletion thresholds. Thresholds range from 20% to 90% depletion from plant available water. Results from season analysis using 36 years of weather data at Town Creek, Alabama

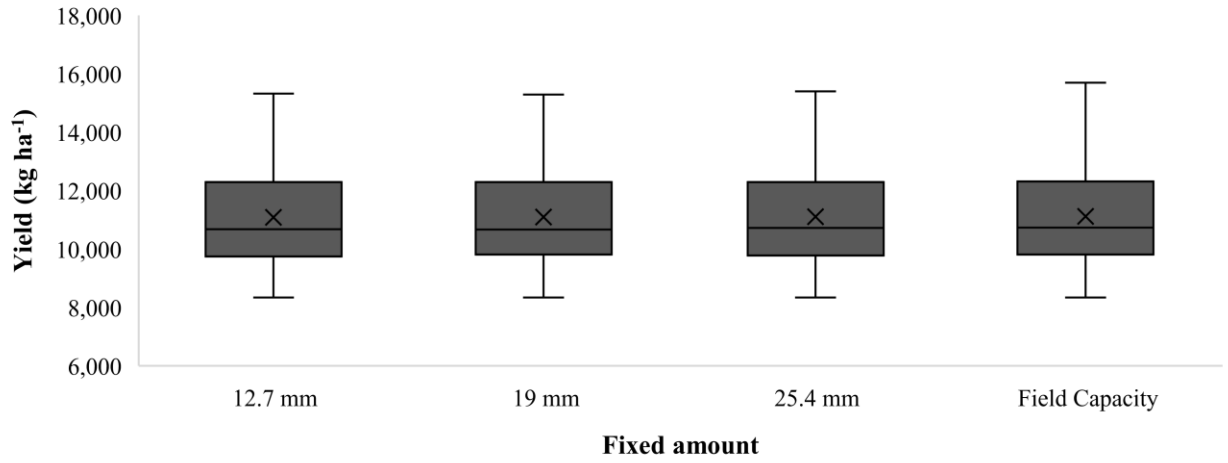

Figure 2.11 Box plot of simulated corn yield by different irrigation fixed rates applications. The fixed rates were 12.7, 19, 25.4 mm and the fixed rate required to refill the soil profile to field capacity. Results from seasonal analysis using 36 years of weather data at Town Creek, Alabama

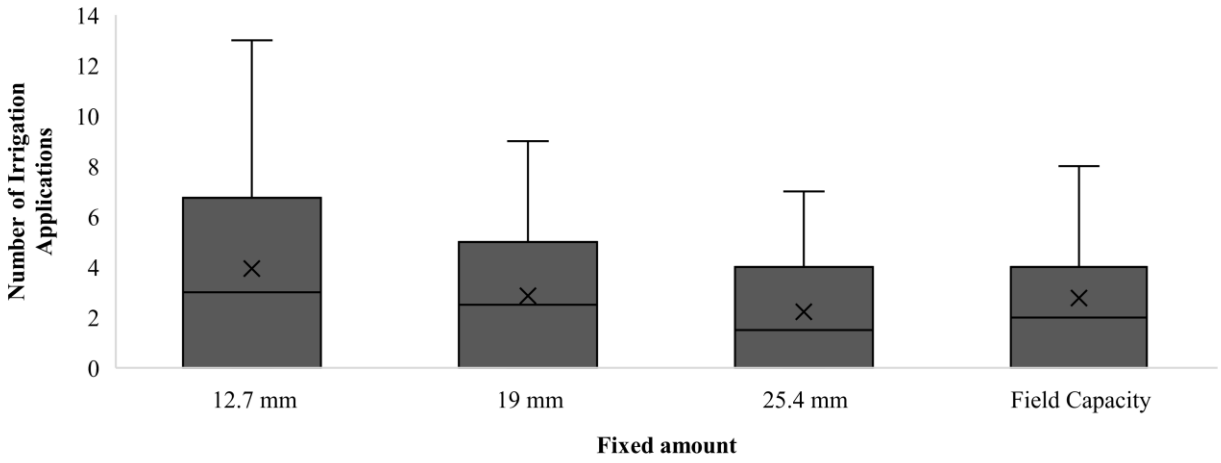

Figure 2.12 Box plot of simulated number of irrigation applications for different irrigation fixed rates needed when the soil is a 70% soil water depletion. The fixed rates were 12.7, 19, 25.4 mm and the fixed rate required to refill the soil profile to field capacity. Results from seasonal analysis using 36 years (1984-2019) of weather data at Town Creek, Alabama

REFERENCES

Allen, R. G., Pereira, L. S., Raes, D., & Smith, M. (1998). Crop Evapotranspiration-Guidelines for computing crop water requirements. *FAO Irrigation and Drainage Paper 56*, *300*, D05109.

Anderson-Cook, C. M., Alley, M. M., Roygard, J. K. F., Khosla, R., Noble, R. B., & Doolittle, J. A. (2002). Differentiating Soil Types Using Electromagnetic Conductivity and Crop Yield Maps. *Soil Science Society of America Journal*, *66*(5), 1562–1570. https://doi.org/10.2136/sssaj2002.1562

Broner, I. (2005). Irrigation scheduling. *Colorado State University Cooperative*. Retrieved from www.ext.colostate.edu

Carter, L., Terando, A., Dow, K., Hiers, K., Kunkel, K. E., Lascurain, A., … Schramm, P. (2018). *Impacts, Risks, and Adaptation in the United States: Fourth National Climate Assessment, Volume II*. https://doi.org/10.7930/NCA4.2018.CH19

Chen, S., Shao, D., Li, X., & Lei, C. (2016). Simulation-Optimization Modeling of Conjunctive Operation of Reservoirs and Ponds for Irrigation of Multiple Crops Using an Improved Artificial Bee Colony Algorithm. *Water Resources Management*, *30*(9), 2887–2905. https://doi.org/10.1007/s11269-016-1277-y

Chiericati, M., Morari, F., Sartori, L., Ortiz, B., Perry, C., & Vellidis, G. (2007). Delineating management zones to apply site-specific irrigation in the Venice lagoon watershed. *Precision Agriculture 2007 - Papers Presented at the 6th European Conference on Precision Agriculture, ECPA 2007*, 599–605.

Cook, J. S. (2015). Validating a Prescription Map used in Variable Rate Irrigation using Geographic Information Science. *Resource Analysis*, *18*, 1–13.

Da Silva, J. R., & Alexandre, C. (2005). Spatial Variability of Irrigated Corn Yield in Relation to Field Topography and Soil Chemical Characteristics. *Precision Agriculture*, *6*, 453–466.

De Reu, J., Bourgeois, J., Bats, M., Zwertvaegher, A., Gelorini, V., De Smedt, P., … Crombé, P. (2012). Application of the topographic position index to heterogeneous landscapes. *Geomorphology*, *186*, 39–49. https://doi.org/10.1016/j.geomorph.2012.12.015

Djaman, K., O'Neill, M., Owen, C. K., Smeal, D., Koudahe, K., West, M., … Irmak, S. (2018). Crop evapotranspiration, irrigation water requirement and water productivity of maize from meteorological data under semiarid climate. *Water*, *10*(4), 405.

https://doi.org/10.3390/w10040405

Evans, R. G., LaRue, J., Stone, K. C., & King, B. A. (2013). Adoption of site-specific variable rate sprinkler irrigation systems. *Irrigation Science*, *31*(4), 871–887. https://doi.org/10.1007/s00271-012-0365-x

Evans, R. G., & Sadler, E. J. (2008). Methods and technologies to improve efficiency of water use. *Water Resources Research*, *44*(7), 1–15. https://doi.org/10.1029/2007WR006200

Fang, Q., Ma, L., Yu, Q., Ahuja, L. R., Malone, R. W., & Hoogenboom, G. (2010). Irrigation strategies to improve the water use efficiency of wheat-maize double cropping systems in North China Plain. *Agricultural Water Management*, *97*(8), 1165–1174. https://doi.org/10.1016/j.agwat.2009.02.012

FAO. (2018). *The future of food and agriculture - Alternative pathways to 2050*. Rome.

Fisher, D. K., Hanks, J. E., & Pringle, H. C. (2009). Comparison of Irrigation Scheduling Methods in the Humid Mid-South. *Irrigation Associations Exposition and Technical Conference Proceedings*, *1*, 1–4.

Fraisse, C. W., Sudduth, K. A., & Kitchen, N. R. (2000). Delineation of Site–Specific Management Zones by Unsupervised Classification of Topographic Attributes and Soil Electrical Conductivity. *American Society of Agricultural Engineers*, *44(1): 155*(1), 155–166. https://doi.org/10.1117/12.840574

Fridgen, J. J., Kitchen, N. R., Sudduth, K. A., Drummond, S. T., Wiebold, W. J., & Fraisse, C. W. (2004). Management Zone Analyst (MZA): Software for Subfield Management Zone Delineation. *Agronomy Journal*, *96*(1), 100–108.

Grisso, R., Alley, M., Holshouser, D., & Thomason, W. (2009). Precision farming tools: soil electrical conductivity. *Virginia Cooperative Extension*, *442*(508), 1–6. Retrieved from http://scholar.google.com/scholar?hl=en&btnG=Search&q=intitle:Precision+farming+tools:+soil+electrical+conductivity#7

Haghverdi, A., Leib, B. G., Washington-Allen, R. A., Ayers, P. D., & Buschermohle, M. J. (2015). Perspectives on delineating management zones for variable rate irrigation. *Computers and Electronics in Agriculture*, *117*, 154–167. https://doi.org/10.1016/j.compag.2015.06.019

Harrison, K. (2012). Irrigation Scheduling Methods. *Journal of Chemical Information and Modeling*. https://doi.org/10.1017/CBO9781107415324.004

Hatfield, J. L., Sauer, T. J., & Prueger, J. H. (2001). Managing soils to achieve greater water use efficiency: A review. *Agronomy Journal*, *93*(2), 271–280. https://doi.org/10.2134/agronj2001.932271x

Holzworth, D. P., Huth, N. I., deVoil, P. G., Zurcher, E. J., Herrmann, N. I., McLean, G., … Keating, B. A. (2014). APSIM - Evolution towards a new generation of agricultural systems simulation. *Environmental Modelling and Software*, *62*, 327–350. https://doi.org/10.1016/j.envsoft.2014.07.009

Hoogenboom, G., Porter, C. H., Boote, K. J., Shelia, V., Wilkens, P. W., Singh, U., … Jones, J. W. (2019). The DSSAT crop modeling ecosystem. In *Burleigh Dodds Science Publishing* (pp. 173–216). https://doi.org/10.19103/AS.2019.0061.10

Howell, T. A. (2001). Enhancing water use efficiency in irrigated agriculture. *Agronomy Journal*, *93*(2), 281–289. https://doi.org/10.2134/agronj2001.932281x

Huang, X., Wang, L., Yang, L., & Kravchenko, A. N. (2008). Management Effects on Relationships of Crop Yields with Topography Represented by Wetness Index and Precipitation. *Agronomy Journal*, 1463–1471. https://doi.org/10.2134/agronj2007.0325

Huat, B. B. K., Ali, F. H. J., & Low, T. H. (2006). Water infiltration characteristics of unsaturated soil slope and its effect on suction and stability. *Geotechnical and Geological Engineering*, *24*(5), 1293–1306. https://doi.org/10.1007/s10706-005-1881-8

Irmak, S., Burgert, M. J., & Yang, H. S. (2012). Large-Scale On-Farm Implementation of Soil Moisture-Based Irrigation Management Strategies for Increasing Maize Water Productivity. *American Society of Agricultural and Biological Engineers*, *55*(3), 881–894.

Irmak, S., Odhiambo, L., Kranz, W. ., & Eisenhauer, D. E. (2011). Irrigation Efficiency and Uniformity, and Crop Water Use Efficiency.

Irmak, S, & Haman, D. Z. (2001). PERFORMANCE OF THE WATERMARK® GRANULAR MATRIX SENSOR IN SANDY SOILS, *17*(6), 787–795.

Irmak, Suat, Payero, J. O., VanDeWalle, B., Rees, J., & Zoubek, G. L. (2014). Principles and Operational Characteristics of Watermark Granular Matrix Sensor to Measure Soil Water Status and Its Practical Applications for Irrigation Management in Various Soil Textures, 1-14,.

Irmak, Suat, & Rathje, W. (2008). Plant Growth and Yield as Affected by Wet Conditions Due to Flooding or Over-Irrigation. Retrieved from

https://cropwatch.unl.edu/documents/g1904.pdf

Isasmendi, M. S. T. (2013). *Different Approaches for Improvement of Nitrogen Management in Alabama Corn Grain Production*. Retrieved from http://hdl.handle.net/10415/3776

James, L. A., Watson, D. G., & Hansen, W. F. (2006). Using LiDAR data to map gullies and headwater streams under forest canopy: South Carolina, USA. *Catena*, *71*(1), 132–144. https://doi.org/10.1016/j.catena.2006.10.010

Jeschke, M., Carter, P., Bax, P., & Schon, R. (2012). Putting Variable-Rate Seeding to Work on Your Farm. *Crop Insights*, *22*(1), 1–4. Retrieved from https://www.pioneer.com/home/site/us/agronomy/library/variable-rate-seeding/

Jiang, P., & Thelen, K. D. (2004). Effect of Soil and Topographic Properties on Crop Yield in a North-Central Corn-Soybean Cropping System. *Agronomy Journal*, *96*(1), 252–258. https://doi.org/10.2134/agronj2004.0252

Kaspar, T. C., Pulido, D. J., Fenton, T. E., Colvin, T. S., Karlen, D. ., Jaynes, D. B., & W., M. D. (2004). Relationship of Corn and Soybean Yield to Soil and Terrain Properties. *Agronomy Journal*, *96*(May), 700–709. https://doi.org/10.2134/agronj2004.0700

Kaspar, Thomas C, Colvin, T. S., Jaynes, D. B., Karlen, D. L., James, D. E., & Meek, D. W. (2003). Relationship Between Six Years of Corn Yields and Terrain Attributes. *Precision Agriculture*, (4), 87–101.

Khan, S., Tariq, R., Yuanlai, C., & Blackwell, J. (2006). Can irrigation be sustainable? *Agricultural Water Management*, *80*(1-3 SPEC. ISS.), 87–99. https://doi.org/10.1016/j.agwat.2005.07.006

Kisekka, I., Aguilar, J. P., Rogers, D. H., Holman, J., O'Brien, D. M., & Klocke, N. (2015). Assessing deficit irrigation strategies for corn using simulation. *American Society of Agricultural and Biological Engineers*, *59*(1), 195–222. https://doi.org/10.13031/trans.59.11206

Kitchen, N. R., Drummond, S. T., Lund, E. D., Sudduth, K. A., & Buchleiter, G. W. (2003). Soil electrical conductivity and topography related to yield for three contrasting soil-crop systems. *Agronomy Journal*, *95*(3), 483–495. https://doi.org/10.2134/agronj2003.4830

Ko, J., Piccinni, G., & Steglich, E. (2009). Using EPIC model to manage irrigated cotton and maize. *Agricultural Water Management*, *96*(9), 1323–1331. https://doi.org/10.1016/j.agwat.2009.03.021

Kranz, W. ., Irmak, S., van Donk, S. J., Yonts, C. D., & Martin, D. L. (2008). *Irrigation management for corn*. Retrieved from http://extension.unl.edu/publications

Kravchenko, A. N., & Bullock, D. G. (2000). Correlation of corn and soybean grain yield with topography and soil properties. *Agronomy Journal*, *92*(1), 75–83.

Laboski, C. A. M., Dowdy, R. H., Allmaras, R. R., & Lamb, J. A. (1998). Soil strength and water content influences on corn root distribution in a sandy soil. *Plant and Soil*, *203*(2), 239–247. https://doi.org/10.1023/A:1004391104778

LaRue, J., & Evans, R. G. (2012). CONSIDERATIONS FOR VARIABLE RATE IRRIGATION. In *24th Annual Central Plains Irrigation Conference* (pp. 111–116).

Lena, B. P. (2013). *Consumo hídrico do pinhão-manso (Jatropha curcas L .) irrigado e sem irrigação na fase de formação*.

Li, Y., Shi, Z., Wu, C. F., Li, H. Y., & Li, F. (2008). Determination of potential management zones from soil electrical conductivity, yield and crop data. *Journal of Zhejiang University: Science B*, *9*(1), 68–76. https://doi.org/10.1631/jzus.B071379

Liakos, V., Vellidis, G., Lacerda, L., Tucker, M., Porter, W., & Cox, C. (2018). Management Zone Delineation for Irrigation Based on Sentinel-2 Satellite Images and Field Properties. In *14th International Conference on Precision Agriculture* (pp. 1–11).

Liang, X., Liakos, V., Wendroth, O., & Vellidis, G. (2016). Scheduling irrigation using an approach based on the van Genuchten model. *Agricultural Water Management*, *176*, 170–179. https://doi.org/10.1016/j.agwat.2016.05.030

Lowrance, C., Fountas, S., Liakos, V., & Vellidis, G. (2016). EZZone-An Online Tool for Delineating Management Zones. In *13th International Conference on Precision Agriculture* (pp. 1–17).

Ma, L., Nielsen, D. C., Ahuja, L. R., Malone, R. W., Saseendran, S. A., Rojas, K. W., … Benjamin, J. G. (2003). Evaluation of RZWQM under varying irrigation levels in eastern Colorado. *Transactions of the American Society of Agricultural Engineers*, *46*(1), 39–49. https://doi.org/10.13031/2013.12547

Maestrini, B., & Basso, B. (2018). *Drivers of within-field spatial and temporal variability of crop yield across the US Midwest*. https://doi.org/10.1038/s41598-018-32779-3

Martini, E., Wollschläger, U., Musolff, A., Werban, U., & Zacharias, S. (2017). Principal component analysis of the spatiotemporal pattern of soil moisture and apparent electrical

conductivity. *Vadose Zone Journal*, *16*(10). https://doi.org/10.2136/vzj2016.12.0129

Mcwilliams, D. A., Berglund, D. R., & Endres, G. J. (1999). *Corn Growth and Management Quick Guide*.

Melvin, S. R., & Yonts, C. D. (2009). *Irrigation scheduling Checkbook method*. Retrieved from http://extensionpublications.unl.edu/assets/pdf/%0Aec709.pdf

Mieza, M. S., Cravero, W. R., Kovac, F. D., & Bargiano, P. G. (2016). Delineation of site-specific management units for operational applications using the topographic position index in La Pampa, Argentina. *Computers and Electronics in Agriculture*, *127*, 158–167. https://doi.org/10.1016/j.compag.2016.06.005

Miller, K. A., Lo, T. H., Luck, J. D., & Heeren, D. M. (2014). Combining Site Specific Data with Geospatial Analysis to Identify Variable Rate Irrigation Opportunities in Irrigated Agricultural Fields. *Biological Systems Engineering: Papers and Publications*.

Moore, I. D., Gessler, P. E., Nielsen, G. A., & Peterson, G. A. (1993). Soil attribute prediction using terrain analysis. *Soil Science Society of America Journal*, *57*(2), 443–452. https://doi.org/10.2136/sssaj1993.03615995005700020026x

NASS. (2013). *Farm and Ranch Irrigation Survey*. *Census of Agriculture* (Vol. 3). Retrieved from http://www.agcensus.usda.gov/Publications/2007/Online_Highlights/Farm_and_Ranch_Irrigation_Survey/index.php

NASS. (2017). *2017 Census of Agriculture: United States Summary and State Data*.

Naveed, S., Aslam, M., Maqbool, M. A., Bano, S., Zaman, Q. U., & Ahmad, R. M. (2014). Physiology of high temperature stress tolerance at reproductive stages in maize. *Journal of Animal and Plant Sciences*, *24*(4), 1141–1145.

Ortiz, B. V., Sullivan, D. G., Perry, C., & Vellidis, G. (2011). Delineation of management zones for Southern root-knot nematode using fuzzy clustering of terrain and edaphic field characteristics. *Communications in Soil Science and Plant Analysis*, *42*(16), 1972–1994. https://doi.org/10.1080/00103624.2011.591471

Peel, M. C., Finlayson, B. L., & McMahon, T. A. (2007). Updated world map of the Köppen-Geiger climate classification. *Hydrology and Earth System Sciences*. https://doi.org/https://doi.org/10.5194/hess-11-1633-2007

Perry, C., Barnes, E., Munk, D., Barnes, E., Fisher, K., & Bauer, P. (2012). Cotton Irrigation

Management for Humid Regions.

Perry, C., Fraisse, C., & Dourte, D. (2012). Variable-Rate Irrigation A Management Option for Climate Variability and Change What are the impacts on production.

Pinter, P., Hatfield, J., Schepers, J., Barnes, E., Moran, M., Daughtry, C., & Upchurch, D. (2018). Remote Sensing for Site-Specific Crop Management. *Photogrammetric Engineering & Remote Sensing*, *69*(6), 647–664. https://doi.org/10.2134/precisionagbasics.2016.0092

QGIS Geographic Information System. (2018). Open Source Geospatial Foundation Project. Retrieved from http://qgis.osgeo.org

Qin, C., Zhu, A., Tao, P., & Scholten, T. (2011). An approach to computing topographic wetness index based on maximum downslope gradient. *Precision Agriculture*, *12*(May 2014), 32–43. https://doi.org/10.1007/s11119-009-9152-y

R Core Team. (2019). R: A language and environment for statistical computing. R Foundation for Statistical Computing, Vienna, Austria. URL http://www.R-project.org/.

Raes, D., Steduto, P., Hsiao, T. C., & Fereres, E. (2018). *FAO crop-water productivity model to simulate yield response to water*. *Reference Manual, Chapter 1 – AquaCrop, Version 6.0*. Retrieved from www.fao.org/publications

Ren, Y., Li, M., & Wu, Y. (2015). Design and Application of Distance Education Platform for New Professional Peasant. *International Journal of Emerging Technologies in Learning (IJET)*, *10*(4), 66. https://doi.org/10.3991/ijet.v10i4.4704

Reyes, J., Wendroth, O., & Matocha, C. (2019). Delineating Site-Specific Management Zones and Evaluating Soil Water Temporal Dynamics in a Farmer ' s Field in Kentucky. https://doi.org/10.2136/vzj2018.07.0143

Reyes, J., Wendroth, O., Matocha, C., & Zhu, J. (2019). Delineating Site-Specific Management Zones and Evaluating Soil Water Temporal Dynamics in a Farmer's Field in Kentucky. *Vadose Zone Journal*, *18*(1), 1–19. https://doi.org/10.2136/vzj2018.07.0143

Robert, P. C., Rust, R. H., Larson, W. E., McCann, B. L., Pennock, D. J., van Kessel, C., & Walley, F. L. (1996). The Development of Management Units for Site-Specific Farming. *Precision Agriculture*, (295–302). https://doi.org/10.2134/1996.precisionagproc3.c33

Runge, M., Kelton, J., Birdsong, W., Dillard, B., & Balkcom, K. (2019). *Enterprise Budgets for Row Crops*. Retrieved from https://www.aces.edu/blog/topics/farm-management/enterprise-budgets-for-row-crops/

Sadler, E. J., Evans, R. G., Stone, K. C., & Camp, C. R. (2005). Opportunities for conservation with precision irrigation. *Journal of Soil and Water Conservation*, *60*(6), 371–379.

Saseendran, S. A., Ahuja, L. R., Ma, L., Timlin, D., Stöckle, C. O., Boote, K. J., & Hoogenboom, G. (2015). *Current Water Deficit Stress Simulations in Selected Agricultural System Models*. https://doi.org/10.2134/advagricsystmodel1.c1

Saseendran, S. A., Ahuja, L. R., Nielsen, D. C., Trout, T. J., & Ma, L. (2008). Use of crop simulation models to evaluate limited irrigation management options for corn in a semiarid environment. *Water Resources Research*, *44*(7), 1–12. https://doi.org/10.1029/2007WR006181

Schepers, A. R., Shanahan, J. F., Liebig, M. A., Schepers, J. S., Johnson, S. H., & Luchiari, A. (2004). Appropriateness of Management Zones for Characterizing Spatial Variability of Soil Properties and Irrigated Corn Yields across Years. *Agronomy Journal*, *96*(1), 195–203.

Shock, C., Barnum, J., & Seddigh, M. (1998). Calibration of Watermark Soil Moisture Sensors for Irrigation Management. *Precision Agriculture Technology for Crop Farming*, 177–211.

Soler, C. M. T., Sentelhas, P. C., & Hoogenboom, G. (2007). Application of the CSM-CERES-Maize model for planting date evaluation and yield forecasting for maize grown off-season in a subtropical environment. *European Journal of Agronomy*, *27*(2–4), 165–177. https://doi.org/10.1016/j.eja.2007.03.002

SSURGO. (2018). *Soil Survey Staff, Natural Resources Conservation Service, United States Department of Agriculture. Web Soil Survey. Available online. Accessed [March/07/2018]*.

Stackhouse, P. (2020). Prediction of Worldwide energy resource. Retrieved May 10, 2020, from http://power.larc.nasa.gov

Stanley, J. N., Lamb, D. W., Falzon, G., & Schneider, D. A. (2014). Apparent electrical conductivity (ECa) as a surrogate for neutron probe counts to measure soil moisture content in heavy clay soils (Vertosols). *Soil Research*, *52*(4), 373–378. https://doi.org/10.1071/SR13142

Steele, D. D., Stegman, E. C., & Gregor, B. L. (1994). Field Comparison of Irrigation Scheduling Methods for Corn. *American Society of Agricultural Engineers*, *37*(4), 1197–1203. https://doi.org/10.13031/2013.28194

Sudduth, K. A., Drummond, S. T., & Kitchen, N. R. (2001). Accuracy issues in electromagnetic induction sensing of soil electrical conductivity for precision agriculture. *Computers and*

Electronics in Agriculture, *31*(3), 239–264. https://doi.org/10.1016/S0168-1699(00)00185-X

Sudduth, Kenneth A., Myers, D. B., Kitchen, N. R., & Drummond, S. T. (2013). Modeling soil electrical conductivity-depth relationships with data from proximal and penetrating ECa sensors. *Geoderma*, *199*, 12–21. https://doi.org/10.1016/j.geoderma.2012.10.006

Sui, R. (2017). Irrigation Scheduling Using Soil Moisture Sensors. *Journal of Agricultural Science*, *10*(1), 1. https://doi.org/10.5539/jas.v10n1p1

Sui, R., & Yan, H. (2017). Field Study of Variable Rate Irrigation Management in Humid Climates. *Irrigation and Drainage*, *66*(3), 327–339. https://doi.org/10.1002/ird.2111

van Genuchten, M. T. (1980). A Closed-form Equation for Predicting the Hydraulic Conductivity of Unsaturated Soils. *Soil Science Society of America Journal*, *44*(5), 892–898. https://doi.org/10.2136/sssaj1980.03615995004400050002x

Varvel, G. E., Schlemmer, M. R., & Schepers, J. S. (1999). Relationship between Spectral Data from an Aerial Image and Soil Organic Matter and Phosphorus Levels. *Precision Agriculture*, *1*(3), 291–300. https://doi.org/10.1023/A:1009973008521

Vellidis, G., Liakos, V., Andreis, J. H., Perry, C. D., Porter, W. M., Barnes, E. M., … Migliaccio, K. W. (2016). Development and assessment of a smartphone application for irrigation scheduling in cotton. *Computers and Electronics in Agriculture*, *127*, 249–259. https://doi.org/10.1016/j.compag.2016.06.021

Vellidis, G., Liakos, V., Perry, C., Tucker, M., Collins, G., Snider, J., … Barnes, E. (2014). A smartphone app for scheduling irrigation on cotton. *Proceedings of the 2014 Beltwide Cotton Conference*, (1987). Retrieved from http://dev.smartirrigationapps.org/wp-content/uploads/2014/04/Smartphone-Cotton-App-Beltwide-2014-Paper-15551.pdf

Vellidis, G., Tucker, M., Perry, C., Kvien, C., & Bednarz, C. (2008). A real-time wireless smart sensor array for scheduling irrigation. *Computers and Electronics in Agriculture*, *61*(1), 44–50. https://doi.org/10.1016/j.compag.2007.05.009

Wang, D., Prato, T., Qiu, Z., Kitchen, N. R., & Sudduth, K. A. (2003). Economic and environmental evaluation of variable rate nitrogen and lime application for claypan soil fields. *Precision Agriculture*, *4*(1), 35–52. https://doi.org/10.1023/A:1021858921307

Willmott, C. J. (1982). *Some comments on the evaluation of model performance. Bulletin - American Meteorological Society* (Vol. 63). https://doi.org/10.1175/1520-

0477(1982)063<1309:SCOTEO>2.0.CO;2

Yadav, S. B., Patel, H. R., Patel, G. G., Lunagaria, M. M., Karande, B. I., Shah, A. V, & Pandey, V. (2012). Calibration and validation of PNUTGRO (DSSAT v4 . 5) model for yield and yield attributing characters of kharif groundnut cultivars in middle Gujarat region. *Journal of Agrometeorology*, *1*, 24–29.

Yan, L., Zhou, S., & Feng, L. (2007). Delineation of Site-Specific Management Zones Based on Temporal and Spatial Variability of Soil Electrical Conductivity. *Pedosphere*, *17*(2), 156–164. https://doi.org/10.1016/S1002-0160(07)60021-6

Yang, C., Sui, R., & Lee, W. (2016). Precision agriculture in large-scale mechanized farming. *Precision Agriculture Technology for Crop Farming*, 177–211.

Yari, A., Madramootoo, C. A., Woods, S. A., Adamchuk, V. I., & Huang, H. H. (2017). Assessment of field spatial and temporal variabilities to delineate site-specific management zones for variable-rate irrigation. *Journal of Irrigation and Drainage Engineering*, *143*(9), 1–7. https://doi.org/10.1061/(ASCE)IR.1943-4774.0001222